JOURNAL OF MECHANICAL ENGINEERING AND SCIENCES (JMES)
ISSN: 2289-4659 e-ISSN: 2231-8380
VOL. 15, ISSUE 2, 8095 – 8140
DOI: https://doi.org/10.15282/jmes.15.2.2021.13.0638

ORIGINAL ARTICLE

Nature-inspired solutions to bluff body aerodynamic problems: A review

N.A.Siddiqui[1], M.Agelin-chaab[1]

[1] Faculty of Engineering and Applied Science, Ontario Tech University, 2000 Simcoe Street, North, Oshawa, ON, L1G 0C5, Canada

ABSTRACT – This review investigates the nature-inspired techniques for the optimization of the aerodynamic forces on bluff bodies. To provide a rich understanding of these nature-inspired phenomena, three distinct zones of the species fishes (nektons), birds (avians) and the fast running land animals are considered. This allows contextualizing different capabilities of the species in different environmental necessities. The review follows a trend in which drag reduction capabilities of individual parts of these species, including body shape & size, tails, fins, surface structure, wings, and wingtips, have been explored in detail. By focusing on specific parts, the review examined the methods and physics involved, which provides space to narrate the development of ideas and our current understanding of the nature-inspired drag reduction and their application to bluff body aerodynamics. Consequently, nature-inspired promising areas for future endeavor related to the bluff body has been discussed in detail. It was found that, though, aerospace field has found several bird inspired application but the bluff body flow modification have only few. Similar is the case with fishes and land animals which have not been explored yet for aerodynamic use on the bluff bodies. The crucial importance of passive devices are also highlighted along with the review of their application on the bluff bodies inspired by nature. Furthermore, several of nature-inspired techniques are proposed and compared to facilitate the research in this direction. It provides a fundamental method to develop nature-inspired flow control devices for the bluff bodies.

ARTICLE HISTORY
Received: 18th Nov 2019
Revised: 23th Sept 2020
Accepted: 7th Oct 2020

KEYWORDS
Drag reduction;
biomimicry;
flow control in nature;
land animals and dra;
bird drag reduction;
nature-inspired vehicles;
wingtips;
fish

INTRODUCTION

Nature was never a field of engineering concern worldwide [1, 2]. The production of both journal publication and commercial patents mimicking nature's inspiration increased drastically for three decades. It was reported that from 1985 to 2005, the worldwide patents with keywords `biomimetic' or `bio-inspired' had increased by a factor of 93, but for non-biomimetic, it was only 2.7 [3]. The diversity of nature's mastery and its inspiration can be found from the fishing net all the way to airplane wings [4]. Due to the immense advancement, several review papers have been written to summarize, provide a research gap, and future possibilities taking inspiration from nature [5, 6, 7–14, 15–19]. However, this review paper focuses on nature-inspired drag reduction devices. Therefore, it is imperative to discuss the existing review papers to distinguish the methodology of the current work. Bio-inspiration is a broad term and amalgamates biological objects that can be stimulated to research on non-biological science [20]. Biomimicry, nature-inspired, bionic, and bio-inspiration are used interchangeably in this review paper.

The most striking breakthrough was the disregard of the smooth surface as the only drag reduction phenomena. Reif et al. [21] found that the sharkskin hierarchical structures can reduce the friction drag, which [22] has investigated significantly affects the drag reduction. Due to several works on this line, numerous review papers have been written from different perspectives [6, 23–28]. Bushnell and Moore [7] reviewed the drag reduction in both swimmers and fliers with three objectives, to identify the methods from nature that can be applied to the technology; identify artificially developed devices that nature already possesses like wingtips, and improve our understanding of the animal form and function. Pressure, skin friction, and lift induced drag were discussed regarding swimmers and fliers. Bechert et al,. [29] discussed the effect of the structure and surfaces of biological creatures on the flow control. It discussed wall shear stress and boundary layer separation of shark riblets. Anders [30] reviewed the kinematics and aerodynamics of bird and insect flights. He argued that the scale of the flier has a major effect on the flight's system and for this reason, birds and insects have completely different mechanisms. This distinct mechanism might have evolved the different number of feather and tip designs. Fish and Lauder [14] observed that sea animals manipulate airflow using active and passive devices. Passive devices relate to a morphological and structural constituent of the body like riblets. On the other hand, active flow control manipulates the appendage or body musculature to influence the wake structure. They reported the performance of the fish and mammals and argued that if a trailing animal follows the tangential velocity vortex formed by a leading animal, the body experiences less relative velocities which can decrease the drag. Keeping the same methodology of [14] and by including insect flight, an elaborated review has been done by [31].

Dean and Bhushan [32] discussed the drag reduction mechanisms in turbulent flows, and riblet inspired drag reduction theories. This special focus on riblet reviewed its performance, optimal geometry, riblet topped shark-scale replica, optimal riblet dimensions, and the latest manufacturing techniques. A fuel saving of 3% was achieved by riblets in-flight applications. Therefore, it is expected that the greater drag reduction may be seen if the biomimetic application

*CORRESPONDING AUTHOR | N.A. Siddiqui | ✉ naseeb.siddiqui@ontariotechu.net

of hydrophobic surfaces is explored at riblet valleys, peaks, or across the surface. Roper et al,. [33] reviewed the concepts, underlying biological principles of aquatic locomotion, biomimetic swimming devices developed so far, trends in design principle, and research gap. Furthermore, [34] reviewed three aspects of biologically inspired designs, including manufacturing research, methods of identifying and applying biology to new problems, and examples related to it. The uniqueness of their review lies in the case made by the authors that much work has reported the inspired design but few specifically elaborated on the methodology of identification and selection of biological designs. Hence, the two methods explored are solution-oriented, where bio-inspiration needs research for potential applications, and problem-oriented for which solutions from biomimetic is explored for a specific problem. Their discussion and review also include other related review papers [10–12, 35–41]. Abdulbari et al. [42] discussed mechanisms to reduce drag using riblets and commercialization of riblet technology. Categorization of the five approaches using riblets, the effect on drag, the effect of riblet groove on non-Newtonian fluids, the effect of groove on laminar and transition flow, and technological applications was discussed. Recently, the unique features of fliers and swimmers that constantly change their shape to accelerate/decelerate the flow has been reviewed to highlight their differences with classical fluid dynamics [43]. There are others review papers which can be referred for more clarification [5, 9, 12, 25, 27, 31–33, 38, 40, 44–51].

There is no dedicated review paper that surveyed the nature-inspired techniques of drag reduction, which can be applied to bluff bodies mostly ground vehicles like a car. However, few works have shown the capability of nature-inspired devices to reduce vehicle drag, which makes this endeavor worth exploring [52, 53]. Also, previous review papers ignored the aerodynamic motivation inherent in the fast land animals. Therefore, this review focuses on promising areas of nature-inspired aerodynamics, including swimmers, flyers, and land animals. Besides, only passive devices have been discussed, which means that the flow dynamics during motion are not considered. Hence, flapping and vibrational motions are not included in this review, like an application is made by the from flapping wing [54]. On land animals, not much work has been done concerning drag analysis. So, fast-moving animals are included to expand the existing perspectives on drag and the associated parameters.

Drag Behaviour of Fishes

The total drag is a combination of pressure and friction drag, which depend on the geometry and nature of the surface. In streamline bodies, the significant portion of drag is contributed by the friction, and in bluff bodies, it is the pressure [55]. Flow around the fish is controlled by combining body shape and appendages with the active and passive interface. Based on the outline of this paper, only the body and appendages will be reviewed without considering their interface and dynamic manipulation of the flow.

Effects of Body Shape on Drag

Aerodynamics of the streamlined shape

It is known that laminar flow is more prone towards separation than the turbulence flow because eddying motion transfers the outer momentum to the inner wall region that delays separation [56]. To create the turbulence, some species use roughness at the maximum girth position. Scombroidei is a family of fast-moving fishes that evolved so that near the maximum girth or body width, the laminar boundary layer is changed into a turbulent layer that delays the flow separation. When these fishes move at Reynolds number above 2 x 106 all the flow is believed to be either transitional or turbulent [57]. This relation between body shape and size has a connection with active swimming in the epipelagic zone in the ocean. Nektonics fishes are in the range of 15-30 cm in length because, below this range, they cannot resist the ocean waves [58]. The same kind of argument has been reported by [59–61]. The question if the fishes are living in the same environment, then why are there differences in shapes and sizes? One argument may be the alteration in the pressure according to the depth a fish is capable of swimming but based on the purely evolutional method; this needs to be addressed. It is essential because it was concluded through numerous studies during the 20th century that the overall drag of the swimming fish can be calculated by the analogy of a rigid body prototyping the fish [59, 62–65]. Due to such calculations, [66] formulated the hypothesis that the power needed to obviate the water drag is higher than the available muscle power in the fish, which is known as Gray's paradox.

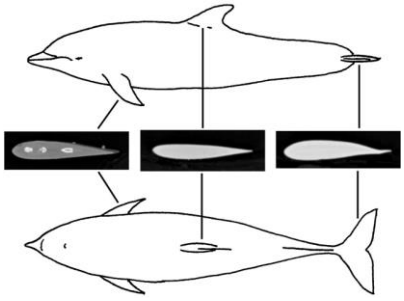

Figure 1. Shape and cross-section of a bottlenose dolphin. Left: Flippers, Middle: Dorsal, Right: Flukes [67]

Figure 1 shows the flippers, dorsal fin, and flukes of the dolphin along with streamlined shapes that were predicted to reduce drag by delaying the flow separation. Webb [68] used the fineness ratio (FR), a ratio of maximum length to the maximum thickness to describe the extent of the streamlines of a body. For an optimal FR, the drag will be minimum at maximum volume [69]. The FR for dolphins and whales are in the range of 3.3 to 8 [70]. This is in line with the argument by [71] who studied mathematically related bodies of revolution of the hull and demonstrated the minimum resistance at FR 7. Mises [69] also argued that a decrease in hair density shows drag reduction. Additionally, [57] formulated a relation between drag and the position of maximum girth, while [72] stated that dolphins have a maximum thickness at 34-45% of the body length. This particular shape is similar to any hydrodynamic foil by maintaining the pressure gradient and laminar boundary [68]. Hence, the flow separation is delayed and observed in the later part of the body just back to the dorsal fin [73]. No significant separation was reported when the experiment was done on the live swimming of dolphins under bioluminescent (production and emission of light by living organism) sea [74]. Rohr [74] argued that the existence of the turbulent flow could not be assumed from the existence of bioluminescence. So, bioluminescence is expected to occur around the dolphin regardless of the flow type. It has also been argued that fish change body shape during motion [75]. However, skin friction drag does not directly depend on the shape of the body. Hence to avoid large flow separation, fish must act to maintain laminar flow for the most part. This can only be done through streamlined shapes. However, [76] stated for the best shape of a fish that exhibits attached flow with a laminar boundary layer at a large Reynolds number. Because of this, dolphins have been recorded to have no separation and wake vortex. Additionally, the volumetric friction coefficient (C_v) does not depend on the shape of the body but rather on the Reynolds number. This is also the minimum drag on a rigid body revolution and valid for laminar attached flow. The range of this minimum possible value is .0015< C_v <.002 that is only possible for an animal with a slender shape. Similarly, [77] performed a three-dimensional simulation on a fish like a model and found that with an increase in swimming movement, the drag was increased. There is a critical velocity at which the thrust and drag were equal, which shows a linear relationship between drag and swimming velocity. All such considerations are due to the streamlined shape of the fish. Similar studies have been reported by[78–81].

However, [82] doubted this assertion and claimed that [66] did not have complete data for dolphin and got the higher values of muscle power that creates no objection to the theoretical drag power requirement. Later, researches unraveled different reasons for such wrong assertion, which they claim are also associated with the drag mechanism of the fishes. Hence, the approach to apply streamline body to fish proved not entirely correct when researchers started to consider the undulating shape of the fish shown in Figure 2. During motion, the fish does not remain straight; preferably, it has a curvy shape [56].

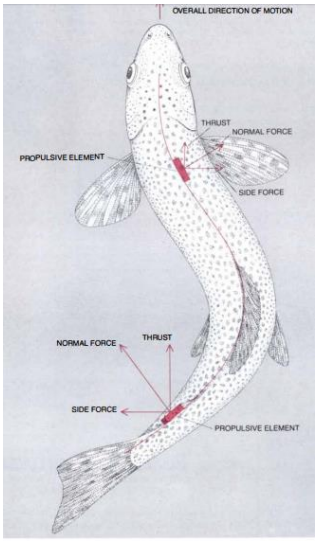

Figure 2. Active forces on undulating fish [83]

During the second and third quarters of the 20th century, inspired by Gray's paradox, investigations were done to understand the swimming behaviors of the fish [57, 84]. Rosen [85] experimented on a small fish in a water tunnel because he thought all the existing experiments had some flaws. The results were not following the established ideas of laminar and turbulent flow. Furthermore, the unusual motion of the quanta was in contradiction with the fundamental laws of motion. This gap led to the developing two hypotheses, namely the vortex peg and scale the force according to which the propulsive forces are due to the vortices of two-third of the fish body and after fins and tail surfaces. These forces originate from centrifugal forces inside the vortex core and angular momentum associated with it. Due to this deviation, [85] argued that the drag calculation of the streamlined shape does not work for undulating fish shape. Taneda and Tomonari [86] at first, proposed that the high swimming of the fish depends on the progressive wavy type motion. He performed a water tunnel experiment on a rubber sheet of 222 cm. They showed that when c/U0 <1, there is an isolated vortex at each trough, but when c/U0 >1, there is no vortex, where c is the wave velocity of the fish and U0 uniform water velocity. Swimming

motion tends to shift the turbulent boundary layer into the laminar boundary layer and reduce the wall shear stress. The same methodology was extended to a later study by the same author. The idea about the waving motion was no longer a mystery; however, [87] proposed enhanced locomotion in fishes and fliers through wavy motion. As a model, they replaced the bird wing and fish tail with large aspect ratio wing. They found a general trend whereby the transverse velocity of the wave was utilized by the wing for optimal motion. This led to enhanced incidence on the wing increasing thrust at crest and trough locations.

While discussing the differences between undulatory and oscillatory motion persistent in aquatic animals, [83] decomposed the forces acting on the undulating body shape. The position of researchers was much clear that waving movement inspired by the fish did reduce drag and improve the propulsion, but there was no experimental evidence on the real fish like model. Triantafyllou and Triantafyllou [88] built a robotic tuna fish model to study real behavior as never done before, see Figure 3. They were concerned about the capability of fishes to reverse movement in a small radius and without slowing down the speed.

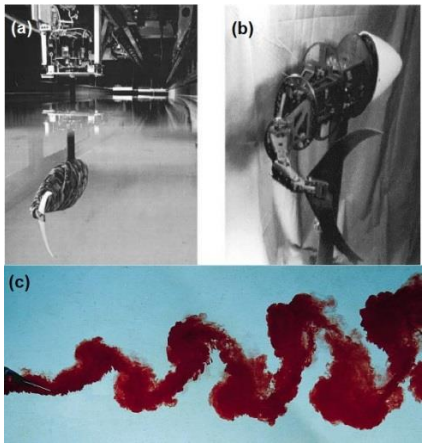

Figure 3. MIT RoboTuna and its vorticity development at the back [89]; (a) Robo Tuna in the tunnel, and (b) Close-up view of Tuna, (c) Vortex development

The unique vortex of tuna fish shown in Figure 3(c) has counter-rotating vortices behind the wake. The order of circulation is clockwise, followed by anticlockwise due to the tails waving moves. The authors argued that fishes maintain the timing and spacing between the vortices for efficient swimming. That was the main conclusion regarding the wavy shape inspired by the fish. The same authors later put together a more recent work [89] outlining three mechanisms during wavy shape; separation elimination, turbulence reduction, and energy extraction from the oncoming flow. This line of research attracted a lot of attention [90–92]. A great deal of research effort was put to investigate this issue where the body shape of the fish became the sole parameter of undersea investigations also [33, 78, 93–99].

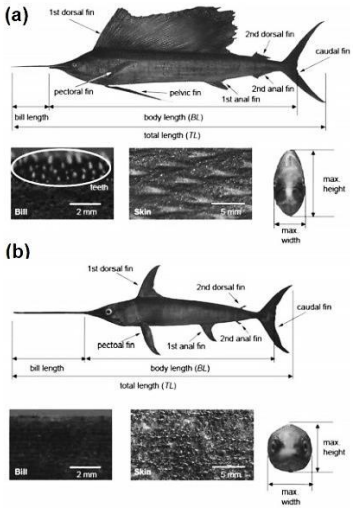

Figure 4. Sailfish with dimensions [100]: (a) Sword fish and (b) Sail fish

On the other hand, swordfish and sailfish shown in Figure 4 have the highest speed in the ocean animals, which is around 110 km/h [101]. In a hydrodynamic study by [100] on sailfish and swordfish inside the wind tunnel, it was found that the drag coefficients of sailfish are .0075 and swordfish .0091. Such coefficients are significantly less than the tuna and small fish like dogfish. The interesting point that velocity measurement showed was the absence of flow separation

from the entire body even without the bill. Additionally, it was also found that sailfish generally fold the first dorsal, first anal, and pelvic fins during gliding and cruising. However, that is not the case with swordfish. Sailfish and swordfish both evolved with a long bill and [102] for the first time investigated its use and found that the legislation is used to feed on prey by inserting into the school of prey without showing off an attack. Later on, they attack singles by lateral motions with large accelerations ever recorded. This investigation removes the ambiguity over the use of bill in such fishes. In a comparative study between swordfish, manta ray, and the killer whale by [103], it was found that the friction drag remains almost the same. However, form drag is in the order of swordfish < Killer Whale < manta ray. So, if the fastest animals under the ocean do not vary in terms of friction drag, then what are the other reasons giving that fish such speed? Information about the form drag elaborates the effect of shape on the aerodynamics, but not much work has been done in this direction. Table 1 summarizes the important information.

Table 1. Summary of the important progress in understanding fish body shape

Mechanism	Investigation method	Significance	References
Movement of fish	Experiment	Gray's paradox- The muscel power is less than the resistence	Gray [66]
Flippers, dorsal fin, and flukes	-	Drag reduction	Fish [67]
Fineness ratio	-	Provide the extent of how much a body is streamline	Mise [69] [104],[70]
Live swimming of dolphins	Experiment	No separation at the body	Rohr [74]
Best body shape	Theory	Should have attached laminar flow	Nesteruk [76]
Drag and thrust relation	CFD simulation	At a critical speed both Drag and thrust are same	Zhang et al., [77], Epps et al., [78], Liu et al.,[79], Triantafyllou et al., [80]
Undulating fish shape	Experiment	Streamlined body method is not applicable to Wavy shape of the fish	Rosen [85]
Wavy shape	Experiment	Tends to change the turbulent bounday into laminar	Taneda and Tomonari [86]
Vortex of tuna	Experiment	fishes maintain the timing and spacing between the vortices for efficient swimming	Techet et al., [89]
Swordfish and sailfish	Experiment	drag coefficients of sailfish are .0075 and swordfish .0091	Sagong et al., [100]

Aerodynamics of the Blunt Fish Shape

Contrary to the expected streamlined shape for better aerodynamics, circumstantial factors led to the development of bluff body shape in the ocean. The boxfish (Ostracion Meleagris) has a similar shape, like a bluff body shown in Figure 5 [105].Such a unique design of the boxfish with fins off maneuverability in a limited space at approximately near zero turning radiuses with 180° change in the direction.

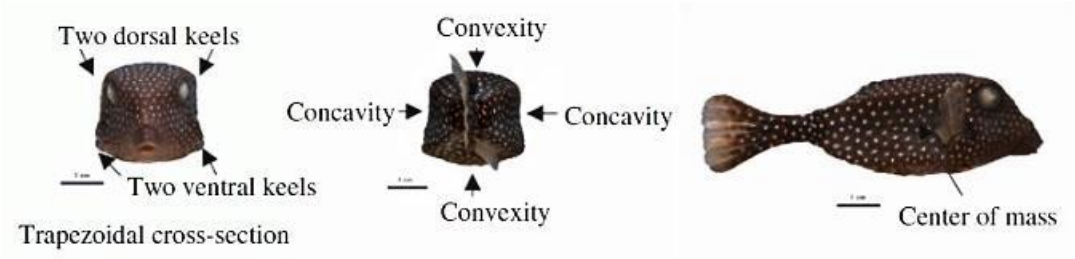

Figure 5. Spotted boxfish Ostracion Meleagris [105]

Also, the role played by the pectoral and caudal fin becomes more important [106]. Quantitative investigations by [107] revealed that swimming is fast with high endurance. The boxfish's speed varies concerning body length covered in one second and is dynamically stable. Their parasitic drag is like a good streamline body. The experiment shows that although the shape might say otherwise, boxfishes are competitive with other body-caudal fins (BCF) operated fishes because the calculated total cost of transport was same as BCF swimmers. That is why its body design and execution is one of the most complicated. Later on, [108] reported that as per rectilinear speed, boxfish use different fins to accommodate movement. When fish travels less than five body lengths per second, the only median, paired, and caudal fins seem to be used for steering. Greater than five body length was managed by burst-and-coast in which the prime factors were the body and caudal fin. The vertical flow structure behind the boxfish was studied by[109] that showed the development of strong longitudinal vortices coming out from keels of fish varying with the angle of attack. The pressure was low, where the concentric vortex was created on the carapace surface. They predict that self-correcting motion is made by the ventral keels in all the boxfishes [105]. The difference between the aerodynamics of real fish and a model fish was investigated by [110]. They experimented on living and a prototype boxfish to know their stability capabilities and found that in live fishes, the strength of vortex circulation was higher than in the model due to the pectoral fin interaction with kneel-induced flow. The power of boxfishes to alter the underlying self-correcting system with fins is an essential factor for stability and maneuver. However, the most crucial point is that the passive system of keels has reached such stability equilibrium. The generated vortices stabilize the boxfish automatically otherwise these will create flow separation leading to huge drag, but such consequences are being handled free of cost. Amalgamating such unusual design factors, the boxfish also has a speed of six body lengths per second for Ostracion Meleagris and Lactophrys triqueter boxfishes. Bartol et al,. [110] also found vertical flows similar to the fish model in the live fishes in the water tunnel. As the pitch angle increases, vortex strength also increases but was higher in live boxfish. This higher vortex might be due to pectoral fin interaction with keel flow. Nevertheless, previous studies led to a paradox: how can a boxfish are forwardly stabilizing at the same time turning quickly? To resolve this, [111] shows through experiment and simulation over boxfish that drag reduction performance is lower than the general fish morphology. The drag coefficient consistently decreases with speed, and a minimum was recorded as 0.26. Additionally, they have found destabilizing moments responsible for the optimal maneuverability. It is due to the different functions of the active fins. This argument is in line with the ecological necessity for efficient turning and tilting, they argue. The results seem contrary in terms of stability hence more data is needed to validate the claim. Again an aerodynamic study of boxfish shape in terms of drag coefficient was done by [112] both experimentally and numerically to initiate a method to implement the bioinspired design to vehicles. They found that the special shape of boxfish has a drag coefficient of 0.10 which is far less than any other model available in the market. Due to the diffusion from all sides, it contributes to the recovery of pressure and reduces the drag coefficient. More recently [113] studied the aerodynamic shape of a boxfish model and found the drag coefficient to be 0.24. These authors stated that features of the boxfish were implemented over the passenger car's front end only without defining what do those features mean. Nevertheless, the car model has a drag coefficient of 0.28, a 50% reduction compared to the Holden car model. This huge variation in the drag coefficient needs to be resolved before any concrete concepts could be made on boxfish. A proper investigation is necessary to judge the claim by [111] that boxfish may not be the ideal choice for car manufacturers, due to self-correcting stabilization of what is called `vortex lift' that keeps boxfish in a straight line. So, it would require large energy for a car to take a turn with such a self-correcting device. However, this debate seems to have huge potential for further research because not all the functions of such fishes are understood, and results appear inconsistent.

This section reviewed the important progress made towards understanding the natural shape like streamline and blunt body. The discussion on streamline shape stresses the shifts in the understanding of flow behavior. The rigid body shape, flexible body, and wavy body shape provide a complex picture of natural flow control techniques. However, the streamlined shape is not the only peculiarity in nature because the blunt body is said to give a relatively low coefficient of drag. Hence, the discussion on shape obscures the authenticity of assumptions about the mysteries of real energy harnessing techniques. Now, through boxfish design, nature again struck human's capability to understand the fundamental flow problems. Furthermore, it is not just a change in structure rather the understanding of basic axioms we have formulated. It means, how the flow behaves is not yet established even in a general sense because streamline and bluff body are two natural shapes. Given that water resistance is much higher than the air, the reduction of the drag coefficient is interesting for such a shape. What then from the combination of shape and passive devices of the fishes can be employed not only to ground vehicles but also to aerospace? Table 2 summarizes the important information.

Table 2. Summary of the important progress in understanding blunt fish shape

Mechanism	Investigation method	Significance	References
Boxfish shape	Experiment	maneuverability in a limited space at approximately near zero turning radiuses with 180° change in the direction	Bartol et al., [105]
Boxfish shape	Experiment and simulation	drag coefficient consistently decreases with speed, and a minimum was recorded as 0.26	Wassenbergh et al., [111]
Pressure recovery in boxfish	Experiment and simulation	Due to the diffusion from all sides, it contributes to the recovery of pressure and reduces the drag coefficient to 0.10	Kozlov et al., [112]
Boxfosh inspired car	Experiment	the car model has a drag coefficient of 0.28, a 50% reduction compared to the Holden car model	Islam et al., [113]

Effects of Appendages on Drag

Aerodynamics of the fins and tails

The streamline behavior is not specific to the body itself; rather, appendages like fins, flukes, and flippers are also streamlined. Lang [114] used three fins of different dolphins, which are all streamlined in cross-section, but the pressure distribution over them does not correspond to the typical airfoil. These fins appear to eliminate both laminar and turbulent boundary layer through the pressure gradient near the nose, and cusp-shape pressure gradients of fin A & B combined with adverse pressure gradient for turbulence create a near-uniform boundary layer to optimize the length of laminar flow. Van Dam [115] studied the unique crescent-shaped fins of the fishes. Long-distance cruising tail fins of aquatic mammals have this particular characteristic shown in Figure 6.

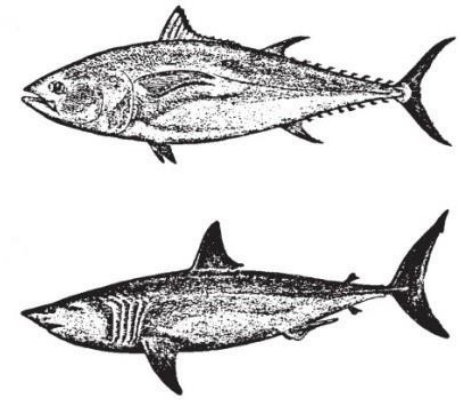

Figure 6. Crescent-shape tail fins [115]

It was found that aerodynamic efficiency has improved owing to increased backward curvature. Due to the combination of large induced efficiency and wingspan for a given loading, drag is reduced. Pavlov [116] examined the dependency between skin structure and dorsal fin of the harbor porpoise through the computational method. It was found that fin and fin cross-sections are related to skin structure which influences hydrodynamic parameters. Therefore, the skin structure is controlled by the fin flow mechanism. This is an exciting proposal because the reliance on each other will not only include skin structure rather the whole-body shape and size. It means the drag-reducing techniques related to the surface are linked to streamline shape and depends on the Reynolds number. Flukes of mammal's cetaceans help to create hydrodynamic thrust, stability, and maneuverability. It is also associated with lift and drag, which [117] has proved computationally. They used flukes' profile at 50% span for a numerical investigation that shows flukes are better lifting generating devices than existing foils, and out of 19 cetaceans, Tursiops has the largest coefficient of lift superior by 12-19% over-engineered. Table 3 summarizes the important information.

Table 3. Summary of the important progress understanding fins and tails

Mechanism	Investigation method	Significance	References
fins, flukes, and flippers shape	Experiment	These fins appear to eliminate both laminar and turbulent boundary layer through the pressure gradient near the nose,	Lang [114]
Crescent shape of fish tail	Experiment	aerodynamic efficiency has improved owing to increased backward curvature. Due to the combination of large induced efficiency and wingspan for a given loading, drag is reduce	Dam [115]
fins	Simulation	fin cross-sections are related to skin structure which influences hydrodynamic parameters	Pavlov [116]
flukes	Simulation	flukes are better lifting generating devices than existing foils upto 12-19%	Fish et al., [117]

Aerodynamics of the Flippers

Similarly, whale's flippers shown in Figure 7 got research attention due to its unusual leading structure called tubercles. It functions to create excitation in the flow that delays the stall for high angles of attack [118]. Watts and Fish [119] did a simulation on a wing with and without tubercles and found that it increases the lift by 4.8%, reduces the induced drag by 10.9%, and increases the lift to drag ratio 17.6%. The delay in the stall was then reported by [120] through the wind tunnel experiment over-idealized humpback whale flippers. They found a 40% delay in the stall compared to smooth wing, along with drag reduction and increased lift. The reason for the delay in stall was the flippers' higher lift at a large angle of attack. During post-stall, flippers maintain the low drag at high lift. This mechanism is auspicious to whale during feeding and maneuvering.

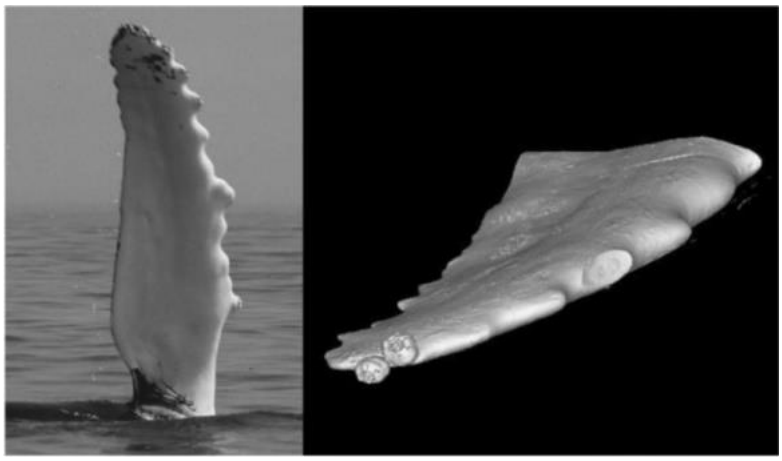

Figure 7. Whales Humpback whale (M. novaeangliae) flippers. Detail views of pectoral flipper showing leading-edge tubercles [121]

van Nierop [122] devised an aerodynamic model for whale flippers that details the reason for delayed stall. They changed the morphology of a smooth wing according to whale flippers to see the effects of bumps. The control properties of flippers are related to the amplitude of the bumps; if the amplitude increases, the lift curve flattens and remains indifferent with wavelength. Similar results have been reported in a water tunnel experiment by [123]. Based on the modification of airfoil NACA0021 by mimicking flippers, tubercles [124] revealed that due to the streamwise formation of the vortices modified by tubercles, the tonal noise of the airfoil is reduced. It is supposed to be influencing the stability of the boundary layer. Later on, the same authors[125] reported that these tubercles work more efficiently on NACA 65-021 than the NACA 0021. Higher amplitudes provide higher lift coefficient and stall. Besides, during post-stall, it works

even better by delaying the stall angle, increasing the maximum lift coefficient and other performance parameters up to a specific wavelength. The flow behind the smooth and tubercles wing was further reported that lateral to crest and downstream vortices interact with the oncoming flow from tubercles [126]. The pair of vortices from the inward-facing side due to the tangential velocities change towards the trailing edge of the wing. Also, the tubercle peak accelerates the flow further downstream after mingling with the vortex pair. These effects altogether stop the separation of the downstream tubercles flow, and this led to shift the stall line further backward. These tubercles again stress the impact of wavy surfaces already discussed before. This led [127] to argue that such protrusions on the whale flippers are not unique to the only whale from tubercles. He proposed alternative forms that equally provide some kind of benefits for better agility and maneuverability. As shown in Figure 8 different types of wavy patterned foils which he investigated for comparison with the whale tubercles. A similar study was done by [128], [129]. Almost all the studies have suggested improvements in aerodynamic performance duet to tubercles.

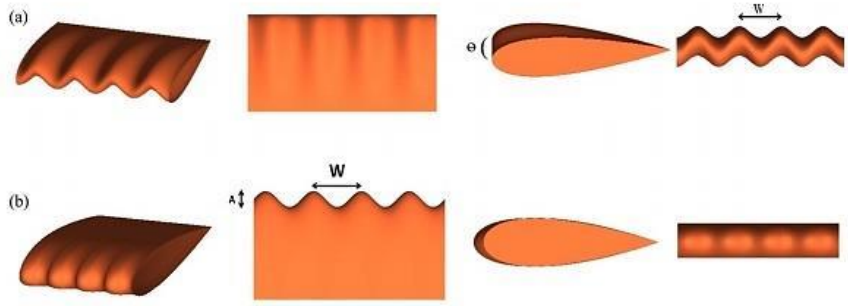

Figure 8. (a) Wavy wing section and (b) Tubercles wing section [127]

However, the flow mechanisms for these improvements are still not clear with several hypotheses, such as the boundary layer momentum, angle of attack, vortex lift, and effective angle [130]. The authors have reviewed such a competing hypothesis, which is useful for further research in this direction. Nonetheless, it was believed that flukes of cetaceans produce the power for swimming, and flippers create the desired lift and torque for maneuver. However, recently [131] demonstrated, for the first time, an additional function of the whale flippers. The active stroke of flapping creates lift and increases propulsive thrust. These strokes can grow massive forward-oriented forces that can enhance lung feeding performance.

This section discusses the aerodynamic effects of various appendages of the Fish. It revealed that fins, flippers and tails provide an exciting, aerodynamic benefit and further motivatein-depth research on different sub-parts. However, the practical implication of these parts still needs the attention of the scientific community. Significantly, the critical features of the flippers had great potential in different applications. Table 4 summarizes the important information.

Table 4. Summary of the important progress in understanding the flippers

Mechanism	Investigation method	Significance	References
Whale's flippers	Simulation	it increases the lift by 4.8%, reduces the induced drag by 10.9%, and increases the lift to drag ratio 17.6%.	Watts and Fish [119]
Humpback whale flippers	Experiment	40% delay in the stall compared to smooth wing, along with drag reduction and increased lift	Miklosovic et al., [120]
Protrusions on the whale flippers	Simulation	such protrusions on the whale flippers are not unique to the only whale from tubercles. He proposed alternative forms that equally provide some kind of benefits for better agility and maneuverability	Rostamzadeh et al., [127]
Stroke of flapping	Simulation	active stroke of flapping creates lift and increases propulsive thrust. These strokes can grow massive forward-oriented forces that can enhance lung feeding performance.	Segre et al., [132]

Aerodynamics of the Surface Structure

Reif and Dinkelacker [21] were the first to discover the complex shape of the sharkskin micro-grooved surfaces that reduce drag in the turbulent conditions. The reason behind this drag reduction is the thickness of the viscous sublayer. If the thickness is greater than the roughness of the contact surface, than these rough surfaces will be immersed into it, hence the friction is transformed into viscous resistance [15]. The structure of sharkskin evolved with micro-grooved structures that consist of riblets. It was suggested that these grooved surfaces are the reason for reduced viscous drag and turbulence intensity.

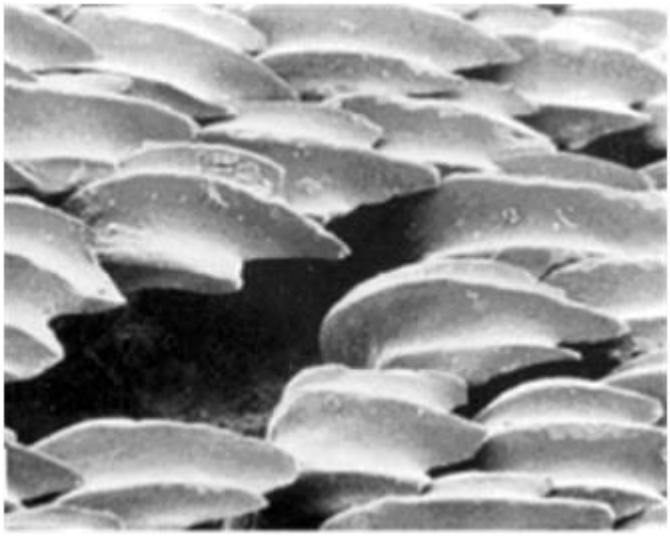

Figure 9. Skin of white shark [133]

Walsh [22, 134] reported a maximum of 8% drag reduction due to longitudinal grooves of shark skin riblets. They kept the dimensions of grooves of the same order as the turbulent wall streaks and bursts. Also, the optimum rib shape is a sharp peak groove with valley curvature. The skin of a white shark is shown in Figure 9. The effect of riblet parameters that can affect the hydrodynamic has been developed. The viscous sub boundary layer due to the longitudinal rib of the shark has been theoretically analyzed [135]. The theoretical calculation predicted the origin of the velocity profile from the riblets. It lies below the tips of riblets, in general, 10-20% distance of rib spacing called `protruding height' theory. Later, 5-8% reported drag reduction was improved by [136] to 10% compared to smooth surfaces through oil tunnel experiments. By taking inspiration from nature, sharkskin riblet has then been modified to suit engineering problems. Nugroho et al,. [137] reported the experimental results in converging-diverging riblets in the turbulent boundary layer with zero-pressure. Due to large scale periodicity in the turbulent boundary layer in the spanwise direction, the boundary layer thickness is significantly affected. Hence, the local mean velocity increase and turbulent intensity decrease make the boundary layer thin. Taking the same line of research, Recently [138] investigated the effect of streamwise riblets in turbulent boundary layers with particle image velocimetry. They found a reduction in friction velocity and Reynolds stress inside the turbulent boundary layer, hence reporting drag reduction. The correlation between hairpin vortices and momentum distribution is that increases in streamwise riblet surface decrease the hairpin vortices. These are in contrast with the smooth surfaces. Similar studies have been reported in this direction, making sharkskin riblet an undisputed technique to reduce drag reduction [8, 139–143].

However, the effect of riblet cannot be understood until all the affecting factors to the movement of sharks are known. Lang et al,. [144] investigated the existing proposals that sharkskin can bristle their scales while in motion. The experiment showed an increase in momentum close to the slip area that forms above the scales. Hence, the increase in velocity can be attributed to boundary layer control that is due to separation control. This is a separate issue to be explored. Like Lang and colleagues [8] brought a different perspective that deals with the angle of attack over sharkskin scales. The angle of attack is a highly influential factor in reducing drag and turbulence intensity. The scales change with swimming conditions. They also stated that the sophisticated morphology of scales behaves as a super-hydrophobic surface with a contact angle of more than 150°. This creates boundary slipping at the interface of fluid-solid, which can reduce the velocity gradient along with resistance due to the viscous effects. One more critical point is the working of nanochain mucus that stretches within the boundary layer creating a more stable and steady flow. They also highlighted the variation of shark riblets throughout the body and found no similar second rib on the entire surface. Domel et al,. [145] designed a new kind of riblets inspired by denticles that have shown significant improvement in the aerodynamics of the wing. This inspired device shown in Figure 10 can improve the drag to lift ratio by 323%, which outperformed the existing vortex generators at a low angle of attack.

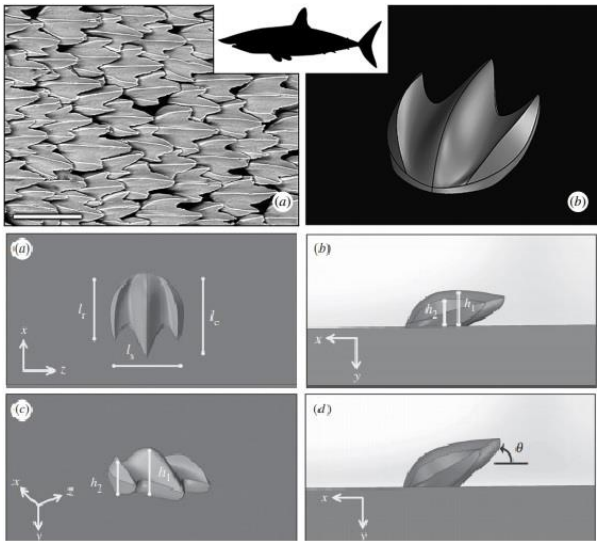

Figure 10. Shark denticle inspired surface structure [145]

This reduction was the alteration of the flow pressure by separation bubbles at the wake of denticles, which improve the suction. The loss of momentum due to skin friction was made up of the streamwise vortices. The importance of this study is that apart from the drag reduction mechanism discussed in existing literature, it has introduced the lift and lift to drag ratio parameters, which were significant in understanding the role of denticles.

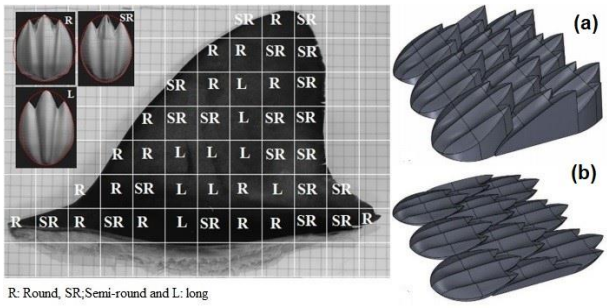

Figure 11. Shark mako's dorsal fin denticles inspired structures. (a) Rounded inclined and (b) Rounded horizontal [146]

By focusing on the shortfin mako shark [146] has designed structures from the dorsal fin. The dorsal fin has somewhat different structures than the body, and the mimicked designed structure was rounded, semi-rounded, and long, as shown in Figure 11. They have found the best drag reduction with rounded and long denticles. The lowest drag coefficient of 0.011 was recorded for long and rounded at 9.5º angle of attack with 5 m/s speed.

uperhydrophobic surfaces have been embellished with sinusoidal surface texture through direct numerical simulations [147]. They found microgroove inspired asymmetric secondary flows that oscillate in the streamwise direction. It is found that transverse shear strain on top of the sinusoidal microgroove is like a stokes spatial layer (SSL). Simulation and experimental studies have been undertaken by [148] to see the effect of the micro-grooved surface on the blade of air engine. They found that a micro-grooved blade has a higher drag reduction performance than un-textured. They also optimized the position of texture on the blade surface. A bunch of application-oriented investigation has been done inspired by riblets [28, 141, 149–153]. Similarly, the protrusions at the surface of sailfish were investigated for friction drag reduction [101]. They found that there was no significant improvement in the drag by the riblets of sailfish. The reported skin friction drag reduction was only 1%. This is in contrast with the improved aerodynamic performance by the shark riblets. What are the evolutional and aerodynamic differences between these two structures need further investigation?

In this section, the aerodynamic effects of the surface structure of the fishes has been discussed. The physical understanding of such structures like Riblets, denticles of the shark led to the development of new kinds of vortex generators providing impressive drag reduction. Fishes structures provide an exciting line of research, which includes the basic physical understanding of shapes, wavy shape, geometries of tails & fins and the surface structure. These are some of the concepts that improve our understanding of fluid flow. The implementation of engineering problems has not been fully discovered yet, so there is a lot of research yet to be done.

Table 5. Summary of the Important progress in understanding the surface structure

Mechanism	Investigation method	Significance	References
sharkskin micro-grooved	Experiment	Reduce drag in the turbulent conditions	Reif & Dinkelacker [21]
longitudinal grooves of shark skin riblets	Experiment	Maximum of 8% drag reduction	[22], [154]
Sharkskin riblet modification	Experiment	Increased drag reduction compared to original	Nugroho et al,. [137]
Shark at angle of attack	Experiment	highly influential factor in reducing drag and turbulence intensity and behaves as a super-hydrophobic surface with a contact angle of more than 150°	Lang [8]
Riblets inspired by denticles	Simulation	improve the drag to lift ratio by 323%, which outperformed the existing vortex generators at a low angle of attack	Domel et al,. [145]
Shortfin mako shark	Experiment	The lowest drag coefficient of 0.011 was recorded for long and rounded at 9.5º angle of attack	Patricia et al., [146]

Applications to Bluff Body Aerodynamics

Engineering applications of nature-inspired body shape has a long history that has been implemented both in aerospace and ground vehicles. Though a high drag reduction was achieved with such a non-aesthetic look, it was not attractive to the people [155, 156]. Arabacı and Arabacı [157] developed a bus inspired by the shape if beluga whales shown in Figure 12. The experimental and numerical study of six different bus models, a drag reduction of 21.06%, was achieved. This would give an approximately 12.64% reduction in fuel consumption. Similarly, the body shape of a sailfish has been studied for the alternative of the fuselage of an airplane. It is well known that sailfish is the fastest animal in the water. Taking inspiration, [158] modified the nose of the fuselage. Sailfish features proved to be aerodynamically more efficient than the conventional fuselage. This led to a reduction of 10% drag force, which points to the importance of elliptical cross-section over circular. This has been discussed because the potential application of this design to the front of tractors and buses is huge [159].

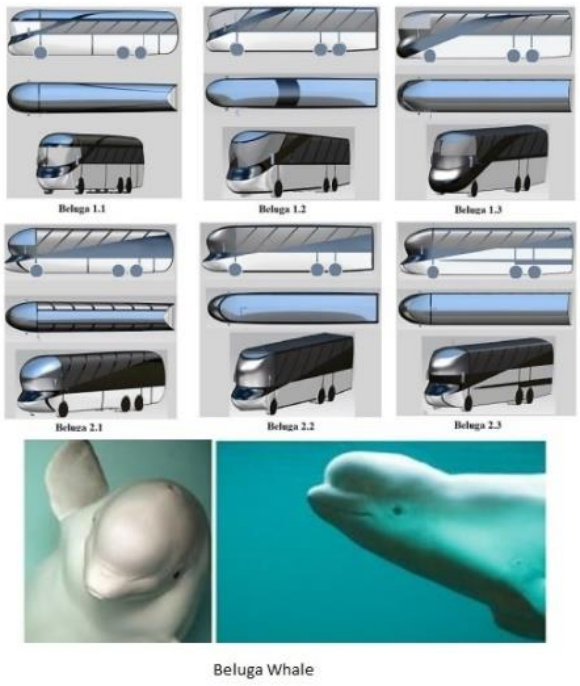

Figure 12. Six models of buses inspired by Beluga whales [157]

Similarly inspired by sailfish diplets at the torso fin used to rise from the pockets of air and water scales were imbedded onto a P1 hypercar. This texture was installed inside the duct that connects to the engine. It increased the volume of air by 17% to the engine, hence improving the car's efficiency. It was a necessary task because this electric Hypercar has 903 horsepower, which needs air in large quantities [160]. The car is shown in Figure 13.

Figure 13. Sailfish inspired P1 Hypercar designed by McLaren [160]

Similarly, a rather unusual shape of the boxfish led to the development of a whole new car design by Mercedes Benz. By mimicking a female boxfish, a car was developed that has a 0.24 drag coefficient, shown in Figure 14 [161]. Though detailed features are not available in the open literature, Figure 16 shows the shape as the significant adoption. This design created a controversy that while in a straight motion, it will be difficult for a car to turn due to morphological reasons. But this destabilizing moment is the reason for enhanced maneuverability in boxfish [111].

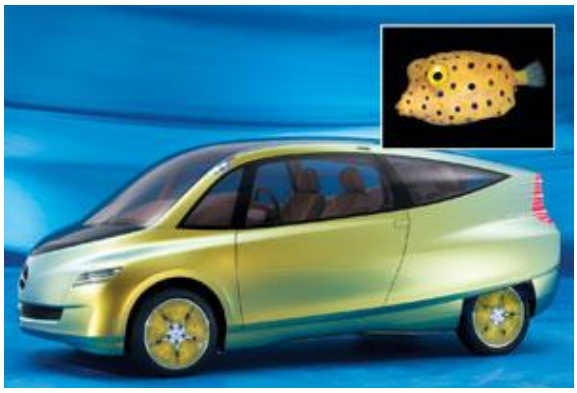

Figure 14. Boxfish inspired car [161]

It was argued that what is called in-course stabilization of boxfish due to vortex lift generated from the edges will make a car bound to a track like a train, and aberration from this linear path requires enormous energy, argues [162]. Hence what benefits can the rare maneuverable capability of boxfish be applied to a car driving at a much higher speed? As rightly pointed out using features and shapes to specific locations rather than adopting whole shape design is an area that needs research attention. Recently, [163] have tried to adopt some features of the boxfish, though not specifying again about the features itself. From Figure 15, it seems their focus was to mimic the shape of the boxfish, which gave a drag coefficient of 0.28. Specifically, the frontal shape of the boxfish, which at the later stage was optimized for better aesthetic looks as well, was examined.

Figure 15. Boxfish inspired car model that claims to use some features [163]

What then can be acquired from the shapes of fishes into engineering applications? As [156] stated that vehicle design is not always about looking at aerodynamic gains rather it is much more complex. Hence, it is imperative to look for the important features that can be mimicked in some parts of the vehicle. Bio-inspired material is a great example that is creating far better-performing materials than inventions made earlier [164, 165].

The application of non-smooth surface that was started by [154] on airplane fuselage did not excite the researcher to apply the same on ground vehicle design. However, [166], for the first time, tried to implement it on a vehicle structure. The size and dimension of the non-smooth surface cart are shown in Figure 16. Only the engine cover lid and vehicle body cap were tested with such non-smooth surfaces. They argued that 10.31% of drag reduction was achieved by controlling the boundary layer. This control lessened the burst and loss associated with turbulent kinetic energy.

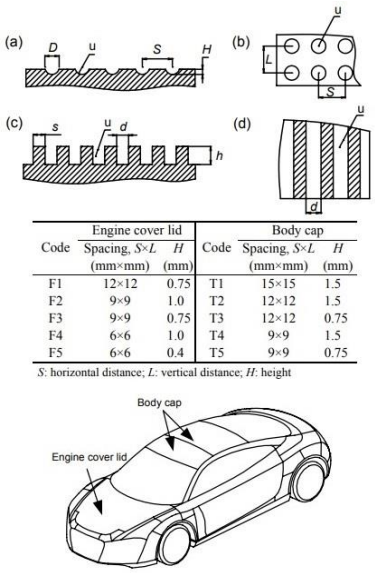

Code	Engine cover lid Spacing, $S\times L$ (mm×mm)	H (mm)	Code	Body cap Spacing, $S\times L$ (mm×mm)	H (mm)
F1	12×12	0.75	T1	15×15	1.5
F2	9×9	1.0	T2	12×12	1.5
F3	9×9	0.75	T3	12×12	0.75
F4	6×6	1.0	T4	9×9	1.5
F5	6×6	0.4	T5	9×9	0.75

S: horizontal distance; *L*: vertical distance; *H*: height

Figure 16. (a) and (b) Pits in uniform distribution (c) and (d) Uniformly divided grooves. The table shows the length and card model indicate the location of non-smooth surfaces.[166]

The same analysis has been done considering the non-smooth surface of beetle and shell by the same authors [167]. Variation in the groove size and shape affects the aerodynamics behaviors, which have been extensively studied [26, 135, 166, 168].

This section describes the fish inspired engineering application attempted till now. However, it does not provide the methodology which can provide a way of selection, at least in terms of applying features of the fishes to engineering. It seems there is a lot of work that needs to be done at this front. Table 1 summarize the application of fish inspired devices.

Table 6. Summary of Important progress in bluff body applications

Drag reduction through fishes				
Flow control Method inspiration	**Investigation method**	**Device**	**Significance**	**References**
Beluga whales	Experiment and CFD simulation	Bus design	21.04% drag reduction	Arabacı and Arabacı [157]
Sailfish diplets	Manufactured	P1 hypercar	Volume of air increased by 17%	Chawla [160]
Female boxfish	Manufactured	Mercedes Benz car	0.24 drag coefficient	Sharfman[161]
Boxfish	Experiment	Car design	50% drag reduction	Chowdhury [163]
Shark's groove like non-smooth surface	CFD	Surface modification	10.31% drag reduction	Song et al., [166]

Drag Behavior in Non-Flapping birds

The first book about human's journey on the path to flight was *`Progress in flying machines'* by *Octave Chanute* in 1894, exploring the strong possibility of natural flyers to solve the engineering problems [169]. Indeed, the complete grasp of natural flyers and their implementation of the engineering problem is neither easy nor required in every case. However, the aerodynamic system of flyers is robust, autonomous, and environmental-friendly; hence the question researchers are looking at whether flyers can become a premise to solve engineering problems in a sustainable way than man-made solutions [30]. Jacob [170] argued that it is imperative to know different aspects of flyers related to engineering

problems, especially wing aerodynamics, structures, and control systems. Due to the flyer's complex wing surfaces, flexibility, and control over agility in maneuvering, they are difficult to study [171]. The mechanical properties influence a lot on aerodynamics, which has been studied by various researchers [170, 172–175], but that will not be reviewed here. The focus of this section is about drag and lift inspiration from flyers, but it will exclude any specific designs which have already been reviewed. However, wherever necessary, they will be referenced for further reading.

Effects of Body Shape on Drag

Air and ground vehicles had motivation in the birds due to streamline shape [155, 156]. The drag associated with bird flight is classified into three components; parasitic drag, profile drag, and induced drag. The parasitic drag is due to the bird's body without the wings [176]. The power required by birds due to their body was theorized by [177], which related flight power and speed. He argued that body drag (drag of non-lifting parts) depends on the freestream velocity and chose the flat plate equivalent area to calculate the parasitic drag associated with the body, as shown in Figure 17. The power required to surpass this drag was calculated.

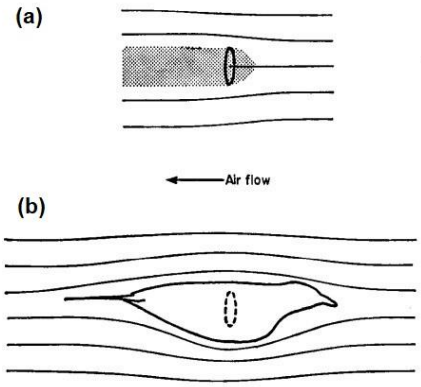

Figure 17. Bird body as an equivalent flat plate area [177]; (a) Flat plate cross-section, (b) Bird body

However, [178] argued that the calculation of drag and associated power had not been compared with the measured values. So, he compared the predicted values with the experimental data and proposed some modifications in the theory. He also adds that parasitic drag is related to Reynolds's number; hence for bird-like body shape, the drag coefficient decreases when the Reynolds number goes higher than a specific range, so the flat plate area needs to be modified with speed. This dependence on the Reynolds number is not predicted by the [177] theory. Moreover, for an actual bird, there is no established functional relation between the Reynolds number and the parasitic drag coefficient. The boundary layer over the bird body varies as per the locations. Accordingly, [178] has formulated the new equation for parasitic power.

Later on, [179] measured the frontal area of large birds related to power through the body mass. The drag coefficients do not vary much after the Reynolds number of 150 000. The drag coefficient ranges from 0.26 to 0.38 for the different birds used in the experiment. Other measurements obtained varied values of body drag that led [180] to resolve this problem and establish a definite body drag on Harris hawk. He reported that the mean minimum drag coefficient of a wingless dry, frozen body is 0.24, and a smooth-surfaced model has 0.14. A similar study was performed by [181]. There are methodological restrictions in the experiment to find out the actual interference drag of the body. Tucker [182] introduced a new method stating that the existing rules to find isolated body drag is the difference between the body on strut minus the strut alone. However, strut influence the freestream flow and creates additional interference drag. Not only the body size and shape but also the position of the head affects the body drag. Tucker [183] argued that while chasing the prey, peregrine falcons bends head about 40 degree but that should also increase the drag due to this bending. This is a paradox because both are existential phenomena. He further experimented in a wind tunnel using pitching and yawing angle on the birds and found that with a turned head, drag increases by 50%. Moreover, [184] has shown that differences in body size deliberately affect the drag pattern along with speed. They showed using auklets bird minor fluctuations in shape but large variations in drag coefficient with speed. It also pointed out the difference in measurement for the smooth and feathered version of the model. That means turbulent transition flow at the front is not only affected by the shape but also the feathers. Moreover, the data shows a higher effect of the feather on the drag magnitude than the shape of the body itself. The effects of body shape and size are not the only factors that influence the drag of the bird body rather, the presence of a tail in birds reduced the parasitic drag. Maybury and Rayner [185] did a wind tunnel experiment on European startling Sturnus vulgaris. They found that the absence of tail rectrices and dorsal and veneral coverts increases the parasitic drag by 55%. This enhancement is large, considering a small portion of the tail compared to the body of the bird. The tail and associated feathers operate as a splitter plate that modifies the boundary layer which ultimately delays the separation and reduced the drag.

Along with the paradox mentioned above, there is a fundamental problem related to the measurement of the drag coefficient of the bird body, which is highlighted by several studies [178, 179, 182]. The ambiguity is that the drag coefficient values determined by experiments using the model were as low as 0.14 to 0.17, which were almost equal and

sometimes lower than the importance of the fundamental values of the best axis-symmetric convex bodies in a similar flow range [186]. Through flow visualization, the authors proposed that this deviation is due to the bird's non-axisymmetric and non-convex shape. This special structure creates a turbulent boundary layer, and the extensive flow separation occurs at the dorsal area of the neck and tail. These two features help to create a scarf vortex starting from the neck and running over the whole body till the tail. This vortex stabilizes flow over the body by controlling the flow separation at the necessary point. Hence, a bird's shape has its own way of controlling the flow, which is not experimentally determined in a live flying bird [187]. When the wings remain motionless and flexed with respect to the body, the intermittent flight of a small bird improves. It means heavy birds cannot remain motionless in the air for more time, but small birds can [188].

From the above discussion, it becomes clear that the complete grasp of bird shape has not been understood yet because, after two decades of work, researchers are still trying to develop improved data on the parasitic drag [189]. Similarly, how other appendages of the birds affect the body drag is also not understood like the wing-body interference. The design of nature has evolved so that it always harnesses the maximum energy, which sometimes seems to be contrary to the general understanding of science. For example, the navigation of bats occurs through echolocation by extending the ears. But [190] showed by experimenting on two small and large ear bats that the large ear bat has high body drag but brings forth relatively higher lift.

In this section, the historical development in the understanding of flow around a bird body is investigated. Different bird body shape shows the range of drag coefficient and then the measurement problem has been highlighted. Additionally, live birds experience different deformation during flights and adjust their body according to the necessity of the conditions of the flow. However, such degrees of freedom are difficult to create in the wind tunnel with various parameters. Future research can resolve this dispute over body drag and find out the proper methodology to calculate different interference drag and lift generation.

Table 7. Summary of the Important progress in understanding Bird body shape

Mechanism	Investigation method	Significance	References
Parasitic drag theory	Experiment	body drag (drag of non-lifting parts) depends on the freestream velocity and chose the flat plate equivalent area to calculate the parasitic drag	Tucker [176]
Drag coefficient of bird body	Experiment	mean minimum drag coefficient of a wingless dry, frozen body is 0.24, and a smooth-surfaced model has 0.14	Tucker and Heine [180]
tail rectrices	Experiment	absence of tail rectrices and dorsal and veneral coverts increases the parasitic drag by 55%.	Maybury and Rayner [185]
non-axisymmetric and non-convex shape	Experiment	special structure creates a turbulent boundary layer, and the extensive flow separation occurs at the dorsal area of the neck and tail. These two features help to create a scarf vortex starting from the neck and running over the whole body till the tail. This vortex stabilizes flow over the body by controlling the flow separation at the necessary point	Rayner and Maybury [186]

Effects of Appendages on Drag

Aerodynamics of bird tails

The appendages of the birds can broadly be divided into two parts, wing, and tail which along with the body, complete the three kinds of drag known as parasitic drag, profile drag, and induced drag [177]. However, only the wings are conventionally excluded while calculating the aerodynamic forces on the bird [182]. Due to the critical contribution of the tail to the drag and lift, it is divided into tail and wing in this paper.

The structure of tails varies dramatically within the flyers. For example, a small bird *Euplectes progne,* has a tail worth 1m long, and the bird *Uropsalis lyra* showed a complex tail that is approximately 8 times the body length [191]. Such a complex shape in their relation to aerodynamics is far from established. Smith [192] argued that the birds use the tail as a horizontal control surface by providing stability. But why did the birds evolve in a horizontal tail rather than vertical is a big mystery yet to be solved? In addition to this, [193] showed that the tail area fluctuates as per the flight speed. For a Harris Hawk, it varies from 10% in fast flight to 20% of the low flight of the wing area[180]. It has been argued that the tails have two objectives, to produce large forces during slow flight and maneuvering. During the slow flight, the wing has to generate a high lift that shifts the center of aerodynamic pressure forward, which destabilizes the flow by changing the pitching moment. At this junction, the tail acts as a control surface and modifies the flow coming, which delays the stall [193]. Similarly, it has been proposed that the variation in tail structure and its length is associated with the kind of vortex generation coming backward by [194]. In the vortex ring gait to allow the bound vortex across the body, this factor

may have influenced the positioning of the tail. The tail may evolve into a rounded trailing edge. He also stated that the drag associated with the elongated tail depends on the surface area. If the area is high, so would be a drag, and that is why the elongated tails have less width and some even end like a wire-like tail. By analyzing the different aspects of the bird's tail [195] wanted to establish the aerodynamic theory of tail on the basis of slender lifting surface theory.

The above discussion reveals an inconclusive understanding of the tail aerodynamics and differences in the lengths available. Balmford et al,. [196] attempted to calculate the flight cost associated with elongated tail by integrating aerodynamic and data on sexual dimorphism. For the experiment, they considered four different elongated tail size models depicting the original birds shown in Figure 18, at a spread angle of 120 degrees. The aerodynamic cost was formulated in terms of lift to drag ratio. A graduated tail has the highest lift to drag (L/D) ratio and a shallow fork the lowest. This suggests that to avoid the aerodynamic cost, a tail must evolve with elongated length but less in width; otherwise, the penalty is a high drag. Later on, [197] using the same method stated that natural selection could explain these tail variations. The tail does reduce the L/D ratio of birds but helps to maintain stability, creating lift and turning the flight. They found that large birds with high L/D have a short length; on the contrary, birds that generally need maneuverability more than any other parameter are evolved with a long tail.

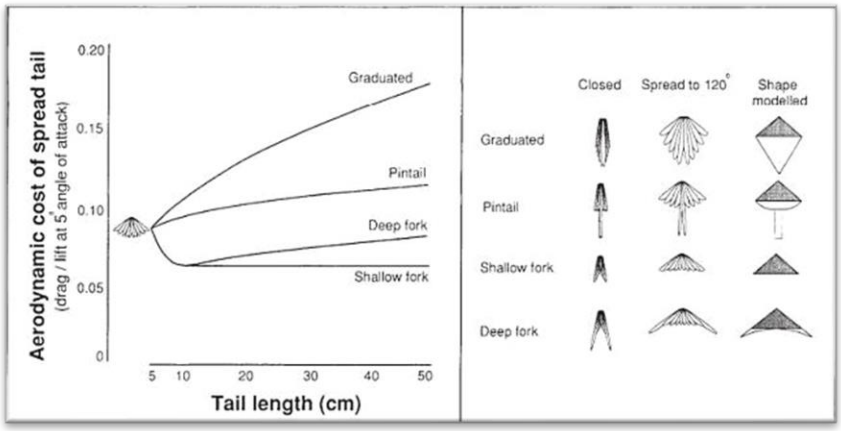

Figure 18. Right side shows the shape of the tail with the spreading angle along with the associated model shape tested. The left side provides the aerodynamic cost corresponding to the tail shape [196]

Also, those birds in need of maximum turning moments on a fixed drag value evolved with long and forked tails that provide such flexibility. Thomas and Balmford [197] have made several predictions that proved to be correct and others wrong. The prediction that if the aspect ratio increases, the tail length should decrease, an increase in flying speed should decrease the tail length, and an increase in outer feather tail length also improves maneuverability were found to be correct.

Furthermore, there was another line of research on the tail that owes to the delta-wing theory. Evans et al. [195], Evans [196] reported the recent debate over applying high-speed delta-wing theory to the slow-moving birds. They proved through an experiment that both delta wing models and bird's tail similarly generate the lift at the narrow spread of tails and low angle of attack. However, this is not true for the high angle of attacks where the actual lift production does not match the theoretical prediction of the theory. Hence there are limits on which a bird's tail can be regarded as a delta-wing. From another perspective, there is a lack of evidence supporting yawing stability due to the tail. So Sachs [200] experimentally showed that in case of disturbance in a sideslip, tails create a yawing moment that brings stability. He also concluded that the horizontal structure of the tail contributes positively to the stability due to yaw and can be compared with the magnitude of the wing when it comes to strength. In the same direction, other researches can be explored [201–204]. However, another study by [205] over hummingbirds' tail stressed that their forked tail is due to the sexual selection. This contrasts with the general opinion on the tail evolution discussed above. On the other hand, the prediction that long-range migrant birds should have a short length of tail found no evidence. To better understand the effect of a tail, a long-eared bat model was tested by [206] in a wind tunnel showing that the absence of tail significantly decreases the pitching moment but does not affect the living generation. Also, the existence of tail increased the lift, drag, and pitching moment. From these data, the authors argued that tails are essential in improving agility and maneuverability. There are different narratives available for bird tail [207, 208] but those are not directly related to the scope of this paper.

The discussion reveals no consensus on whether the evolution of the tail is due to natural selection or sexual selection. Besides, the variation of tail length and its supposed effect as a control surface and maneuverability needs further work by considering the interference of tail-body combination. Similarly, the tail affects both drag and lift generation by manipulating oncoming vortices from the body and wing. This line also needs detailed experimental and numerical work while also taking account of flexibility and feather characteristics. Therefore the question of why the tail is horizontal rather than vertical is still open. How does this influence not only the yaw and pitch but also rolling moments need investigation? At last, the theoretical foundation of the tail and aerodynamics are not established.

Table 8. Summary of the Important progress in understanding Bird's tail

Mechanism	Investigation method	Significance	References
Birds Tail	Theory	horizontal control surface by providing stability	Smith [192]
Tails fucntions	Experiment	to produce large forces during slow flight and maneuvering. During the slow flight, the wing has to generate a high lift that shifts the center of aerodynamic pressure forward, which destabilizes the flow by changing the pitching moment	Tucker [193]
Vortex	Theoritical analysis	the variation in tail structure and its length is associated with the kind of vortex generation coming backward. Also drag associated with the elongated tail depends on the surface area	Thomas [194]
Tail length	Experiment	A graduated tail has the highest lift to drag (L/D) ratio and a tail must evolve with elongated length but less in width; otherwise, the penalty is a high drag	Balmford et al,. [196]
Tails evolution	Experiment	tail does reduce the L/D ratio of birds but helps to maintain stability, creating lift and turning the flight. They found that large birds with high L/D have a short length; on the contrary, birds that generally need maneuverability more than any other parameter are evolved with a long tail	Thomas and Balmford [197]
Delta wind and tail	Experiment	and bird's tail similarly generate the lift at the narrow spread of tails and low angle of attack	Evans et al. [195], Evans [196]
Stability	Experiment	in case of disturbance in a sideslip, tails create a yawing moment that brings stability	Sachs [200]
Agility and maneuverability	Experiment	absence of tail significantly decreases the pitching moment but does not affect the living generation. Also, the existence of tail increased the lift, drag, and pitching moment. From these data, Also, tails are essential in improving agility and maneuverability	Gardiner et al., [206]

Aerodynamics of bird feathers

The major portion of the lift and drag in a bird flight is contributed by the wings. It is the wing that creates the induced drag at the tip understood by the Helmholtz hypothesis [155]. However, the basic structure and morphology of birds are not empirical; they vary from insects to large soaring birds. Some birds fly at low Reynolds number, and some are at quite a high speed with high Reynolds number [209]. Birds flying over land have their specific differences to the birds flying above the sea. The morphology of bird feathers is vital to know the reason behind such unique configurations directly involved in the performance improvement during the flight [210]. A feather is made of a shaft and vanes while the vane becomes resistant to the aerodynamic forces due to inclination in the barbs. Due to differences between vanes and shaft, there exists a moment, but due to multiple feathers, it cancels out [211]. The morphology and working mechanism of feathers affect the mechanical behavior of the wings. Primary feathers, importantly at the tip play a high resistive role to forces than the inner ones [212]. Tip feathers of a bird's wing reduce the drag by allowing air to pass through and use tip reversal upstroke [213]. Due to considerable low wing size and speed, the Reynolds number remains around 10^5. In large birds, the Reynolds number can go up to the transition zone, reducing drag and increasing the lift coefficient. Most of the large soaring birds have a Reynolds number ranging from 75000 to 10^6, and the critical Reynolds number for smooth bird-like airfoil is around 75000, [214]. The aerodynamic performances much depend on the morphology of the bird feather. Their size, shape affects the overall lift and drag coefficient [215].

Significant acceleration has been seen during the second wingbeat of take-off, and feathers are the significant contribution for acceleration compared to other parts of the bird body [216]. During the cruise, the primary feather tip becomes vertically curved with slots between each of them. This shape increases the span of a feather. In the planar wing, where shape remains the same from root to tip, does not contribute to reduce the vorticity as a non-planar surface does in the case of bird feather [217]. A more detailed view of the slotted wingtips has been given by [218] in which he considered Harris hawk in flight and developed the configuration. The length of the half wing from root to tip is 1.06m, and from the

head-on side, it is 0.92 m. Following this shape, which disburses the vorticity vertically, the bird feather directly reduces the induced drag. Induced drag is the significant portion of the drag during landing and take-off. Vertically slotted feather tip increases the span, area, and modifies the size of the feather. All these factors directly or indirectly influence the induced drag. Generally, an increase in wing efficiency is achieved by splitting the feathers vertically at the tip, but the best performance can be attained by spreading the feather over a large dihedral angle [219].

Henderson and Holmes [220] stated that to reduce the induced drag, the main criteria are increased in aspect ratio, elliptical loading, and low coefficient of lift, which is supported by the classical theory of aerodynamics. Nevertheless, these criteria have limitations due to design implementations. The weight constraint counters increment in aspect ratio. So, the choices have to be made if only the planar wing is considered. To get relief from this situation [221] argued for a non-planar wing that can reduce the induced drag and stated that the induced drag could not be less than the:

$$C_{D_{imin}} = \frac{L^2}{\frac{1\rho V^2 \pi b}{2}} \tag{1}$$

Later on [209] showed that the plane planar tandem wings could not decrease the drag and echoed the line of reasoning of Munk. Following this [222] gave the analytical solution of non-planar wings as well. Similarly, it was then argued that following the lifting line theory, advanced methods can be developed to reduce induced drag, and the major shift was the development of non-planar surfaces that disburse the drag in a vertical direction like wingtip shapes [223]–[225]. Following this approach, arguments and methods have been developed to retrieve energy from the wingtips, the non-planar wing [226]–[230].

The important takeaway of the above discussion is that bird wings are naturally non-planar due to their unique configuration during flight. They can reduce both the induced drag and profile drag of the surface because the surface of feathers is unique for aerodynamics.

Tucker and Parrott [231] experimented over a flacon that glided in the wind tunnel and reported that at 12.5 m/s speed bird showed the maximum lift to drag ratio. With an increase in speed, the bird decreases its lift coefficient, wing area, and span. Withers [215] investigated the aerodynamic characteristics of the bird's wing in detail at Reynolds number 1-5 × 10^4 and reported the contrasts with insects and real airplane wings. He found that due to low Reynolds number operation, bird wing shows a large minimum drag coefficient between .03-0.13, with a low maximum lift coefficient of 0.8-1.2 and low lift to drag ratio (L/D) between 3-17. Compared to conventional airfoils, the bird has low efficiency due to high profile drag. However, the author makes it clear that the flow structure over the bird wing satisfies the aerodynamic theory. Figure 19 shows the lift and drag coefficient for different bird wings:

Species	$C_{D,\,pro}$	$C_{L,\,max}$	$(C_L/C_D)_{max}$	$dC_L/d\alpha$	$1/\pi$ ARe	Reference
Swift	0·030 (+1°)	0·80 (+8°)	17 (+5°)	0·1	0·02	Present study
Petrel	0·070 (0°)	0·88 (+13°)	4·0 (+8°)	0·08	0·32	
Woodcock	0·082 (+2°)	0·90 (+15°)	3·5 (+8°)	0·05	0·33	
Wood duck	0·096 (+1°)	0·90 (+20°)	3·8 (+8°)	0·06	0·16	
Quail	0·055 (+3°)	1·10 (+25°)	6·0 (+8°)	0·05	0·21	
Starling	0·125 (0°)	1·00 (+15°)	3·3 (+7°)	0·06	0·23	
Nighthawk	0·051 (+3°)	1·15 (+15°)	9·0 (+6°)	0·08	0·08	
Hawk	0·074 (+2°)	1·0 (+25°)	3·8 (+6°)	0·06	0·27	
Vulture primary	0·024 (0°)	1·15 (+12°)	17 (+5°)	0·08	0·07	
Thrush	0·05	0·8	—	0·03	0·36	Nachtigall & Kempf (1971)
Sparrow	0·16	1·0–1·1	—	0·05	0·28	
Duck	0·11	0·9	—	0·06	0·34	
Snipe	0·11	1·0	3	0·06	0·33	Reddig (1978)
Pigeon models	0·06–0·13	0·8–1·2	2–8	0·12–0·27	0·1–0·7	Nachtigall (1979)

Figure 19. Lift and drag coefficient of different bird wing reported by [215]

Two, different birds [214] studied the bird's wing aerodynamics by a gliding bird in a wind tunnel. Both Falcon and Vulture glide freely by reducing the wingspan. This change in wingspan increases the induced drag, but due to an airfoil section, the bird's wing has; it has a minimum value of profile drag coefficient near one while a conventional wing has a value of 0. The same method [180] experimented with a Harris hawk in a speed range between 1.1 to 16.2 m/s gliding freely in a wind tunnel. This time the maximum lift to drag ratio was 10.9. He stated that the relation between airspeed, glide angle ad wingspan is evident given that when speed or glide angle goes up, the bird's wingspan reduces. Similar studies have been done to establish the wing span and its relation with drag and lift [232, 233]. The detrimental effects of an asymmetric wing have three significant effects stated by [234] that the total span will be changed, which influences drag & lift, it will create an imbalanced yawing and rolling moment, and lastly, due to this, the turning performance will be vitiated. The same thing has also been reported by [196]. An article published in nature by [235] highlighted the problem of extra lift in insect flight. It means, according to acronymic theory insects cannot fly because they produce more lift in flapping than in steady flight, but the reason for that high lift was not unknown. Through flow visualization,

they found that it is due to a leading-edge vortex formed on the top of a wing. This vortex is generated due to dynamics stall and does not depend on the rotational lift. However, later on, it was found that this unconventional lift generation device is not restricted to insect flight, but swifts also show such a leading-edge vortex. In normal conditions, this leading-edge vortex begins at the large angle of attacks. To use this vortex, it must be nearby the wing itself. To achieve this goal, insects beat the wings, and swifts sweep their wings backward. Another turnaround on the bird's wings comes from the active control of the wings shape and span by the birds. This natural morphology brings aerodynamic effects [236]. Based on the same idea, [237] experimented on a swift in gliding flight and controls the wingspan along with sweep angle during glide. They found that extended wings work well during turns and slow gliding; on the contrary, swept-wing is beneficial in fast gliding and turning. Where swept wings are not good in creating lift but can resist large loads. The authors' attached such advantages to the aerodynamic consequences.

Bird is controlling the force coefficients through alteration of wing shapes, speed, and angle of attack. Additionally, [238] showed that the primary feathers of swift are remarkably rough due to the overlapping of vanes and extended shafts and formed roughness height of 1-2% of the chord length at the upper surface. This roughness height is considerable compared to the sailplane surface as large as 10,000 times. The fundamental difference between conventional sailplane and the swift surface is that the sailplanes try to minimize the drag and increase the laminar boundary layer area from the smooth surface; in contrast, the swift utilizes roughness to do that. They measured the laminar flow over a swift wing in a low-turbulence wind tunnel. They showed that the laminar area over the swift wing is around 69% of the total during gliding motion, which increases their distance of flight and duration. Due to the long run of the flow without separation, it can reduce the drag. This revelation resonates with the drag reduction mechanism used by shark and whales through non-smooth surfaces discussed in the section of swimmers [122, 142]. Is the question do all birds have such characteristics? If yes, why have they not been implemented into applications? Besides, how is this sweeping phenomenon different than conventional swept wings? Recently [239] have explored this question by comparing the sweep of the swift with straight and traditional swept wings experimentally. The forces were taken between angles of 0° to 24°, and the data shows that innovative sweep greater than zero produces high lift and increases the stall until 24°. The aerodynamic performance at low Reynolds number and increase in lift is the departure point from a conventional wing. The importance of sweep is not only related to lifting, drag, and stall parameters but [240] investigated its role to affect yawing moment. Compared to the conventional wing, the wings of birds have sideslip due to sweep leading to a substantial increase in the yawing moment. They used gullwing in an experiment that shows significant stability improvement with an increase in the lift coefficient. On the contrary, much less yawing moment was recorded for the unswept condition. The inspiration has already been highlighted previously, and the mathematical yawing moment derivative was calculated with experimental and numerical methods, see, for example, [241–243].

One more important feature of the bird's wings that attracted researchers recently is a secondary feather. It was highlighted by [244] that secondary feathers of the bird pop up during landing. He argued that due to flow separation, the reverse flow occurs, and to respond to this reverse flow, these secondary feathers pop up. Figure 20 shows the wing and secondary feathers.

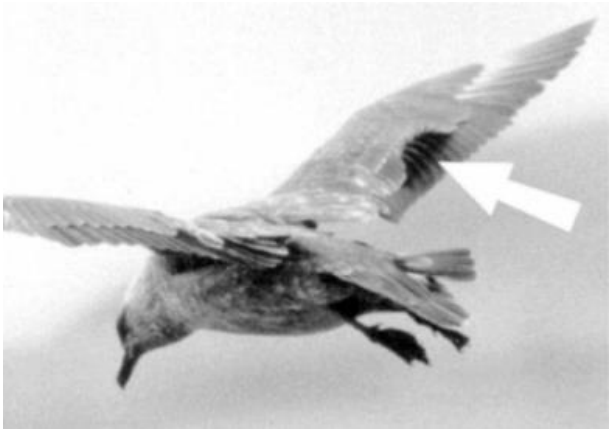

Figure 20. Birdwing showing the pop up secondary feather at the suction side [245]

Taking inspiration from this feather [136] developed a flap that was implemented on a two-dimensional airfoil HQ17 and HQ41 and resulted in a 10% lift enhancement from the one without flap. The size of flaps was the key point explored, and a 22% flap length even increased the lift by 18%. The physics behind self-activation due to flow separation is the key to such a unique configuration that makes it a passive device, saving extra energy used inactive devices. The author also tested the new concept over practical airplane applications such as a glider plane and received the same enhancement. It shows that at the time of flow separation, the flap popped up automatically and resulted in a 7% increase in the lift. To explore the various transformations related to flaps like size, chord length, configuration, the Reynolds number variation, and material used to conduct an experimental study at Reynolds number of 1000000 [246]. It was found that the best width ranged between 10%-40% of chord length and below the 10% width is ineffective due to sudden stall, and more than 40% does not work correctly due to pressure drop. Also, the flap should be located at the mid-chord, and this

increased the maximum lift by 15%. Later on, [247] applied this same concept of lift enhancement to low Reynolds number between 30,000 to 40,000, considering its use in micro air vehicle applications. Variations of the flap were tested in a water tunnel on airfoils. They reported that the most popular airfoil for MAV SD8020, when adorned with a flap length of 0.2c at x/c=0.6, increased the lift by 50%. It can tremendously improve payload and flight performance. Similarly, one more experimental study was done at a Reynolds number 85000 by [245] who manufactured a new airfoil and attached flaps. Study in the same fashion as previous studies highlighted to improve the lift by 6.4%, reducing the drag by 13.2%, and a reduction of 8.3% was achieved in pitching moment. All these recent studies have almost established the promising capability of secondary feathers to improve aerodynamic performance.

Mazellier et al. [53] used the porous flaps inspired by the birds. The porosity in the birds' wings has special functions. Though the idea to use porosity for aerodynamic means was not new because during the 1960's it has already been proposed and formulated by [248–250]. However, one of the first known experiments on owl feathers porosity was done by [251], who glided owl in an aeroacoustics laboratory to record data on noise reduction and attributed this noise reduction to the flexibility of the wings. Muler and G. Patone [211] measured the air transmissivity of owl's wing due to porosity from ventral to dorsal and reverse and found the mean difference between these two opposite directions was only 10%. However, they reported the significant differences in air transmissivity between inner and outer vanes of remiges and coverts. The outer vanes show more transmissivity, and its significance forms a smooth and continuous smooth surface. This difference in porosity agitates feathers on each other that create pressure gradients. If these differences over the bird's wing contrast with the conventional wing surface, which is smooth and without permeability than what would happen to the aerodynamic parameters like lift, drag, and moment coefficients along with the aerodynamic center location? [252] attempted to solve this problem by manufacturing a wing with forwarding the impermeable forward part and permeable aft part. The results show that the lift slope coefficient is reduced while increasing permeability, and the value shifts to the width of the forwarding membrane part. Similarly, the aerodynamic center moves to the quarter chord of the forward membrane. He concluded that the permeable wing is not practical for high-speed flow. Also, the seepage drag due to seepage velocity can be contained by maintaining the aft part width to less than half of the chord length [253]. Adding to this porosity problem [254] built a passive actuation system enshrouding the airfoil's suction side with a coating inspired by the bird feather. The coating has three features, porosity, anisotropy, and compliance, but care was taken that while not working must not harm the flow. It modified the length scale of the vortices leading to significant drag reduction, and it also changes the near airfoil flow topology by adopting flow separation. Thus, one wonders if porosity works similarly in all birds. It is known for a long time that the feathers of owls evolved in such a way actually todump the noise created out of flow variations. Bachmann and Winzen [255] stated that owls have large wings compared to the mass of their bodies and special profile of the wing which provides sizable lift at low speeds. The wings are embellished with velvety textures at surface able to dilute the friction noise and by regulating boundary layer delay the separation of flow. Uniquely, they reduce the turbulent eddies through serrations at leading edge and fringes at the trailing. Also, plumage being dense and porous works as an acoustic absorber damping noise at the point of creation. However, a physical mechanism is yet to be known. A similar study has been done by [256]. Another study only focusing on the aerodynamic influence of the velvet was already done by [257, 258] showing the redistribution of turbulent kinetic energy at higher Reynolds numbers $40{,}000 \leq Re_c \leq 120{,}000$ number that enforces pre-attachment of the flow. The separation bubble at the suction side gets reduced due stabilization of the flow due to the velvet surfaces. Wagner et al,. [259] reviewed the recent developments related to owl's wing and its various dimensions that can be referred for further information. However, existing studies focus only on a particular dimension of the bird feather but recently [19] enriched the airfoil similar to NACA0012 with leading edge waves, serration at the trailing edge and ridges at the surface as a concept of flow control. Through large eddy simulation it was found that compared to conventional NACA0012 airfoil, the biomimetic airfoil reduces the sound level and provides an overall sound pressure whereas no change in drag has been identified. It also changed the shedding vortices to horseshoe type vortices that reduce the noise around the biomimetic airfoil. Nevertheless one detrimental effect of porosity has also been reported by [260] by experimenting on a porous rectangular wing and a symmetric airfoil. They have used standard equation to calculate lift coefficient for porous wing also and found it suitable. However, the lift slop decreased with gain in porosity and at the low porosity decrease but after, grows with porosity. These bird feathers have different surface structure throughout the span with specific shapes. Effect of surface texture has been recently studied by [261] using different shape and sizes of feather surface on NACA4412 tapered wing at 4×10^5 Reynolds number at several locations. They found that surface roughness decreases the lift and stall. The minimum drags and maximum lift were located at 75% to 95% of mean chord distance from leading edge. Table 9 summarized the important progress.

Table 9. Summary of the Important progress in understanding Bird's feather

Mechanism	Investigation method	Significance	References
morphology	Experiment	A feather is made of a shaft and vanes while the vane becomes resistant to the aerodynamic forces due to inclination in the barbs. Due to differences between vanes and shaft, there exists a moment, but due to multiple feathers, it cancels out	Muler and Patone [211]

Table 10. Summary of the Important progress in understanding Bird's feather (cont.)

Mechanism	Investigation method	Significance	References
Air transmission	Experiment	Tip feathers of a bird's wing reduce the drag by allowing air to pass through and use tip reversal upstroke	Crandell and Tobalske [213]
Reynolds number	Experiment	Due to considerable low wing size and speed, the Reynolds number remains around 10^5. In large birds, the Reynolds number can go up to the transition zone, reducing drag and increasing the lift coefficient	Tucker [214]
wingbeat	Experiment	during the second wingbeat of take-off, and feathers are the significant contribution for acceleration compared to other parts of the bird body	Berg et al.,[216]
Induced drag	Theory	to reduce the induced drag, the main criteria are increased in aspect ratio, elliptical loading, and low coefficient of lift, which is supported by the classical theory of aerodynamics maneuverability more than any other parameter are evolved with a long tail	Henderson and Holmes [220]
Non-planar wing	Experiment	non-planar wing can reduce the induced drag. Also, plane planar tandem wings could not decrease the drag and echoed the line of reasoning of Munk which is followed by analytical solution of non-planar wings as well	Newman [209], Munk [221],Cone et al., [222]
L/D ratio	Experiment	at 12.5 m/s speed bird showed the maximum lift to drag ratio. With an increase in speed, the bird decreases its lift coefficient, wing area, and span	Tucker and Parrott [231]
Low Reynolds number	Experiment	due to low Reynolds number operation, bird wing shows a large minimum drag coefficient between .03-0.13, with a low maximum lift coefficient of 0.8-1.2 and low lift to drag ratio (L/D) between 3-17	Withers [215]
Wingspan	Experiment	relation between airspeed, glide angle ad wingspan is evident given that when speed or glide angle goes up, the bird's wingspan reduces. Similar studies have been done to establish the wing span and its relation with drag and lift	Tucker and Heine, [180], Pennycuick [232],Tucker [233]
Asymmetric wing	Experiment	three significant effects stated by [234] that the total span will be changed, which influences drag & lift, it will create an imbalanced yawing and rolling moment, and lastly, due to this, the turning performance will be vitiated	Balmford et al., [234]
Roughness height	Experiment	primary feathers of swift are remarkably rough due to the overlapping of vanes and extended shafts and formed roughness height of 1-2% of the chord length at the upper surface. This roughness height is considerable compared to the sailplane surface as large as 10,000 times.	Lentink and Kat [237]
Sweep in wing	Experiment	The importance of sweep is not only related to lifting, drag, and stall parameters but [240] investigated its role to affect yawing moment. Compared to the conventional wing, the wings of birds have sideslip due to sweep leading to a substantial increase in the yawing moment	Voloojerdi and Mani [239], Sach [240]

Table 11. Summary of the Important progress in understanding Bird's feather (cont.)

Mechanism	Investigation method	Significance	References
Secondary feather	Experiment	due to flow separation, the reverse flow occurs, and to respond to this reverse flow, these secondary feathers pop up	Liebe [244]
Secondary feather inspired flap	Experiment	10% lift enhancement from the one without flap. The size of flaps was the key point explored, and a 22% flap length even increased the lift by 18%	Bechert et al., [139]
porous flaps	Experiment	glided owl in an aeroacoustics laboratory to record data on noise reduction and attributed this noise reduction to the flexibility of the wings	Gruschka et al., [251]
velvet		redistribution of turbulent kinetic energy at higher Reynolds numbers $40{,}000 \leq Re_c \leq 120{,}000$ number that enforces pre-attachment of the flow	Winzen et al., [257]

Aerodynamics of bird wingtips

Graham [210] suggested a possible relation between feather slot and drag reduction through imagined flow past the wingtips. Because feather wingtips are without muscle, the author believed the formation of slotted wingtips is due to the pressure of the air. The formation of wingtips is attributed to the primary feather of the bird. Due to the aerodynamic loads' tips rises above the trailing edge of the wing. The distinction is necessary between conventional winglets designs that were inspired by the 1970's oil crisis and motivated [262] to develop new non-planar slotted devices to reduce the induced drag [222]. Those conventional wingtip designs are not treated here, but detailed discussion can be found in [50]. Here the discussion will be focused on bird wingtips only.

This special winglet like configuration in bird feathers was investigated by [263] to understand the aerodynamics. He used three different wingtip designs: the first was made of the primary feather of a Harris hawk, the second was made of balsa wood similar to the Clark Y airfoil without slot, and the third was made of balsa wood with the slot. These wingtips were set up on a base wing. There was a 12% drag reduction with a feathered tip compared to a hypothetical wing with the same span and lift. The vital point of flow visualization shows is the dispersion of vorticity in both horizontal and vertical directions with wingtips. Also, the lift to drag ratio (L/D) was higher for a feathered tip. The author argues for a strong connection between bird feather tip and reduction of drag. Later on, the same author [217] glided a Harris hawk in a wind tunnel at one time by clipping the slots and then with slotted wingtips. He found that slotted wingtips showed a 70-90% drag of the un-slotted wingtips. He calculated for a wingspan of 0.8m; slotted wing tips showed induced drag factor 0.56 and un-slotted 1.10, which is a large difference. Not all the birds have a similar configuration of the wingtips; rather, they differ significantly, as shown in Figure 21.

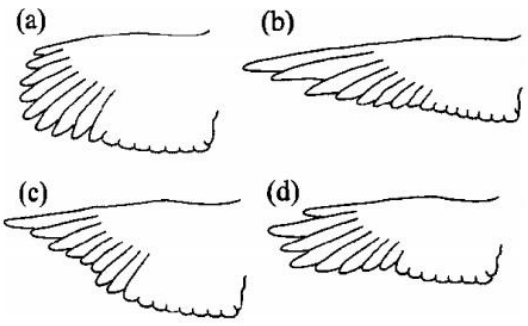

Figure 21. Wing shapes (a) Rounded (b) Pointed (c) Concave (d) Convex [46]

Aerodynamically pointed tips should disburse the vortex smoothly in contrast to the rounded tip that discharges a large volume of a vortex and increases the induced drag. However, the round wing seemed to work efficiently with a round tip in reducing induced drag and functionally better than an elliptical wing. It might be due to special vertical and horizontal primary feather tips [46]. This wingtip shape affects the flight performance shown by [264] in an interspecies study over European Startling's. The rounded tip seemed useful, providing steeper take-off but the reason behind this shape and takeoff is not clear. These slotted feather tips are not separated vertically rather have sweep inside. What is the effect of this sweep on the aerodynamics has been done by [265]. Through numerical simulation, they found that the sweep provides a significant increment in yaw moment with lift coefficient. The comparison was made with tips without sweep that showed less yawing moment. There was also a second reason for yawing stability due to sweep at the wingtip.

It is due to the drag force during the positive yaw angle. During positive yaw, the drag force at the right-wing is higher than the left wingtip, and this difference in drag force settles the yaw stability.

By taking the inspiration from birds, new wingtips were designed to see the effect which differs from the conventional winglet designs. [266] designed a spiroid wingtip mimicking bird feather shown in Figure 22, especially to report lift and drag parameters. It was found that the lift-induced drag reduced by 75% at the coefficient of lift (C_L) of 0.95, the lift slope increases by 9%. Total drag reduction was highest at the coefficient of lift (C_L) 0.95, which is 50%, and during no-stall trade-off, the lift to drag ratio was maximum at 7.1%.

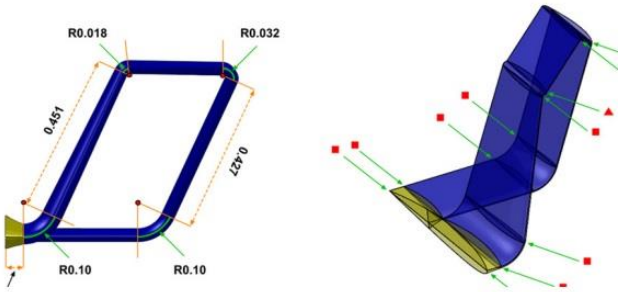

Figure 22. Feather inspired spiroid wingtips [267]

The flows around slotted feather tips were spotted through particle image velocimetry in a wind tunnel of bird jackdaw. Flow visualization reveals that each primary feather generated individual vortex that re-stressed the multi-slotted functioning of the tips. These multi-vortices expanded, improving aerodynamic efficiency. This happened in both gliding and flapping. Nevertheless, what effect does the gap between wingtips has on the aerodynamics parameters? [268] studied this point. By varying the wingtip gap sizes between 0%-40% of the mean chord of the wing, both planar and non-planar were experimentally tested at a Reynolds number of 100,000. In the planar wing that has a 20% wingtip gap, it showed an increase in mean lift coefficient of 7.25%. On the contrary, it was 5.6% for without gap tips. The important point was the independence of wingtip gap effects from planar and non-planar wingtip devices. This conclusion may be true when the emargination length and curved configuration of the feather tip are not considered. Siddiqui et al,. [269] mimicked the feather tip by comparing the curved and flat condition of the tips considering the flexibility and rigidity of the feather at a Reynolds number of 3.7 x 10^5. The experiment shows a 20% increase in the L/D ratio compared to the base wing. This improvement has been compared with forty other variations of wingtips and was found to be the maximum. Though they have not changed the size of the gap, the planar and non-planar wing does make a huge difference when it comes to bird flight.

Apart from the separation in the primary feather,[270] highlighted one more zone within the tips. As shown in Figure 23, the inner vane has a barb from which small barbules protrude outside.

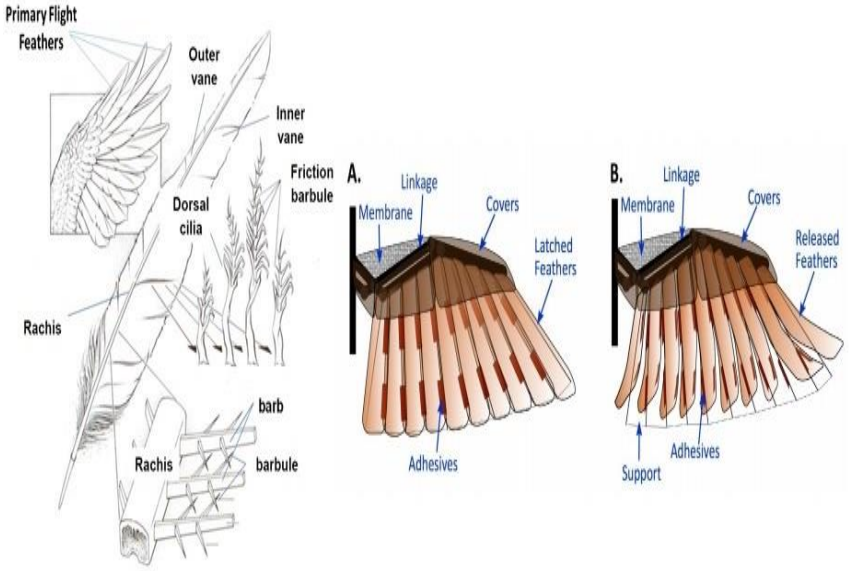

Figure 23. Single feather with membranes. A. shows the lathed condition of barbules, and B. shows the high speed or gust condition [270]

In normal conditions, these barbules remain in close contact, but during high speed or gust, they separate and delay the stall. The authors have mimicked this feature on airfoil through the experiment at a 18º angle of attack. It was found

that unlatching reduces the lift generated, which is useful in gusty conditions. Between the latched and unlatched cases, the maximum difference in lift and drag was 17% and 32%. This configuration provides avenues for further research, and it seems from open literature; the area is available for further exploration.

It is clear from the critical literature discussed that wingtip's unique attributes and their variation with flight conditions had been referred to natural selection. However, the effect of wingtips and bird capabilities influenced the aerospace sector, but bluff body aerodynamics is still a large area to be considered for its implementation. Only a few studies have been done in this direction, but there are parts of the bird body that does deal with the flow separation similar to the bluff body like secondary feathers [7]. What affects the texture of bird feather could have on the bluff body or how the characteristics of wingtips and its variation can be implemented to the bluff body still needs to be analyzed. The possibility and physics of tails that have evolved with kinds of variation can give promising techniques for various Reynolds number conditions. In addition to these separate promising extremities, large birds show a great deal of synchronization during flight. That bird flies in a unique V shape known for a long time [155]. In a study reported in Nature by [271] brought out some important insights as the aerodynamic reasons behind such V shape flight was elusive. He argues that the V shape agrees with predictions of theoretical aerodynamics. During V flight, the flapping phase provides side following the bird to harness the upwash coming towards it. This energy capture is not possible when the bird follows just behind because they lack the wingtip coherence path, and flapping becomes anti-phase. However, one wonders how such a sophisticated mechanism is adopted? And for the author, it cannot be until an awareness of the spatial vortex structure of nearby birds exists either by precise sensing ability or by predicting it. This brings investigations to the psychological richness of the birds that is still a question to answer. Others suggested that during V flight, birds use 20% to 30% less energy. What are the possibilities of such a unique shape to influence the aerodynamics of bluff bodies? Is it possible to change the laminar flow to turbulent by disturbing the flow with the V shape? Like this, there are other special patterns in nature that can influence aerodynamically.

In this section, the important appendages of the bird have been discussed and it was found that the flow around the tail and its evolution is yet to be understood. Moreover, the features of feather and tips have been investigated from different perspective and its applications are made in the aerospace sector. However, there is still a considerable scope of study on the bird's feather, tips, and its application on the bluff bodies. Table 10 Summarizes the important progress.

Table 12. Summary of the important progress in understanding Bird's tip

Mechanism	Investigation method	Significance	References
Feather tip	Theory	a possible relation between feather slot and drag reduction through imagined flow past the wingtips. Because feather wingtips are without muscle, the author believed the formation of slotted wingtips is due to the pressure of the air	Graham [210]
Tip's aerodynamics	Experiment	There was a 12% drag reduction with a feathered tip compared to a hypothetical wing with the same span and lift. The vital point of flow visualization shows is the dispersion of vorticity in both horizontal and vertical directions with wingtips. Also, the lift to drag ratio (L/D) was higher for a feathered tip	Tucker [263]
Neccesity of wingtip	Experiment	slotted wingtips showed a 70-90% drag of the un-slotted wingtips. He calculated for a wingspan of 0.8m; slotted wing tips showed induced drag factor 0.56 and un-slotted 1.10, which is a large difference	Tucker [217]
Tip shape	Experiment	pointed tips should disburse the vortex smoothly in contrast to the rounded tip that discharges a large volume of a vortex and increases the induced drag. However, the round wing seemed to work efficiently with a round tip in reducing induced drag and functionally better than an elliptical wing	Lockwood et al., [46]
Wingtip inspired spiroid wingtip	CFD simulation	lift-induced drag reduced by 75% at the coefficient of lift (C_L) of 0.95, the lift slope increases by 9%. Total drag reduction was highest at the coefficient of lift (C_L) 0.95, which is 50%, and during no-stall trade-off, the lift to drag ratio was maximum at 7.1%.	Guerrero et al., [267]

Applications to bluff body aerodynamics

There are great works on the bio-inspired technique used in the aerospace, which has been well documented, and the process is still ongoing. However, few studies have been done on the application of bird-inspired techniques to the bluff body aerodynamics. Inspiration from the bird's secondary feather led [53] to investigate the effect of self-activated feathers on the bluff body using a squared cylinder. In addition to adapting the only flap, they also considered the porosity existing in feathers in their flap. The flap was installed at the side of the cylinder and tested at both controlled and uncontrolled flow with different Reynolds numbers. Experimental data reveals an average of 22% reduction in the drag. The reason behind such a huge decline is attributed to the flow modification in the vicinity of the flap and wall of the cylinder. The motion of the flaps has a strong relationship with the vortex shedding and is influenced by the Reynolds number. That much drag reduction is hardly achieved by other devices. Recently the same feather inspired flap was installed at the back of a generic vehicle model called Ahmed body by [52]; they got this new device automatic moving deflector (AMD). Different sizes and materials were used for AMD at Reynold numbers of $1.0 \times 10^5 - 3.8 \times 10^5$. Flow visualization shows that there is a drag reduction of 19% due to pressure recovery at the slant by delaying the flow separation and through suppression of the vortices coming out from the edges. Figure 26 shows the model with flaps.

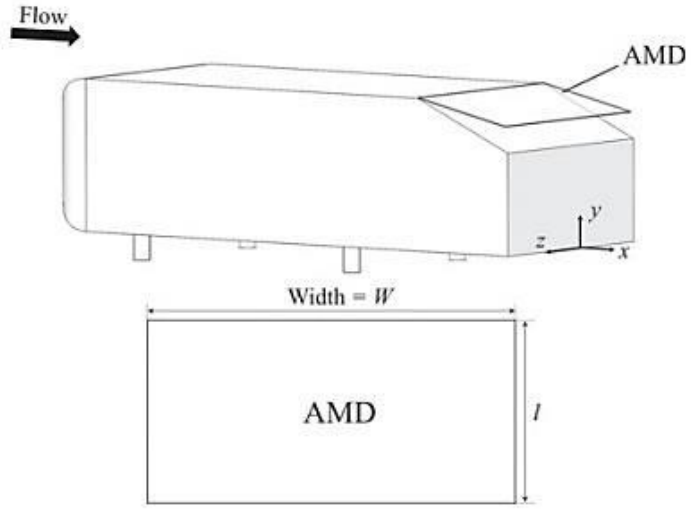

Figure 24. A generic vehicle models with automatic movable deflectors [52]

From the same secondary feather of bird wing [272] found another device from the riblets, the length of which decreases from the shaft towards the fringe. They have manufactured herringbone riblets having smooth edges and, through experiment, found a drag reduction of 16%. This feather inspired microstructure drag reduction device is superior to the other microgroove surfaces used traditionally. Drag reduction was due to the change in shear stress distribution to nearby riblets tips compared to another microstructure. Additionally, compared to other surfaces, the depth of the viscous sublayer transformed into a thicker layer, and these changes in the boundary led to drag reduction.

More recently, the bullet train in Japan was investigated to reduce the noise problem. The noise was created due to three distinct reasons not related. The first was due to vibration between the train structure and ground at high speed. The second was the aerodynamic noise due to the blunt-body of front and pantographs that joined the train to catenary wires, and third was a sonic boom that came into existence when the train moves into the tunnels. The second aerodynamic noise was the formation of Karman vortex sheets, which are the alternate and opposite eddies traveling in the back of the object. To solve this issue, the serration of owl feathers was investigated and found to work like a vortex generator. After modification, they have used a V-shaped triangular cross-section arrayed at both sides of the turbulence line to suppress the Karman vortex and to tune the airflow in a parallel manner. The third problem of the tunnel was more serious. When the train enters the tunnel, atmospheric waves pass through the tunnel end at sonic speed, generating a sonic boom. To solve this problem, the shape of a kingfisher was investigated. Through a large scale model and computational study, it was found that the working principle of kingfisher and train was the same as they both change the pressure environment from less dense to denser. The bill shape has especial morphology of consistent circular cross-section when implemented, provided 30% less air resistance and reduced power consumption by 13%. The final shape of the bullet train is shown in Figure 25 [273–275]. Table 2 summarize the bird inspired devices for the bluff body. Table 11 Summarizes the important progress.

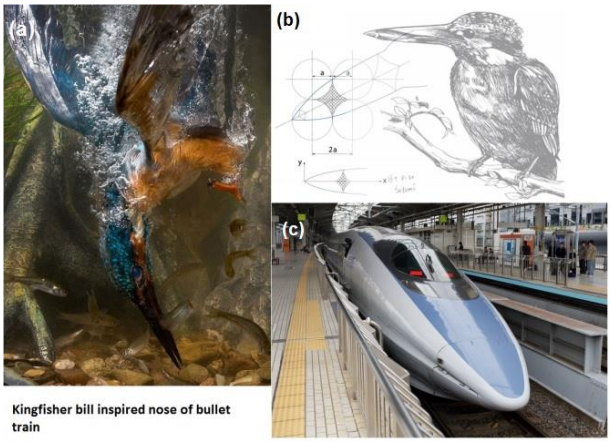

Figure 25. Kingfisher bill inspired circular cross-section of the bullet train that increased the speed by 10% [273], [274]. (a) Kingfisher inside the water, (b) the bill shape, (c) Modified bullet train

Table 13. Summary of non-flapping bird inspired devices on the bluff body

Drag reduction through fishes				
Flow control Method inspiration	**Investigation method**	**Device**	**Significance**	**References**
Bird's secondary feather	Experiment	Passive flap device	22% drag reduction	Mazellier [53]
Bird's secondary feather	Experiment	Self-activated flap device	19% drag reduction	Kim et al., [52]
Riblets of the secondary feather	Experiment	herringbone riblets	16% drag reduction	Chen et al., [272]
serration of owl feathers and kingfisher bill	Experiment, CFD and Manufactured	V-shaped triangular cross-section on Japan's bullet train modification	Noise reduction 30% less air resistance and 13% less power consumption	McKeag [273]

Drag Behaviors of Land Animals

Effects of body shape on drag

Mammals that walk overland have distinct qualities different from one another. Some are excellent at running, so some have a considerable amount of strength and live longer [276]. It would not be an out of context question to know how a small tiger beetle can run as fast as 9 km/h (around 125 body length per second) [277] or a cheetah, which is small compared to any vehicle, can go up to 93 km/h [278]. However, not much work is available from aerodynamics perspectives, but the motivation to understand such kinds of questions existed for a long time. Hildebrand [276] has listed previous results on morphology and adaptions of cheetahs, but there was only one crucial work on the motion by [279]. Hence [276] was the first who comparatively studied the movement of a horse and a cheetah. The difference between them is that the horse is the most efficient animal ever evolved with such untiring and long adaptations in the long run. On the other hand, the cheetah is the fastest animal for short distances. What difference motivates such drastic change? The author found the variation between the galloping of both the animals, as shown in Figure 26.

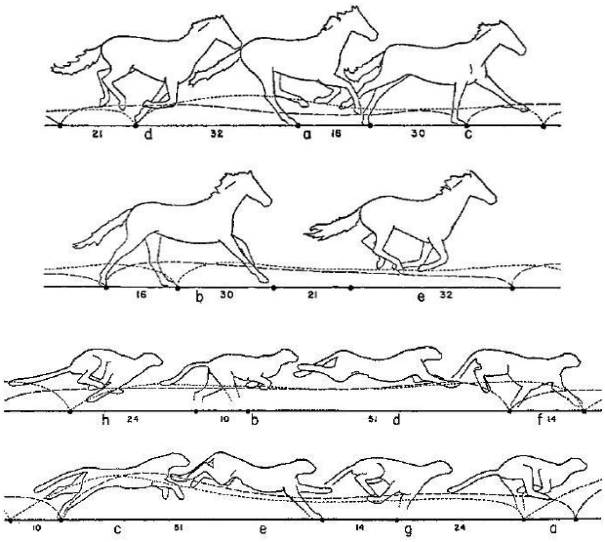

Figure 26. Galloping motion of a horse and Cheetah at different positions [276]

The galloping and movement of legs of the horse and cheetah differed, and the data has been corrected later on by the same author [280]. The author states that the speed of animals depends on its length and its stride duration; both are functions of body size. It means that if the form of the animal is the same with mass then body size does not matter; hence a red fox can match the horse, but due to differences in the mass, that is not possible. The reason lies in the directly proportional relationship between the length of strides and linear measure. Additionally, it can be concluded that if the mass of the cheetah and horse is the same, they can run the same speed. How is it possible for large and small body size to have the same mass? This is not the only version of Cheetah's power and speed relation. Hudson et al,. [281] argue that this power is generated from the back musculature, and pitching moment can be handled by powerful psoas muscle around the hip, providing the cheetah to cover long strides. Moreover, the effect of the tail has found attraction from an aerodynamics point of view. Patel [282] studied the motion of the cheetah tail by developing a mathematical model, feedback control, and a novel robotic platform due to the tail's supposed influence on the maneuverability. The roll axis motion helps to provide stability at high speeds. When the tail moves in the pitch axis, it stabilizes rapid acceleration in maneuvers. He also found that the tail motion is a combination of pitching and yawing that caters to continuous torque while tuning. A similar fashion [283] further developed this method to calculate the aerodynamic force on the cheetah tail. They produced robotic models of a tail in a rigid form by creating all three axis rolling, yawing, and pitching.

By applying Euler-Lagrange, a rigid tail model was developed and investigated. The wing tunnel testing shows that the fur on the tail doubles the frontal area without influencing the mass itself. The aerodynamic force was calculated to be:

$$F_a = \frac{1}{2}\rho C_d (V_T \cos(\alpha))^2 dr \tag{2}$$

Similarly, aerodynamic drafting of the horses has been discussed by [284], which is a way to reduce drag generated from the leading horse by following close to its leading one. They considered the horse as a bluff body and to calculate power to overcome drag, considered the C_d as 1.0 and the frontal area to be 1 m^2 with the formula:

$$P = \frac{1}{2} C_d \rho A V^3 \tag{3}$$

But the quantification of this slipstreaming was later on reported by [285], who found a drastic change in drag. A 66% drag reduction was recorded when two horses raced in front and 54% for four horses. Nevertheless, for both animals, there was no discussion about the aerodynamics around the body, which shows the similarity between almost all the fast running land animals.

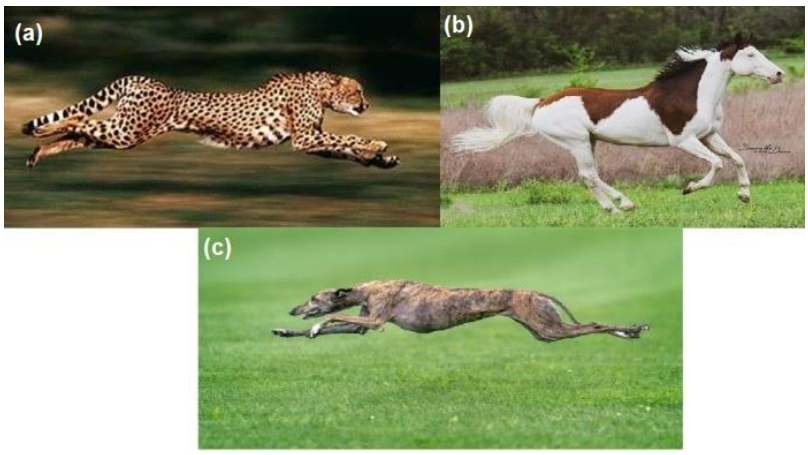

Figure 27. (a) Cheetah, (b) Horse, (c) Greyhound dog [286]

Figure 27 shows the cheetah, horse, and greyhound during fast running. The similarity between these three animals lies in their body form that is concave in the middle portion of the bottom side up to a certain distance starting from the front legs. Similarly, the upper surface of the curvature portion is also convex but not in all the areas but rather to some specific lengths. However, the radius of curvature differed, with the bottom curvature shows a higher radius than the upper portion. The position of the tail, head, and legs also offers important forms similar in all. This characteristic can be seen in almost all the ground mammals that walk and run. The obvious question is to investigate these unique body shape because if Gray's paradox [67] between available power and drag is real for dolphin, then it must be applied to these fast running bluff body animals also why natural selection evolved this only convex curvature, which contrasts the bodies of swimmers and flyers with a combination of convex and concave shapes. If biologists and aerodynamicists argue that it is due to optimizing the drag force reduction, the same applies to these convex shapes as well. But how these shapes reduce the drag and what is the significance of it, can be explored in the future. Also, why this issue of convex and concave according to the environment?

The fast-running land animals are discussed briefly while considering their shape as an aerodynamics opportunity. Gray's paradox revealed that muscle power could not alone alienate the drag. Hence, it implies that the especial shape might be a cause and; however, that needs to be investigated in length.

Applications to bluff body aerodynamics

Taking inspiration from the Dung beetle and shell [167] have incorporated the non-smooth surface over the engine cover lid and body cap. The non-smooth surface was with pits and grooves of different sizes. Through CFD simulation, it was found that at the vehicle sped of 30 m/s the drag reduction was 10.31%. Peng et al., [287] has done an aerodynamic study on tiger beetle. They have mimicked the beetle body in solid works and simulated for aerodynamic parameters. To a surprise, there was no vortex generation behind the beetle body; hence the curved portion reduced the flow separation. Taking this inspiration, a MIRA fastback model was modified according to the beetle body. The curved portion at the beetle's abdomen and cercus were mimicked to the rear window, trunk lid and chasis of the MIRA model
as shown in Figure 28. A simulation provided a 3.4% drag reduction compared to the base model. was reported. Experimental study can highlight more about this bionic inspiration. Table 3 summarizes the application to bluff bodies. Table 12 Summarizes the important progress.

Table 14. Summary of land animals inspired devices on the bluff body

Flow control Method	Investigation method	Device	Drag reduction	References
Active device	CFD simulation	Movable underbody diffuser	4%	Kang et al.,[288]
	Experiment	Steady blowing	1%	Heinemann et al., [289]
	Experiment		6 to 10.4%	Mestiri et al.,[290]
	CFD simulation		20%	Rouméas et al., [291]
	CFD simulation		6.4%	Wassen & Thiele [292]
	Experiment		5.7%	Krentel et al.,[293]
	CFD Simulation		11.1%	Wassen et al.,[294]

Table 15. Summary of land animals inspired devices on the bluff body (cont.)

Flow control Method	Investigation method	Device	Drag reduction	References
Active device	Experiment	Steady blowing	9-14%	Aubrun et al.,[295]
	Experiment and CFD simulation		2.6%	McNally et al.,[296]
	Experiment	Synthetic Jets	4.29%	Park et al.,[297]
			8.5%	Kourta & Leclerc,[298]
			10%	Tounsi et al.,[299]
	Experiment	Pulsed Jet	6 to 8%	Joseph et al., [300]
			20%	Gilliéron et al.,[301]
			20%	Gillieron & A. Kourta, [302]
	Experiment	Steady suction	17%	Kourta & Gilliéron, [303]
			6%	Lehugeur et al., [304]
			9.5%	Wassen & Thiele [305]
			10%	Whiteman & Zhuang, [306]
	Experiment	Plasma Actuator	8%	Boucinha et al. [307]
			3.65%	Shadmani et al., [308]
			20%	Khalighi et al., [309]
Passive Flow Control	Experiment	Vortex Generator	12%	Aider et al., [310]
	CFD Simulation		2.2%	Kim & Chen, [311]
	Experiment		10%	Pujals et al., [312]
	CFD Simulation		10%	Filip et al., [313]
	CFD Simulation		11.7%	Krajnović [314]
	CFD Simulation		10%	Mazyan [315]
	Experiment and simulation		4.53%	Shankar & Devaradjane, [316]
	CFD Simulation	Spoiler	5%	Kim et al., [317]
	Experiment	Flaps	17.6%	Beaudoin & Aider, [318]
	Experiment		19%	Kim et al., [52]
	Experiment		21.2%	Tian et al.,[319]
	CFD simulation	Body modification	10%	Marklund et al.,[320]
	CFD simulation		8.4 %	Cho et al.,[321]
	CFD simulation		5.639%	Song et al., [322]
	Experiment and CFD simulation		13.23%	Hu et al., [323]
	CFD simulation		5.20%	Wang et al.,[18]
Combined Active and Passive	CFD simulation	Blowing jets with a porous layer	30%	Bruneau et al., [324]

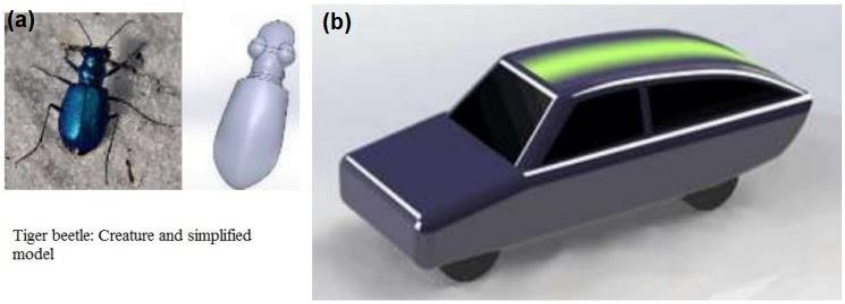

Figure 28. Tiger beetle and inspired MIRA fastback car design [287] (a) Tiger beetle, (b) Inspired car model

Table 163. Summary of land animals inspired devices on the bluff body

Drag reduction through fishes				
Flow control Method inspiration	**Investigation method**	**Device**	**Significance**	**References**
Dung beetle and shell	CFD simulation	non-smooth surface	10.31 % drag reduction	Song et al., [167]
tiger beetle	CFD simulation	Body modification of MIRA fastback model	3.4% drag reduction	Peng et al., [287]

Potential Future Research Areas in Bluff Body Aerodynamics

After reviewing the bio-inspired aerodynamic opportunities within three distinct species, it is clear that they manipulate the flow by both active and passive mechanisms. However, their aerodynamic control is far more enriching than any human technology. The active mechanism is just started to be explored and has a long way to go with promising opportunities to develop sustainable solutions. However, about the structure of this article to focus on the bluff body, passive devices provide more drag reduction capabilities than active once shown in Table 4. The comparison is shown in Figure 29, which shows the comparatively better performance of passive devices than active once even after ignoring the energy input required to operate the active devices [325]. Flaps as an add-on device seem far better than any other active systems.

Furthermore, the legal requirements of safety are a hindrance to applying active devices and, in some cases, passive devices too. Relatively, passive devices are the best available option to reduce fuel consumption rather than using fuel to reduce fuel. Bio-inspiration to the bluff body and especially to vehicle aerodynamics, has vast potential to work as passive devices that are explored in this section. Different types of flaps have been used to reduce the drag of vehicles. [318] have used approximately rectangular flaps at the back of the Ahmed body. These flaps were installed along the edges of the end. The results showed that 25% drag reduction, along with 105% of lift reduction was achieved. At the lateral position, which was found to be the best, there were no longitudinal vortices, and through downflow, the separation was delayed. However, it has been discussed that sailfish and swordfish are the fastest fish in the ocean. The first dorsal fin at the top surface of both the fishes seems promising. Their shapes are curved, and they are flexible as well. This inspired design can be implemented as a passive device on the edges of the Ahmed body, which produces the major C-vortex. These special devices will disturb the oncoming flow at the separation point. Some existing shapes are shown in Figure 30 [326–328].

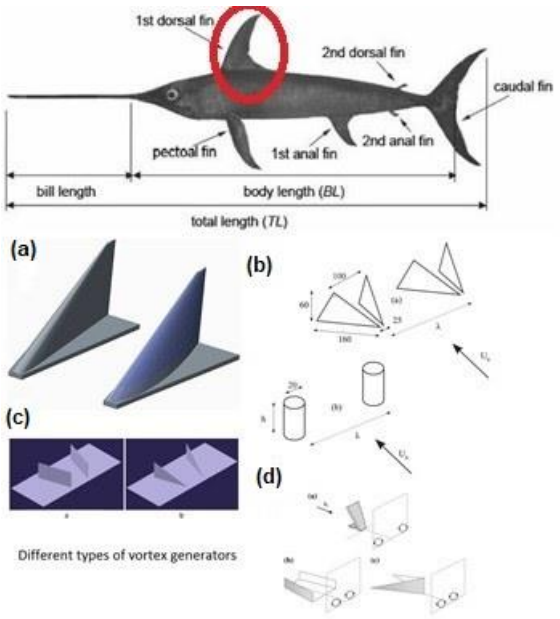

Figure 29. different types of flaps as vortex generators (a) [327] (b) [326] (c)[329] (d) [318] and promising device marked with the red circle

Contrary to these small passive devices that can manipulate the individual boundary layer and vortex, [330], [331] argued for a different version with aerodynamic improvements. However, specific to the discussion [332] have considered an elliptical shape flap, which was optimized through simulation. This elliptical shape reduced the drag by 11.1% at 0.12 m semi-major axis on a TGX MAN long-haul truck. The optimal mounting angle was found as 50º. However, nature has already developed this device in crescent type tail shape at the end of fishes like sailfish, swordfish, thunnus thynnus and Isurus oxyrinches to name a few, which have been shown in Figure 30 along with elliptical flap shape.

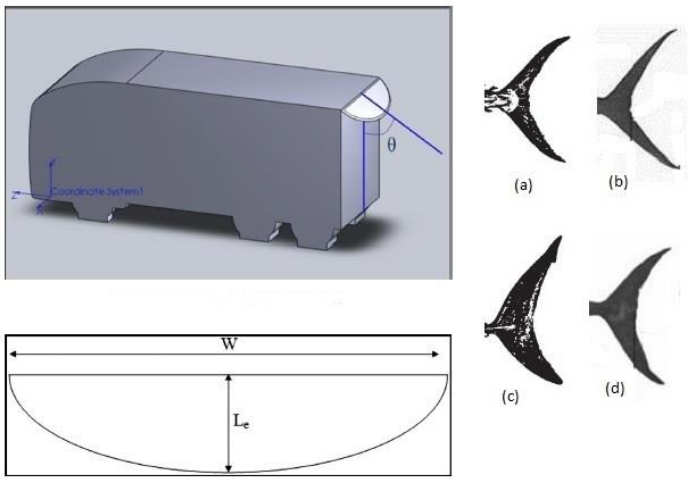

Figure 30. Ahmed body with elliptical shape flap [332] and fish crescent type tails were (a) Thunnus thynnus (b) Sailfish (c) Isurus oxyrinches (d) swordfish [100, 115]

The importance of crescent type tails has already been discussed by[115] but taking inspiration from elliptical flaps and its aerodynamic performance, the crescent shape has possibilities to affect the drag performance. This unique design varies in width, length, and the sweep angle that cannot be without aerodynamics and stability reasons. A whole bunch of studies is possible in this direction, referring to bluff body aerodynamics. In addition to this shape, bringing the flexibility factor of a bird's secondary feather discussed by [52] can further motivate the investigations. Along with it, the effect of porosity can also be included as discussed by [44], and around 45% reduction was achieved with the porous front surface over a two-dimensional Ahmed body by [333]. Nevertheless, there is another kind of flap design available from feathers. Only one aspect of it from the secondary feathers pop-up idea has been Tested by [52]. The wing of large birds has somewhat parabolic shape when seen from the front. So, they are not exactly circular or elliptic. Along with it, they evolved with slots at the end, not without reason [270]. Hence, the new flap design would mimic this unique feature along with perfect curvature and slots at the proper locations shown in 31. Not only this but also such flaps can be

symmetrical add-on device which might cancel out the vortex formation when they pop-up. It would be rather good to use two symmetric flaps of this kind rather than one to fully grasp the dynamics of flow structures.

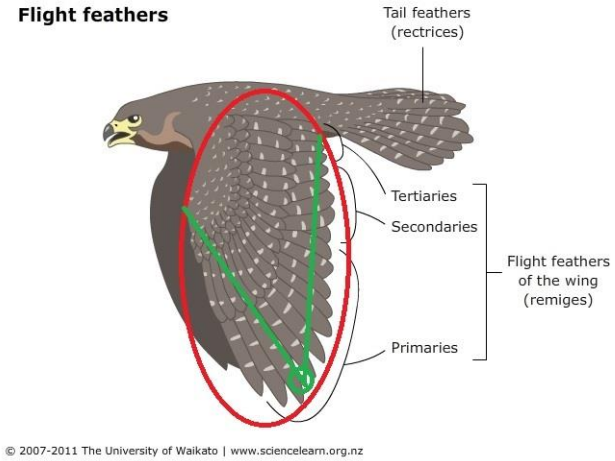

Figure 31. The unique configuration of large birds. The shape is somewhat parabolic nature, whose center can be assumed at the small green circle [270]

The question of what the ideal size of this unique flap would be, need to be studied because it does not necessarily be at the whole slant surface of the body. This flap can be put at the top and side of the body to modify the boundary layer if used in small sizes. Recently the Canadian government has reviewed the drag reduction devices for the high-speed long combination vehicles (LCV). They highlighted the drag contribution of the gap between tractor and trailers along with different passive devices developed [159]. Now, instead of using filler or side skirts, this bio-inspired flexible flap could be placed between the gaps, and that would not require any fixed apparatus which influences maneuvering. It can also be studied at the end of a truck similarly, and the best combination can be analyzed. Its success in drag reduction will not only reduce fuel consumption but also reduce the snow and ice weight, which would otherwise assemble on the appendages of any fixed apparatus like fillers and side skirts. It is an essential factor to consider because during winter in Canada -15º temperature increases the drag by 11.6%, and at -30º, it goes up to 18.5% compared with 15º temperature. Hence, assembly of snow and ice are serious problems in Canada to be investigated. This small device could replace the use of bot tail that adds weight if investigations prove it worth for application.

It is evident and established in vehicle aerodynamics, as stated by [334] that vortices coming out of the side edges called `C' vortex, provide the significant part vortex behind the Ahmed body. He also confirms that this vorticity is the same that a finite wing generated from its edges. Considering this fact, birds have developed the slotted tips at their primary feather to disburse the vorticity. As was discussed earlier that during gliding, the birds raise their tips in a spiral form, and their tips vary in length with slots between each [269]. These tips disburse the vortex both horizontally and vertically stated by [217]. Hence, taking inspiration from this particular shape, a passive and automatic device can be invented. Mimicking the feather tips, a good amount of drag reduction and delay in a stall has been achieved [266]. To apply this wingtip design to the bluff body, the longitudinal edges would seem best for the investigation. The secondary position may be at the slant surface of the Ahmed body because bio-inspired coating at the surface has been proved positive in an aerodynamic sense inspired by shark denticles. They have not reported the forces and coefficients but found it to be promising [335].

Moreover, the slant surface of the vehicle can be filled with micro passive devices inspired by the wingtips. These micro passive devices can work as the vortex generator stated by [7] if this device can disburse the C-vortex coming from the longitudinal edges into the horizontal and vertical direction, that would ultimately reduce a large amount of drag as it seems from the existing literature [310, 334, 336].

The forebody of the buses has been predicted to contribute 60-70% of pressure drag [159]; hence the adoption of wingtips or any other passive devices depends on the kind of vehicle in question. With spoiler at forebody 22.59% and with NACA2415, 10.94% of drag reduction was achieved. This revelation further strengthens the argument for the front and rear end passive devices to manipulate the C-vortex generation. The special design of shark flippers with tubercles have been discussed to accelerates the flow due to vortex pair formation at the back of the leading edge. This acceleration stops the separation and shifts the stall towards the trailing end of the wing. This tubercles shape with peak and crest can influence the flow around the bluff bodies as well. The working mechanism described by [126] seems also to modify the incoming flow from the forebody towards the rear end of the vehicle. This can be tested by providing tubercles on the same locations at the forebody [159]. The edge preparation of the vehicle can be done in a wavy form inspired by the flippers as done by [127].

Recently wave drag reduction on the blunt bodies has been investigated by [337]. They considered three spike shapes and performed a numerical simulation to see the effect. Due to low-pressure formation at the front just ahead of the blunt spike configuration, it outperformed the others in terms of drag reduction. The blunt body configuration, coupled with

blunt-tipped, gives the minimum drag coefficient, which is 0.3. The relation of such devices to reduce aerodynamic drag at supersonic speed resembles the already investigated blunt type bill nose of kingfisher [273]. Due to incredible improvements in the bullet train aerodynamics, the bill of kingfisher can be employed in supersonic flow. The simple reason is that the bill is blunt from the tip, but it has a consistent increasing constant circular cross-section. From the sides, it has a curved portion that distinguishes from the purely blunt body.

The shape designs for which the bullet train has been investigated fall into the nose design of the kingfisher. These birds change the environment almost instantly without losing any aero or hydrodynamic capability. Even the eyes of birds are non-affected by such huge change. These provide an area for further research in high-speed vehicle designs.

In this section, the possible application of nature-inspired devices discussed so far have been proposed for the bluff body and major are summarised in Table 5. Several devices are devised by taking inspiration from the fish and birds. Similarly, few pieces of research in this direction are also included. However, the scope of such devices on the bluff body is enormous, and it just begins to be recognized.

Table 17. Summary of the proposed nature inspired devices

Inspiration	Device	Application	Promising influence
Sailfish First dorsal	Vortex generators	At the edges of the bluff body	C-vortex & separation point
Crescent shape of the fish tails	Passive flap devices	At the back of the bluff body	Delay in the separation
Parabolic shape of bird feather	Passive flap device	At the back of the bluff body	Delay in the separation
feather tips	Passive flow modifier	At the side edges of the bluff body	C-Vortex
tubercles	Flow modifier	At front of the bluff body	C-Vortex

CONCLUSIONS

What can be concluded from the above nature-inspired optimization of aerodynamic forces based on the discussion and reviews of three distinct species of fishes, birds, and land animals? The important point is that these species have a highly developed and complex mechanism of flow control at low Reynolds number with certain active techniques employed as and when necessary, so not all the methods can be mimicked from nature. In the review of fishes, the focus was to see the aerodynamic effects of body shape and various strategies employed by researchers along with the main conclusions drawn. Also, the debate over streamline shapes of large fishes was contrasted with the discussion of boxfish, which surprisingly shows less drag coefficient than well-shaped fishes and models. The debate between these two body shapes is not finished yet; hence further studies can be focused on that. Similarly, passive devices like fins, tails, and flippers have been discussed and shown the capabilities to reduce drag, increase lift, and delay stall. Along with it, the structures of fishes, especially shark's with microgroove, provide drag reduction higher than a smooth surface. Again, this concept inspired a huge debate, and a lot of work has been dedicated to it have been analyzed. Following the same methodology, the aerodynamic effects of the un-flapping aerodynamics around the bird's body, tail, wing, and wingtips have been discussed. It was noted that the study of bird aerodynamics by and large restricted to aerospace applications, and few techniques are employed in the bluff body, especially in road vehicle flow control. The self-pop-up mechanism of secondary feathers and wingtips of primary feathers provides vast potential to delay the flow separation and disperse the vorticity behind the wake. However, while discussing the drag opportunities inland animals, it was found that less work is available in the open literature. Hence, flow around large animals like the cheetah and horse have been discussed along with the use of their tails.

After embarking on such a trigonal voyage to find inspiration that can embellish the bluff body and especially vehicle flow control, promising future research inspirations have been discussed in detail. This discussion proposes the techniques and how they can be implemented to bluff bodies. However, throughout this review, it was highlighted that nature does not support the notion of smooth surface drag reduction. Rather fishes, flyers, animals overland show no smooth surfaces. Therefore, the non-smooth surface should be considered in high importance both in streamlined and bluff bodies. Nature's unconventional designs are questioning conventional concepts about drag and motion. Nature adopted both active and passive methods according to the level of difficulty and necessity involved in the process. Overall, this review paper assembled the ideas from three distinct species that can work as a ready reference for the nature-inspired solution to bluff body aerodynamics.

REFERENCES

[1] J. Scobey-Thal, "Biomimetics: A Short History," *Foreign Policy*, p. 1, Dec. 2014.

[2] E. A. Jamsari, M. A. M. Nawi, A. Sulaiman, R. Sidik, Z. Zaidi, and M. Z. A. H. Ashari, "Ibn Firnas and His Contribution to the Aviation Technology of the World," *Adv. Nat. Appl. Sci.*, vol. 7, no. 1, pp. 74–78, 2013.

[3] R. H. C. Bonser, "Patented Biologically-inspired Technological Innovations: A Twenty Year View," *J. Bionic Eng.*, vol. 3, no. 1, pp. 39–41, Mar. 2006, doi: 10.1016/S1672-6529(06)60005-X.

[4] L. Yongxiang, "Significance and Progress of Bionics," *J. Bionic Eng.*, vol. 1, no. 1, pp. 1–3, Mar. 2004, doi: 10.1007/BF03399448.

[5] G. D. Bixler and B. Bhushan, "Rice and butterfly wing effect inspired low drag and antifouling surfaces: A Review," *Crit. Rev. Solid State Mater. Sci.*, vol. 40, no. 1, pp. 1–37, Jan. 2015, doi: 10.1080/10408436.2014.917368.

[6] B. Bhushan, "Biomimetics inspired surfaces for drag reduction and oleophobicity/philicity," *Beilstein J. Nanotechnol.*, vol. 2, no. 1, pp. 66–84, Feb. 2011, doi: 10.3762/bjnano.2.9.

[7] D. M. Bushnell and K. J. Moore, "Drag Reduction in Nature," *Annu. Rev. Fluid Mech.*, vol. 23, no. 1, pp. 65–79, Jan. 1991, doi: 10.1146/annurev.fl.23.010191.000433.

[8] Y. Luo, Y. Liu, D. Zhang, and E. Y. K. Ng, "influence of morphology for drag reduction effect of sharkskin surface," *J. Mech. Med. Biol.*, vol. 14, no. 02, p. 1450029, Apr. 2014, doi: 10.1142/S0219519414500298.

[9] K. B. Golovin, J. W. Gose, M. Perlin, S. L. Ceccio, and A. Tuteja, "Bioinspired surfaces for turbulent drag reduction," *Philos. Trans. R. Soc. A Math. Phys. Eng. Sci.*, vol. 374, no. 2073, p. 20160189, Aug. 2016, doi: 10.1098/rsta.2016.0189.

[10] J. F. V Vincent, "Biomimetics — a review," *Proc. Inst. Mech. Eng. Part H J. Eng. Med.*, vol. 223, no. 8, pp. 919–939, Nov. 2009, doi: 10.1243/09544119JEIM561.

[11] D. Sameoto and C. Menon, "Recent advances in the fabrication and adhesion testing of biomimetic dry adhesives," *Smart Mater. Struct.*, vol. 19, no. 10, p. 103001, Oct. 2010, doi: 10.1088/0964-1726/19/10/103001.

[12] G. M. Luz, "Mineralized structures in nature: Examples and inspirations for the design of new composite materials and biomaterials," *Compos. Sci. Technol.*, vol. 70, no. 13, pp. 1777–1788, Nov. 2010, doi: 10.1016/J.COMPSCITECH.2010.05.013.

[13] E. C. Goldfield, *Bioinspired devices : emulating nature's assembly and repair process*. 2018.

[14] F. E. Fish and G. V. Lauder, "passive and active flow control by swimming fishes and mammals," *Annu. Rev. Fluid Mech.*, vol. 38, no. 1, pp. 193–224, Jan. 2006, doi: 10.1146/annurev.fluid.38.050304.092201.

[15] Y. Luo, X. Xu, D. Li, and W. Song, "Recent developments in fabricating drag reduction surfaces covering biological sharkskin morphology," *Rev. Chem. Eng.*, vol. 32, no. 1, pp. 93–113, Jan. 2016, doi: 10.1515/revce-2015-0015.

[16] Z. Morris, M. Weissburg, and B. Bras, "Towards a biologically-inspired urban-industrial ecosystem," *Procedia CIRP*, vol. 69, pp. 861–866, Jan. 2018, doi: 10.1016/J.PROCIR.2017.11.055.

[17] G. D. Bixler and B. Bhushan, "Fluid Drag Reduction with Shark-Skin Riblet Inspired Microstructured Surfaces," *Adv. Funct. Mater.*, vol. 23, no. 36, pp. 4507–4528, Sep. 2013, doi: 10.1002/adfm.201203683.

[18] Y. Wang, C. Wu, G. Tan, and Y. Deng, "Reduction in the aerodynamic drag around a generic vehicle by using a non-smooth surface," *Proc. Inst. Mech. Eng. Part D J. Automob. Eng.*, vol. 231, no. 1, pp. 130–144, Jan. 2017, doi: 10.1177/0954407016636970.

[19] J. Wang, C. Zhang, Z. Wu, J. Wharton, and L. Ren, "Numerical study on reduction of aerodynamic noise around an airfoil with biomimetic structures," *J. Sound Vib.*, vol. 394, pp. 46–58, Apr. 2017, doi: 10.1016/J.JSV.2016.11.021.

[20] G. M. Whitesides, "Bioinspiration: something for everyone.," *Interface Focus*, vol. 5, no. 4, p. 20150031, Aug. 2015, doi: 10.1098/rsfs.2015.0031.

[21] A. Reif, W. E., & Dinkelacker, "Hydrodynamics of the squamation infast swimming sharks," *Neues Jahrb. fuer Geol. Palaeontol.*, pp. 184–187, 1982.

[22] M. J. Walsh, "Riblets as a Viscous Drag Reduction Technique," *AIAA J.*, vol. 21, no. 4, pp. 485–486, Apr. 1983, doi: 10.2514/3.60126.

[23] D. W. Bechert, M. Bartenwerfer, G. Hoppe, and W.-E. Reif, "Drag reduction mechanisms derived from shark skin," *ICAS, Congr. 15th, London, England, Sept. 7-12, 1986, Proceedings. Vol. 2 (A86-48976 24-01). New York, Am. Inst. Aeronaut. Astronaut. Inc., 1986, p. 1044-1068.*, vol. 2, pp. 1044–1068, 1986, Accessed: Jun. 20, 2019. [Online]. Available: http://adsabs.harvard.edu/abs/1986icas....2.1044B.

[24] G. D. Bixler and B. Bhushan, "Fluid drag reduction and efficient self-cleaning with rice leaf and butterfly wing bioinspired surfaces," *Nanoscale*, vol. 5, no. 17, p. 7685, Aug. 2013, doi: 10.1039/c3nr01710a.

[25] Y. F. Fu, C. Q. Yuan, and X. Q. Bai, "Marine drag reduction of shark skin inspired riblet surfaces," *Biosurface and Biotribology*, vol. 3, no. 1, pp. 11–24, Mar. 2017, doi: 10.1016/J.BSBT.2017.02.001.

[26] A. Mohammadi and J. M. Floryan, "Groove optimization for drag reduction," *Phys. Fluids*, vol. 25, no. 11, p. 113601, Nov. 2013, doi: 10.1063/1.4826983.

[27] X. Pu, G. Li, and Y. Liu, "Progress and perspective of studies on biomimetic shark skin drag reduction," *ChemBioEng Rev.*, vol. 3, no. 1, pp. 26–40, Feb. 2016, doi: 10.1002/cben.201500011.

[28] V. Stenzel, Y. Wilke, and W. Hage, "Drag-reducing paints for the reduction of fuel consumption in aviation and shipping," *Prog. Org. Coatings*, vol. 70, no. 4, pp. 224–229, Apr. 2011, doi: 10.1016/J.PORGCOAT.2010.09.026.

[29] D. W. Bechert, M. Bruse, W. Hage, and R. Meyer, "Fluid Mechanics of Biological Surfaces and their Technological Application," *Naturwissenschaften*, vol. 87, no. 4, pp. 157–171, Apr. 2000, doi: 10.1007/s001140050696.

[30] J. Anders, "Biomimetic flow control," in *Fluids 2000 Conference and Exhibit*, Jun. 2000, doi: 10.2514/6.2000-2543.

[31] T. Y. Wu, "Fish Swimming and Bird/Insect Flight," *Annu. Rev. Fluid Mech.*, vol. 43, no. 1, pp. 25–58, Jan. 2011, doi: 10.1146/annurev-fluid-122109-160648.

[32] B. Dean and B. Bhushan, "Shark-skin surfaces for fluid-drag reduction in turbulent flow: a review," *Philos. Trans. R. Soc. A Math. Phys. Eng. Sci.*, vol. 368, no. 1929, pp. 4775–4806, Oct. 2010, doi: 10.1098/rsta.2010.0201.

[33] D. T. Roper, S. Sharma, R. Sutton, and P. Culverhouse, "A review of developments towards biologically inspired propulsion systems for autonomous underwater vehicles," *Proc. Inst. Mech. Eng. Part M J. Eng. Marit. Environ.*, vol. 225, no. 2, pp. 77–96, May 2011, doi: 10.1177/1475090210397438.

[34] L. H. Shu, K. Ueda, I. Chiu, and H. Cheong, "Biologically inspired design," *CIRP Ann.*, vol. 60, no. 2, pp. 673–693, Jan. 2011, doi: 10.1016/J.CIRP.2011.06.001.

[35] B. Bhushan and Y. C. Jung, "Natural and biomimetic artificial surfaces for superhydrophobicity, self-cleaning, low adhesion, and drag reduction," *Prog. Mater. Sci.*, vol. 56, no. 1, pp. 1–108, Jan. 2011, doi: 10.1016/J.PMATSCI.2010.04.003.

[36] X. Han, D. Zhang, X. Li, and Y. Li, "Bio-replicated forming of the biomimetic drag-reducing surfaces in large area based on shark skin," *Sci. Bull.*, vol. 53, no. 10, pp. 1587–1592, May 2008, doi: 10.1007/s11434-008-0219-3.

[37] T. Lenau, H. Cheong, and L. Shu, "Sensing in nature: using biomimetics for design of sensors," *Sens. Rev.*, vol. 28, no. 4, pp. 311–316, Sep. 2008, doi: 10.1108/02602280810902604.

[38] Y. Li, J. Zhang, and B. Yang, "Antireflective surfaces based on biomimetic nanopillared arrays," *Nano Today*, vol. 5, no. 2, pp. 117–127, Apr. 2010, doi: 10.1016/J.NANTOD.2010.03.001.

[39] K. Liu and L. Jiang, "Bio-inspired design of multiscale structures for function integration," *Nano Today*, vol. 6, no. 2, pp. 155–175, Apr. 2011, doi: 10.1016/J.NANTOD.2011.02.002.

[40] J. McKittrick *et al.*, "Energy absorbent natural materials and bioinspired design strategies: A review," *Mater. Sci. Eng. C*, vol. 30, no. 3, pp. 331–342, Apr. 2010, doi: 10.1016/J.MSEC.2010.01.011.

[41] L. Raibeck, J. Reap, and B. Bras, "Investigating environmental burdens and benefits of biologically inspired self-cleaning surfaces," *CIRP J. Manuf. Sci. Technol.*, vol. 1, no. 4, pp. 230–236, Jan. 2009, doi: 10.1016/J.CIRPJ.2009.05.004.

[42] H. A. Abdulbari, H. D. Mahammed, and Z. B. Y. Hassan, "Bio-Inspired Passive Drag Reduction Techniques: A Review," *ChemBioEng Rev.*, vol. 2, no. 3, pp. 185–203, Jun. 2015, doi: 10.1002/cben.201400033.

[43] R. Godoy-Diana and B. Thiria, "On the diverse roles of fluid dynamic drag in animal swimming and flying.," *J. R. Soc. Interface*, vol. 15, no. 139, 2018, doi: 10.1098/rsif.2017.0715.

[44] M. A. Aldheeb, W. Asrar, E. Sulaeman, and A. A. Omar, "A review on aerodynamics of nonflapping bird wings," *J. Aerosp. Technol. Manag.*, vol. 8, no. 1, pp. 7–17, 2016, doi: 10.5028/jatm.v8i1.564.

[45] Z. Guo, W. Liu, and B.-L. Su, "Superhydrophobic surfaces: From natural to biomimetic to functional," *J. Colloid Interface Sci.*, vol. 353, no. 2, pp. 335–355, Jan. 2011, doi: 10.1016/J.JCIS.2010.08.047.

[46] R. Lockwood, J. P. Swaddle, and J. M. V. Rayner, "Avian Wingtip Shape Reconsidered: Wingtip Shape Indices and Morphological Adaptations to Migration," *J. Avian Biol.*, vol. 29, no. 3, p. 273, Sep. 1998, doi: 10.2307/3677110.

[47] E. Lurie-Luke, "Product and technology innovation: What can biomimicry inspire?," *Biotechnol. Adv.*, vol. 32, no. 8, pp. 1494–1505, Dec. 2014, doi: 10.1016/J.BIOTECHADV.2014.10.002.

[48] A. M. Savill, "Drag Reduction by Passive Devices—a Review of some Recent Developments," in *Structure of Turbulence and Drag Reduction*, Berlin, Heidelberg: Springer Berlin Heidelberg, 1990, pp. 429–465.

[49] J. V. Shreyas, S. Devranjan, and K. R. Sreenivas, "Aerodynamics of bird and insect flight," *J. Indian Inst. Sci.*, vol. 91, no. 3, pp. 315–327, 2011.

[50] N. A. Siddiqui, W. Asrar, and E. Sulaeman, "Literature review: Biomimetic and conventional aircraft wing tips," *Int. J. Aviat. Aeronaut. Aerosp.*, vol. 4, no. 2, 2017, doi: 10.15394/ijaa.2017.1172.

[51] G. Yunqing, L. Tao, M. Jiegang, S. Zhengzan, and Z. Peijian, "Analysis of Drag Reduction Methods and Mechanisms of Turbulent.," *Appl. bionics Biomech.*, vol. 2017, p. 6858720, 2017, doi: 10.1155/2017/6858720.

[52] D. Kim, H. Lee, W. Yi, and H. Choi, "A bio-inspired device for drag reduction on a three-dimensional model vehicle," *Bioinspir. Biomim.*, vol. 11, no. 2, p. 026004, Mar. 2016, doi: 10.1088/1748-3190/11/2/026004.

[53] N. Mazellier, A. Feuvrier, and A. Kourta, "Biomimetic bluff body drag reduction by self-adaptive porous flaps," *Comptes Rendus Mécanique*, vol. 340, no. 1–2, pp. 81–94, Jan. 2012, doi: 10.1016/J.CRME.2011.11.006.

[54] M. R. Arifin, A. F. M. Yamin, A. S. Abdullah, M. F. Zakaryia, S. Shuib, and S. Suhaimi, "Evolution of the leading-edge vortex over a flapping wing mechanism," *J. Mech. Eng. Sci.*, vol. 14, no. 2, pp. 6888–6894, Jun. 2020, doi: 10.15282/jmes.14.2.2020.27.0539.

[55] J. D. Anderson, *The fundamental of aerodynamics*. New York: McGraw Hills, 2012.

[56] D. M. Bushnell and K. J. Moore, "Drag Reduction in Nature," *Annu. Rev. Fluid Mech.*, vol. 23, no. 1, pp. 65–79, Jan. 1991, doi: 10.1146/annurev.fl.23.010191.000433.

[57] V. Walter, "body form and swimming performance in the scombroid fishes," *Am. Zool.*, vol. 2, no. 2, pp. 143–149, May 1962, doi: 10.1093/icb/2.2.143.

[58] Y. G. Aleyev, "Introduction," in *Nekton*, Dordrecht: Springer Netherlands, 1977, pp. 1–18.

[59] Q. Bone, "Buoyancy and Hydrodynamic Functions of Integument in the Castor Oil Fish, Ruvettus pretiosus (Pisces: Gempylidae)," *Copeia*, vol. 1972, no. 1, p. 78, Mar. 1972, doi: 10.2307/1442784.

[60] V. V. Ovchinnikov, "[Turbulence of the boundary layer as one of the methods of reducing resistance in the movement of certain fishes].," *undefined*, 1966, Accessed: Jun. 27, 2019. [Online]. Available: https://www.semanticscholar.org/paper/%5BTurbulence-of-the-boundary-layer-as-one-of-the-of-Ovchinnikov/8539c623fc8f350e924130bfa5b02d82e1ee940f.

[61] P. W. Webb, "Hydrodynamics: Nonscombroid Fish," *Fish Physiol.*, vol. 7, pp. 189–237, Jan. 1978, doi: 10.1016/S1546-5098(08)60165-X.

[62] E. G. Richardson, "The Physical Aspects Of Fish Locomotion," *J. Exp. Biol.*, vol. 13, no. 1, 1936.

[63] D. A. Parry, "The Swimming of Whales and a Discussion of Gray's Paradox," *J. Exp. Biol.*, vol. 26, no. 1, 1949.

[64] C. C. Lindsey, "Form, Function, and Locomotory Habits in Fish," 1978, pp. 1–100.

[65] D. Gero, "The hydrodynamic aspects of fish propulsion. American Museum novitates; no. 1601," 1952, Accessed: Jun. 27, 2019. [Online]. Available: http://digitallibrary.amnh.org/bitstream/handle/2246/4922/N1601.pdf?sequence=1.

[66] J. Gray, "Studies in Animal Locomotion," *J. Exp. Biol.*, vol. 10, no. 1, 1933.

[67] F. E. Fish, "The myth and reality of Gray's paradox: implication of dolphin drag reduction for technology," *Bioinspir. Biomim.*, vol. 1, no. 2, pp. R17–R25, Jun. 2006, doi: 10.1088/1748-3182/1/2/R01.

[68] P. Webb, "Hydrodynamics and Energetics of Fish Propulsion," *Bull. Fish. Res. Board Canada*, Jan. 1975, Accessed: Jun. 27, 2019. [Online]. Available: https://scholarworks.umass.edu/fishpassage_journal_articles/569.

[69] R. Von Mises, *Theory of flight*. Dover Publications, 1959.

[70] F. E. Fish, "Influence of hydrodynamic design and propulsive mode on mammalian swimming energetics," *AUST. J. ZOOL*, pp. 42--79, 1993, Accessed: Jun. 27, 2019. [Online]. Available: http://citeseerx.ist.psu.edu/viewdoc/summary?doi=10.1.1.734.450.

[71] Morton Gertler, "resistance experiments on a systematic series of streamlined bodies of revolution-for application to the design of high-speed submarines," Washington, 1972. Accessed: Jun. 27, 2019. [Online]. Available: https://apps.dtic.mil/dtic/tr/fulltext/u2/a800144.pdf.

[72] F. E. Fish and C. A. Hui, "Dolphin swimming–a review," *Mamm. Rev.*, vol. 21, no. 4, pp. 181–195, Dec. 1991, doi: 10.1111/j.1365-2907.1991.tb00292.x.

[73] P. E. Purves, W H Dudok van Heel, and J. A, "Locomotion in dolphins Part I: hydrodynamic experiments on a model of the bottle-nosed dolphin," *Aquat. Mamm*, vol. 34, pp. 1–8, 1975.

[74] J. Rohr, M. I. Latz, S. Fallon, J. C. Nauen, and E. Hendricks, "Experimental approaches towards interpreting dolphin-stimulated bioluminescence.," *J. Exp. Biol.*, vol. 201, no. 9, 1998.

[75] F. Fish and G. Lauder, "Not just going with the flow," *Am. Sci.*, vol. 1, 2013, Accessed: Aug. 22, 2019. [Online]. Available: http://www.people.fas.harvard.edu/~glauder/reprints_unzipped/Fish.Lauder.2013.pdf.

[76] I. Nesteruk, G. Passoni, and A. Redaelli, "Shape of Aquatic Animals and Their Swimming Efficiency," *J. Mar. Biol.*, vol. 2014, pp. 1–9, Feb. 2014, doi: 10.1155/2014/470715.

[77] Y. Zhang, H. Kihara, and K. Abe, "Three-dimensional simulation of a self-propelled fish-like body swimming in a channel," *Eng. Appl. Comput. Fluid Mech.*, vol. 12, no. 1, pp. 473–492, Jan. 2018, doi: 10.1080/19942060.2018.1453381.

[78] B. P. Epps, P. Valdivia y Alvarado, K. Youcef-Toumi, and A. H. Techet, "Swimming performance of a biomimetic compliant fish-like robot," *Exp. Fluids*, vol. 47, no. 6, pp. 927–939, Dec. 2009, doi: 10.1007/s00348-009-0684-8.

[79] H. Liu and K. Kawachi, "A Numerical Study of Undulatory Swimming," *J. Comput. Phys.*, vol. 155, no. 2, pp. 223–247, Nov. 1999, doi: 10.1006/JCPH.1999.6341.

[80] M. S. Triantafyllou, A. H. Techet, Q. Zhu, D. N. Beal, F. S. Hover, and D. K. P. Yue, "Vorticity Control in Fish-like Propulsion and Maneuvering," *Integr. Comp. Biol.*, vol. 42, no. 5, pp. 1026–1031, Nov. 2002, doi: 10.1093/icb/42.5.1026.

[81] Q. Zhu, M. J. Wolfgang, D. K. P. Yue, and M. S. Triantafyllou, "Three-dimensional flow structures and vorticity control in fish-like swimming," *J. Fluid Mech.*, vol. 468, pp. 1–28, Oct. 2002, doi: 10.1017/S002211200200143X.

[82] R. Bainbridge, "Problems of fish locomotion," in *Symp. Zool. SOC.*, 1961, pp. 13–32.

[83] Paul W. Webb, "Form and Function in Fish Swimming," *Sci. Am. a Div. Nat. Am. Inc*, vol. 251, no. 1, pp. 72–83, 1984, Accessed: Jul. 05, 2019. [Online]. Available: https://www.jstor.org/stable/24969414?seq=1#metadata_info_tab_contents.

[84] C. M. Breder and C. M. Breder, "The locomotion of fishes," *Zool. Sci. Contrib. New York Zool. Soc.*, vol. 4, no. 5, pp. 159--297, 1926, Accessed: Jul. 05, 2019. [Online]. Available: https://www.biodiversitylibrary.org/part/203769.

[85] Moe William Rosen, "water flow about a swimming fish," California, 1959. Accessed: Jul. 05, 2019. [Online]. Available: https://apps.dtic.mil/dtic/tr/fulltext/u2/238395.pdf.

[86] S. Taneda and Y. Tomonari, "An Experiment on the Flow around a Waving Plate," *J. Phys. Soc. Japan*, vol. 36, no. 6, pp. 1683–1689, Jun. 1974, doi: 10.1143/JPSJ.36.1683.

[87] T. Y. Wu and A. T. Chwang, "Extraction of Flow Energy by Fish and Birds in a Wavy Stream," in *Swimming and Flying in Nature*, Boston, MA: Springer US, 1975, pp. 687–702.

[88] M. Triantafyllou and G. Triantafyllou, "An Efficient Swimming Machine," *Sci. Am.*, vol. 272, no. 3, pp. 64–70, 1995.

[89] A. H. Techet, F. S. Hover, and M. S. Triantafyllou, "Separation and Turbulence Control in Biomimetic Flows," *Flow, Turbul. Combust. (formerly Appl. Sci. Res.*, vol. 71, no. 1–4, pp. 105–118, 2003, doi: 10.1023/B:APPL.0000014923.28324.87.

[90] L. Shen, X. Zhang, D. K. P. Yue, and M. S. Triantafyllou, "Turbulent flow over a flexible wall undergoing a streamwise travelling wave motion," *J. Fluid Mech.*, vol. 484, p. S0022112003004294, Jun. 2003, doi: 10.1017/S0022112003004294.

[91] H. Hu, "Biologically Inspired Design of Autonomous Robotic Fish at Essex," in *Proceedings of the IEEE SMC UK-RI Chapter Conference*, 2006, p. 6.

[92] G. H. Yang *et al.*, "Control and design of a 3 DOF fish robot 'Ichtus,'" in *2011 IEEE International Conference on Robotics and Biomimetics, ROBIO 2011*, 2011, pp. 2108–2113, doi: 10.1109/ROBIO.2011.6181603.

[93] F. Bonnet *et al.*, "Design of a modular robotic system that mimics small fish locomotion and body movements for ethological studies," *Int. J. Adv. Robot. Syst.*, vol. 14, no. 3, 2017, doi: 10.1177/1729881417706628.

[94] J. Gao, S. Bi, J. Li, and C. Liu, "Design and experiments of robot fish propelled by pectoral fins," in *2009 IEEE International Conference on Robotics and Biomimetics, ROBIO 2009*, 2009, pp. 445–450, doi: 10.1109/ROBIO.2009.5420688.

[95] S. Guo, T. Fukuda, N. Kato, and K. Oguro, "Development of underwater microrobot using ICPF actuator," in *Proceedings - IEEE International Conference on Robotics and Automation*, 1998, vol. 2, pp. 1829–1834, doi: 10.1109/ROBOT.1998.677433.

[96] Y. Luo, L. Wang, L. Green, K. Song, L. Wang, and R. Smith, "Advances of drag-reducing surface technologies in turbulence based on boundary layer control," *J. Hydrodyn.*, vol. 27, no. 4, pp. 473–487, Aug. 2015, doi: 10.1016/S1001-6058(15)60507-8.

[97] J. Oyekan, B. Lu, and H. Hu, "A creative computing approach to 3D robotic simulator for water pollution monitoring," 2013. Accessed: Sep. 06, 2019. [Online]. Available: http://www.sonyaibo.net/aboutaibo.htm.

[98] W. Qing-Ping, S. Wang, X. Dong, L.-J. Shang, and M. Tan, "Design and Kinetic Analysis of a Biomimetic Underwater Vehicle with Two Undulating Long-fins," *Acta Autom. Sin.*, vol. 39, no. 8, pp. 1330–1338, Aug. 2013, doi: 10.1016/S1874-1029(13)60049-X.

[99] J. Yu, M. Tan, S. Wang, and E. Chen, "Development of a biomimetic robotic fish and its control algorithm," *IEEE Trans. Syst. Man, Cybern. Part B Cybern.*, vol. 34, no. 4, pp. 1798–1810, Aug. 2004, doi: 10.1109/TSMCB.2004.831151.

[100] W. Sagong, W. P. Jeon, and H. Choi, "Hydrodynamic characteristics of the sailfish (Istiophorus platypterus) and swordfish (Xiphias gladius) in gliding postures at their cruise speeds," *PLoS One*, vol. 8, no. 12, Dec. 2013, doi: 10.1371/journal.pone.0081323.

[101] W. Sagong, C. Kim, S. Choi, W. P. Jeon, and H. Choi, "Does the sailfish skin reduce the skin friction like the shark skin?," in *Physics of Fluids*, 2008, vol. 20, no. 10, doi: 10.1063/1.3005861.

[102] P. Domenici *et al.*, "How sailfish use their bills to capture schooling prey," *Proc. R. Soc. B Biol. Sci.*, vol. 281, no. 1784, Apr. 2014, doi: 10.1098/rspb.2014.0444.

[103] J. M. Zhan, Y. J. Gong, and T. Z. Li, "Gliding locomotion of manta rays, killer whales and swordfish near the water surface," *Sci. Rep.*, vol. 7, no. 1, Dec. 2017, doi: 10.1038/s41598-017-00399-y.

[104] R. Von Mises, *Theory of flight.* Dover Publications, 1959.

[105] I. Bartol, M. Gharib, P. Webb, and D. Weihs, "Body-induced vortical flows: a common mechanism for self-corrective trimming control in boxfishes," *J. Exp. Biol.*, no. 208, pp. 327–344, 2005, Accessed: Jul. 02, 2019. [Online]. Available: http://jeb.biologists.org/content/208/2/327.short.

[106] J. A. Walker, "Does a rigid body limit maneuverability?," *J. Exp. Biol.*, vol. 203, no. 22, 2000.

[107] M. S. Gordon, J. R. Hove, P. W. Webb, and D. Weihs, "Boxfishes as Unusually Well-Controlled Autonomous Underwater Vehicles," *Physiol. Biochem. Zool.*, vol. 73, no. 6, pp. 663–671, Nov. 2000, doi: 10.1086/318098.

[108] J. R. Hove, L. M. O'Bryan, M. S. Gordon, P. W. Webb, and D. Weihs, "Boxfishes (Teleostei: Ostraciidae) as a model system for fishes swimming with many fins: kinematics," *J. Exp. Biol.*, vol. 204, no. 8, 2001.

[109] I. K. Bartol, M. S. Gordon, M. Gharib, J. R. Hove, P. W. Webb, and D. Weihs, "Flow Patterns Around the Carapaces of Rigid-bodied, Multi-propulsor Boxfishes (Teleostei: Ostraciidae)," *Integr. Comp. Biol.*, vol. 42, no. 5, pp. 971–980, Nov. 2002, doi: 10.1093/icb/42.5.971.

[110] I. K. Bartol, M. S. Gordon, P. Webb, D. Weihs, and M. Gharib, "Evidence of self-correcting spiral flows in swimming boxfishes," *Bioinspir. Biomim.*, vol. 3, no. 1, p. 014001, Mar. 2008, doi: 10.1088/1748-3182/3/1/014001.

[111] S. Van Wassenbergh, K. van Manen, T. A. Marcroft, M. E. Alfaro, and E. J. Stamhuis, "Boxfish swimming paradox resolved: forces by the flow of water around the body promote manoeuvrability," *J. R. Soc. Interface*, vol. 12, no. 103, pp. 20141146–20141146, Dec. 2014, doi: 10.1098/rsif.2014.1146.

[112] A. Kozlov, H. Chowdhury, I. Mustary, B. Loganathan, and F. Alam, "Bio-Inspired Design: Aerodynamics of Boxfish," *Procedia Eng.*, vol. 105, pp. 323–328, Jan. 2015, doi: 10.1016/J.PROENG.2015.05.007.

[113] R. Islam, M. Hussein, M. Zaid, and B. Loganathan, "Design of an energy efficient car by biomimicry of a boxfish," *Energy Procedia*, vol. 160, pp. 40–44, Feb. 2019, doi: 10.1016/J.EGYPRO.2019.02.116.

[114] T. G. Lang, "Hydrodynamic Analysis of Dolphin Fin Profiles," *Nature*, vol. 209, no. 5028, pp. 1110–1111, Mar. 1966, doi: 10.1038/2091110a0.

[115] C. P. van Dam, "Efficiency characteristics of crescent-shaped wings and caudal fins," *Nature*, vol. 325, no. 6103, pp. 435–437, Jan. 1987, doi: 10.1038/325435a0.

[116] V. V. Pavlov, "Wing design and morphology of the harbor porpoise dorsal fin," *J. Morphol.*, vol. 258, no. 3, pp. 284–295, Dec. 2003, doi: 10.1002/jmor.10135.

[117] F. E. Fish, J. T. Beneski, and D. R. Ketten, "Examination of the three-dimensional geometry of cetacean flukes using computed tomography scans: Hydrodynamic implications," *Anat. Rec. Adv. Integr. Anat. Evol. Biol.*, vol. 290, no. 6, pp. 614–623, Jun. 2007, doi: 10.1002/ar.20546.

[118] J. Z. Wu, A. D. Vakili, and J. M. Wu, "Review of the physics of enhancing vortex lift by unsteady excitation," *Prog. Aerosp. Sci.*, vol. 28, no. 2, pp. 73–131, Jan. 1991, doi: 10.1016/0376-0421(91)90001-K.

[119] P. Watts and FE Fish, "The influence of passive, leading edge tubercles on wing performance," in *Proc. Twelfth Intl. Symp. Unmanned Untethered Submers. Technol*, 2001, Accessed: Jul. 03, 2019. [Online]. Available: https://www.researchgate.net/profile/Frank_Fish4/publication/229002925_The_influence_of_passive_leading_edge_tubercles_on_wing_performance/links/0c9605233028f7aef1000000.pdf.

[120] D. S. Miklosovic, M. M. Murray, L. E. Howle, and F. E. Fish, "Leading-edge tubercles delay stall on humpback whale (Megaptera novaeangliae) flippers," *Phys. Fluids*, vol. 16, no. 5, pp. L39–L42, May 2004, doi: 10.1063/1.1688341.

[121] F. E. Fish, L. E. Howle, and M. M. Murray, "Hydrodynamic flow control in marine mammals," *Integr. Comp. Biol.*, vol. 48, no. 6, pp. 788–800, Apr. 2008, doi: 10.1093/icb/icn029.

[122] E. A. van Nierop, S. Alben, and M. P. Brenner, "How Bumps on Whale Flippers Delay Stall: An Aerodynamic Model," *Phys. Rev. Lett.*, vol. 100, no. 5, p. 054502, Feb. 2008, doi: 10.1103/PhysRevLett.100.054502.

[123] H. Johari, C. W. Henoch, D. Custodio, and A. Levshin, "Effects of Leading-Edge Protuberances on Airfoil Performance," *AIAA J.*, vol. 45, no. 11, pp. 2634–2642, Nov. 2007, doi: 10.2514/1.28497.

[124] K. Hansen, R. Kelso, and C. Doolan, "Reduction of Flow Induced Tonal Noise Through Leading Edge Tubercle Modifications," in *16th AIAA/CEAS Aeroacoustics Conference*, Jun. 2010, doi: 10.2514/6.2010-3700.

[125] K. L. Hansen, R. M. Kelso, and B. B. Dally, "Performance Variations of Leading-Edge Tubercles for Distinct Airfoil Profiles," *AIAA J.*, vol. 49, no. 1, pp. 185–194, Jan. 2011, doi: 10.2514/1.J050631.

[126] F. E. Fish, P. W. Weber, M. M. Murray, and L. E. Howle, "The Tubercles on Humpback Whales' Flippers: Application of Bio-Inspired Technology," *Integr. Comp. Biol.*, vol. 51, no. 1, pp. 203–213, Jul. 2011, doi: 10.1093/icb/icr016.

[127] N. Rostamzadeh, R. M. Kelso, B. B. Dally, and K. L. Hansen, "The effect of undulating leading-edge modifications on NACA 0021 airfoil characteristics," *Phys. Fluids*, vol. 25, no. 11, p. 117101, Nov. 2013, doi: 10.1063/1.4828703.

[128] D. Custodio, C. W. Henoch, and H. Johari, "Aerodynamic Characteristics of Finite Span Wings with Leading-Edge Protuberances," *AIAA J.*, vol. 53, no. 7, pp. 1878–1893, Jul. 2015, doi: 10.2514/1.J053568.

[129] M. M. Zhang, G. F. Wang, and J. Z. Xu, "Aerodynamic Control of Low-Reynolds-Number Airfoil with Leading-Edge Protuberances," *AIAA J.*, vol. 51, no. 8, pp. 1960–1971, Aug. 2013, doi: 10.2514/1.J052319.

[130] M. D. Bolzon, R. M. Kelso, and M. Arjomandi, "Tubercles and Their Applications," *J. Aerosp. Eng.*, vol. 29, no. 1, p. 04015013, Jan. 2016, doi: 10.1061/(ASCE)AS.1943-5525.0000491.

[131] P. S. Segre, S. M. Seakamela, M. A. Meÿer, K. P. Findlay, and J. A. Goldbogen, "A hydrodynamically active flipper-stroke in humpback whales," *Curr. Biol.*, vol. 27, no. 13, pp. R636–R637, Jul. 2017, doi: 10.1016/j.cub.2017.05.063.

[132] P. S. Segre, S. M. Seakamela, M. A. Meÿer, K. P. Findlay, and J. A. Goldbogen, "A hydrodynamically active flipper-stroke in humpback whales," *Curr. Biol.*, vol. 27, no. 13, pp. R636–R637, Jul. 2017, doi: 10.1016/j.cub.2017.05.063.

[133] D. Bechert and W. Reif, "On the Drag Reduction of the Shark Skin," in *23rd Aerospace Sciences Meeting*, Jan. 1985, doi: 10.2514/6.1985-546.

[134] M. Walsh, "Turbulent boundary layer drag reduction using riblets," in *20th Aerospace Sciences Meeting*, Jan. 1982, doi: 10.2514/6.1982-169.

[135] D. W. Bechert and M. Bartenwerfer, "The viscous flow on surfaces with longitudinal ribs," *J. Fluid Mech.*, vol. 206, pp. 105–129, Sep. 1989, doi: 10.1017/S0022112089002247.

[136] D. W. Bechert, M. Bruse, W. Hage, J. G. T. Van Der Hoeven, and G. Hoppe, "Experiments on drag-reducing surfaces and their optimization with an adjustable geometry," *J. Fluid Mech.*, vol. 338, pp. 59–87, May 1997, doi: 10.1017/S0022112096004673.

[137] B. Nugroho, N. Hutchins, and J. P. Monty, "Large-scale spanwise periodicity in a turbulent boundary layer induced by highly ordered and directional surface roughness," *Int. J. Heat Fluid Flow*, vol. 41, pp. 90–102, 2013, doi: 10.1016/j.ijheatfluidflow.2013.04.003.

[138] g. Cui, c. Pan, d. Wu, q. Ye, and J. WANG, "Effect of drag reducing riblet surface on coherent structure in turbulent boundary layer," *Chinese J. Aeronaut.*, May 2019, doi: 10.1016/J.CJA.2019.04.023.

[139] d. W. Bechert, m. Bruse, w. Hage, j. G. T. Van der hoeven, and G. HOPPE, "Experiments on drag-reducing surfaces and their optimization with an adjustable geometry," *J. Fluid Mech.*, vol. 338, pp. 59–87, May 1997, doi: 10.1017/S0022112096004673.

[140] W. Li *et al.*, "Turbulent drag reduction by spanwise traveling ribbed surface waves," *Eur. J. Mech. - B/Fluids*, vol. 53, pp. 101–112, Sep. 2015, doi: 10.1016/J.EUROMECHFLU.2015.03.009.

[141] S. Martin and B. Bhushan, "Modeling and optimization of shark-inspired riblet geometries for low drag applications," *J. Colloid Interface Sci.*, vol. 474, pp. 206–215, Jul. 2016, doi: 10.1016/J.JCIS.2016.04.019.

[142] L. Tian, L. Ren, Z. Han, and S. Zhang, "Experiment about drag reduction of bionic non-smooth surface in low speed wind tunnel," *J. Bionic Eng.*, vol. 2, no. 1, pp. 15–24, Mar. 2005, doi: 10.1007/BF03399477.

[143] D. Zhang, Y. Luo, X. Li, and H. Chen, "Numerical simulation and experimental study of drag-reducing surface of a real shark skin," *J. Hydrodyn. Ser. B*, vol. 23, no. 2, pp. 204–211, Apr. 2011, doi: 10.1016/S1001-6058(10)60105-9.

[144] A. W. Lang, P. Motta, P. Hidalgo, and M. Westcott, "Bristled shark skin: a microgeometry for boundary layer control?," *Bioinspir. Biomim.*, vol. 3, no. 4, p. 046005, Dec. 2008, doi: 10.1088/1748-3182/3/4/046005.

[145] A. G. Domel, M. Saadat, J. C. Weaver, H. Haj-Hariri, K. Bertoldi, and G. V. Lauder, "Shark skin-inspired designs that improve aerodynamic performance," *J. R. Soc. Interface*, vol. 15, no. 139, p. 20170828, Feb. 2018, doi: 10.1098/rsif.2017.0828.

[146] F.-W. Patricia, D. Guzman, B. Iñigo, I. Urtzi, B. J. Maria, and S. Manu, "Morphological Characterization and Hydrodynamic Behavior of Shortfin Mako Shark (Isurus oxyrinchus) Dorsal Fin Denticles," *J. Bionic Eng.*, vol. 16, no. 4, pp. 730–741, Jul. 2019, doi: 10.1007/s42235-019-0059-7.

[147] P. A. Fuaad and K. Arul Prakash, "Enhanced drag-reduction over superhydrophobic surfaces with sinusoidal textures: A DNS study," *Comput. Fluids*, vol. 181, pp. 208–223, Mar. 2019, doi: 10.1016/J.COMPFLUID.2019.01.022.

[148] C. Zhang and K. Saurav Bijay, "Investigation on drag reduction performance of aero engine blade with micro-texture," *Aerosp. Sci. Technol.*, vol. 72, pp. 380–396, Jan. 2018, doi: 10.1016/J.AST.2017.11.007.

[149] Y. Luo, D. Zhang, and Y. Liu, "recent drag reduction developments derived from different biological functional surfaces: a review," *J. Mech. Med. Biol.*, vol. 16, no. 02, p. 1630001, Mar. 2016, doi: 10.1142/S0219519416300015.

[150] S. Nakao, "Application of V Shape Riblets to Pipe Flows," *J. Fluids Eng.*, vol. 113, no. 4, p. 587, Dec. 1991, doi: 10.1115/1.2926519.

[151] M. Nili-Ahmadabadi, O. Nematollahi, and K. C. Kim, "Effects of coarse riblets on air flow structures over a slender delta wing using particle image velocimetry," *Chinese J. Aeronaut.*, vol. 32, no. 6, pp. 1367–1379, Jun. 2019, doi: 10.1016/J.CJA.2019.03.019.

[152] N. West, K. Sammut, and Y. Tang, "Material selection and manufacturing of riblets for drag reduction: An updated review," *Proc. Inst. Mech. Eng. Part L J. Mater. Des. Appl.*, vol. 232, no. 7, pp. 610–622, Jul. 2018, doi: 10.1177/1464420716641452.

[153] H. H. Zhang, S. S. Nunayon, and A. C. K. Lai, "Experimental study on deposition enhancement of ultrafine particles in a duct flow by riblets," *Appl. Therm. Eng.*, vol. 147, pp. 886–894, Jan. 2019, doi: 10.1016/J.APPLTHERMALENG.2018.10.112.

[154] M. J. Walsh, W. L. Sellers, and C. B. McGinley, "Riblet drag reduction at flight conditions," in *AIAA 6th Applied Aerodynamics Conference, 1988*, 1988, pp. 629–638, doi: 10.2514/6.1988-2554.

[155] J. Anderson, *Introduction to Flight.pdf*, Seventh. USA: McGraw-Hill Education, 2001.

[156] I. Hucho, "Aerodynamics of Road Vehicles," *Annu. Rev. Fluid Mech.*, vol. 25, no. 1, pp. 485–537, 1993, doi: 10.1146/annurev.fluid.25.1.485.

[157] S. K. Arabacı and M. Arabacı, "aerodynamic characteristics of buses inspired by beluga whales in cfd and wind tunnel," 2018. Accessed: Sep. 06, 2019. [Online]. Available: https://www.researchgate.net/publication/333311236.

[158] C. Chhavi and T. Selvakumaran, "Adaptation of Sailfish topology in fuselage design and performance comparison with modern fuselage," in *IEEE Aerospace Conference Proceedings*, Jun. 2018, vol. 2018-March, pp. 1–8, doi: 10.1109/AERO.2018.8396431.

[159] J. Patten, P. Eng Brian McAuliffe, W. Mayda, and P. Eng Bernard Tanguay, "Review of Aerodynamic Drag Reduction Devices for Heavy Trucks and Buses," 2012.

[160] D. S. Chawla, "The car designer who turned a sailfish into a supercar," *BBC News*, 2014.

[161] B. Sharfman, "Mercedes and the boxfish | The Scientist Magazine®," *The Scientist*, 2006.

[162] J. Buehler, "Mercedes-Benz Bionic car: Boxfish stability and agility paradox finally solved.," *Slate*, 2015.

[163] H. Chowdhury, R. Islam, M. Hussein, M. Zaid, B. Loganathan, and F. Alam, "Design of an energy efficient car by biomimicry of a boxfish," in *Energy Procedia*, 2019, vol. 160, pp. 40–44, doi: 10.1016/j.egypro.2019.02.116.

[164] B. Bhushan and Y. C. Jung, "Micro- and nanoscale characterization of hydrophobic and hydrophilic leaf surfaces," *Nanotechnology*, vol. 17, no. 11, pp. 2758–2772, Jun. 2006, doi: 10.1088/0957-4484/17/11/008.

[165] L. Feng *et al.*, "Super-Hydrophobic Surfaces: From Natural to Artificial," *Adv. Mater.*, vol. 14, no. 24, pp. 1857–1860, Dec. 2002, doi: 10.1002/adma.200290020.

[166] X. W. Song, G. G. Zhang, Y. Wang, and S. G. Hu, "Use of bionic inspired surfaces for aerodynamic drag reduction on motor vehicle body panels," *J. Zhejiang Univ. Sci. A*, vol. 12, no. 7, pp. 543–551, Jul. 2011, doi: 10.1631/jzus.A1000505.

[167] X. W. Song, G. G. Zhang, Y. Wang, and S. G. Hu, "Aerodynamic drag reduction analysis of vehicle body with bionic non-smooth surfaces," *Journal of Hunan University Natural Sciences2*, 2010. https://www.researchgate.net/-publication/286869248_Aerodynamic_drag_reduction_analysis_of_vehicle_body_with_bionic_non-smooth_surfaces (accessed Sep. 08, 2019).

[168] R. I. Bourisli and A. A. Al-Sahhaf, "CFD modeling of turbulent boundary layer flow in passive drag-reducing applications," in *WIT Transactions on Engineering Sciences*, 2008, vol. 59, pp. 79–90, doi: 10.2495/AFM080081.

[169] O. Chanute, *Progress in flying machines*. Dover Publications, 1997.

[170] J. D. Jacob, "On The Fluid Dynamics of Adaptive Airfoils," *ASME Int. Eng. Congr. Expo.*, 1998.

[171] W. Shyy *et al.*, "Computational aerodynamics of low Reynolds number plunging, pitching and flexible wings for MAV applications," *Acta Mech. Sin. Xuebao*, vol. 24, no. 4, pp. 351–373, 2008, doi: 10.1007/s10409-008-0164-z.

[172] T. Bachmann, J. Emmerlich, W. Baumgartner, J. M. Schneider, and H. Wagner, "Flexural stiffness of feather shafts: geometry rules over material properties," *J. Exp. Biol.*, vol. 215, no. 3, pp. 405–415, 2012, doi: 10.1242/jeb.059451.

[173] R. Bonser and P. Purslow, "The Young's modulus of feather keratin," *J. Exp. Biol.*, vol. 198, no. 4, 1995.

[174] G. D. Macleod, "Mechanical Properties of Contour Feathers," *J. exp. Biol*, vol. 87, pp. 65–71, 1980.

[175] P. P. Purslow and J. F. V. Vincent, "Mechanical Properties of primary feathers from the pigeon," *J. Exp. Biol.*, vol. 72, pp. 251–260, 1978.

[176] V. A. Tucker, "Body drag, feather drag and interference drag of the mounting strut in a peregrine falcon,falco peregrinus," *J. Exp. Biol.*, vol. 149, no. 1, 1990, Accessed: Aug. 12, 2019. [Online]. Available: https://jeb.biologists.org/content/149/1/449.

[177] C. J. Pennycuick, "the mechanics of bird migration," *Int. J. Avian Sci.*, vol. 111, no. 4, pp. 525–556, Apr. 1969, doi: 10.1111/j.1474-919X.1969.tb02566.x.

[178] V. A. Tucker, "Bird Metabolism During Flight: Evaluation of a Theory," *J. Exp. Biol.*, vol. 58, no. 3, 1973.

[179] C. J. Pennycuick, H. H. Obrecht, and M. R. Fuller, "Empirical Estimates of Body Drag of Large Waterfowl and Raptors," *J. Exp. Biol.*, vol. 135, no. 1, 1988.

[180] V. A. Tucker and C. Heine, "aerodynamics of gliding flight in a harris' hawk, parabuteo unicinctus," *J. Exp. Biol.*, vol. 149, no. 1, 1990.

[181] Anders Hedeenstrom and Felix Liechtifelix Liechti, "Field estimates of body drag coefficient on the basis of dives in passerine birds," *J. Exp. Biol.*, no. 204, pp. 1167–1175, 2001, Accessed: Aug. 12, 2019. [Online]. Available: https://-pdfs.semanticscholar.org/05c3/b12a81057bd22e754413fc1a6963d7cf263e.pdf.

[182] V. A. Tucker, "Measuring Aerodynamic Interference Drag Between a Bird Body and the Mounting Strut of a drag Balance," *J. Exp. Biol.*, vol. 154, no. 1, 1990.

[183] V. A. Tucker, "Gliding flight: drag and torque of a hawk and a falcon with straight and turned heads, and a lower value for the parasite drag coefficient," *J. Exp. Biol.*, vol. 203, no. 24, 2000.

[184] J. Lovvorn, G. A. Liggins, M. H. Borstad, S. M. Calisal, and J. Mikkelsen, "Hydrodynamic drag of diving birds: effects of body size, body shape and feathers at steady speeds," *J. Exp. Biol.*, vol. 204, no. 9, 2001.

[185] W. J. Maybury and J. M. V. Rayner, "The avian tail reduces body parasite drag by controlling flow separation and vortex shedding," *Proc. R. Soc. London. Ser. B Biol. Sci.*, vol. 268, no. 1474, pp. 1405–1410, Jul. 2001, doi: 10.1098/rspb.2001.1635.

[186] J. M. V. Rayner and W. J. Maybury, "The Drag Paradox: Measurements of Flight Performance and Body Drag in Flying Birds," in *Avian Migration*, Berlin, Heidelberg: Springer Berlin Heidelberg, 2003, pp. 543–562.

[187] W. J. Maybury, "The aerodynamics of bird bodies," UNIVERSITY OF BRISTOL, 2000.

[188] B. W. Tobalske, J. W. D. Hearn, and D. R. Warrick, "Aerodynamics of intermittent bounds in flying birds," *Anim. Locomot.*, pp. 401–411, 2010, doi: 10.1007/978-3-642-11633-9_31.

[189] B. W. Tobalske, "Biomechanics of bird flight," *J. Exp. Biol.*, vol. 210, no. 18, pp. 3135–3146, Sep. 2007, doi: 10.1242/JEB.000273.

[190] J. Håkansson, L. Jakobsen, A. Hedenström, and L. C. Johansson, "Body lift, drag and power are relatively higher in large-eared than in small-eared bat species," *J. R. Soc. Interface*, vol. 14, no. 135, p. 20170455, Oct. 2017, doi: 10.1098/rsif.2017.0455.

[191] A. L. R. Thomas, "On the Tails of Birds," *Bioscience*, vol. 47, no. 4, pp. 215–225, Apr. 1997, doi: 10.2307/1313075.

[192] J. M. Smith, "The Importance of the Nervous System in the Evolution of Animal Flight," *Evolution (N. Y).*, vol. 6, no. 1, p. 127, Mar. 1952, doi: 10.2307/2405510.

[193] V. A. Tucker, "Pitching Equilibrium, Wing Span and Tail Span in a Gliding Harris' Hawk, Parabuteo Unicinctus," *J. Exp. Biol.*, vol. 165, no. 1, 1992, Accessed: Aug. 14, 2019. [Online]. Available: https://jeb.biologists.org/content/165/1/21.

[194] A. L. R. Thomas, "The Aerodynamic Costs of Asymmetry in the Wings and Tail of Birds: Asymmetric Birds can't Fly round Tight Corners," 1993. Accessed: Aug. 15, 2019. [Online]. Available: https://www-jstor-org.uproxy.library.dc-uoit.ca/stable/pdf/49894.pdf?refreqid=excelsior%3A765639442334971143396c8759e677cc.

[195] A. L. R. Thomas, "On the aerodynamics of birds' tails," *Phil. Trans. R. Soc. B*, vol. 340, no. 1294, p. 361, 1993.

[196] A. Balmford, A. L. R. Thomas, and I. L. Jones, "Aerodynamics and the evolution of long tails in birds," *Nature*, vol. 361, no. 6413, pp. 628–631, Feb. 1993, doi: 10.1038/361628a0.

[197] A. L. R. Thomas and A. Balmford, "How Natural Selection Shapes Birds' Tails," *The American Naturalist*, vol. 146. The University of Chicago PressThe American Society of Naturalists, pp. 848–868, 1995, doi: 10.2307/2463100.

[198] M. R. Evans, M. Rosén, K. J. Park, and A. Hedenström, "How do birds' tails work? Delta–wing theory fails to predict tail shape during flight," *Proc. R. Soc. London. Ser. B Biol. Sci.*, vol. 269, no. 1495, pp. 1053–1057, May 2002, doi: 10.1098/rspb.2001.1901.

[199] M. R. Evans, "Birds' Tails Do Act like Delta Wings but Delta-Wing Theory Does Not Always Predict the," vol. 270, no. 1522, pp. 1379–1385, 2003, doi: 10.1098/rspb.2003.2373.

[200] G. Sachs, "Tail effects on yaw stability in birds," *J. Theor. Biol.*, vol. 249, pp. 464–472, 2007, doi: 10.1016/j.jtbi.2007.07.014.

[201] D. Alexander, *Nature's flyers: birds, insects, and the biomechanics of flight*. 2002.

[202] R. H. J. Brown, "the flight of birds," *Biol. Rev.*, vol. 38, no. 4, pp. 460–489, Nov. 1963, doi: 10.1111/j.1469-185X.1963.tb00790.x.

[203] CJ Pennycuick -, "Mechanics of flight," *Avian Biol.*, pp. 1–73, 1975, Accessed: Aug. 15, 2019. [Online]. Available: https://ci.nii.ac.jp/naid/10004433287/.

[204] U. M. Norberg, *Vertebrate Flight*, vol. 27. Berlin, Heidelberg: Springer Berlin Heidelberg, 1990.

[205] C. J. Clark, "The Evolution of Tail Shape in Hummingbirds," *Auk*, vol. 127, no. 1, pp. 44–56, Jan. 2010, doi: 10.1525/auk.2009.09073.

[206] J. D. Gardiner, G. Dimitriadis, J. R. Codd, and R. L. Nudds, "A Potential Role for Bat Tail Membranes in Flight Control," *PLoS One*, vol. 6, no. 3, p. e18214, Mar. 2011, doi: 10.1371/journal.pone.0018214.

[207] P. Matyjasiak, J. Matyjasiak, F. de Lope, and A. P. Møller, "Vane emargination of outer tail feathers improves flight manoeuvrability in streamerless hirundines, Hirundinidae," *Proc. R. Soc. London. Ser. B Biol. Sci.*, vol. 271, no. 1550, pp. 1831–1838, Sep. 2004, doi: 10.1098/rspb.2004.2812.

[208] A. P. Møller, A. Barbosa, J. J. Cuervo, F. de Lope, S. Merino, and N. Saino, "Sexual selection and tail streamers in the barn swallow," *Proc. R. Soc. London. Ser. B Biol. Sci.*, vol. 265, no. 1394, pp. 409–414, Mar. 1998, doi: 10.1098/rspb.1998.0309.

[209] B. G. Newman, "Soaring and gliding flight of the {B}lack {V}ulture," *J. Exp. Biol.*, vol. 35, pp. 280–285, 1958, [Online]. Available: http://jeb.biologists.org/cgi/content/abstract/35/2/280.

[210] R. . Graham, "Safety Devices in Wing Birds," *J. R. Aeronaut. Soc.*, vol. 36, no. 253, pp. 24–58, 1932, doi: 10.1017/S0368393100111708.

[211] W. MULler and G. Patone, "Air transmissivity of feathers," *J. Exp. Biol.*, vol. 201 (Pt 18, pp. 2591–9, 1998, doi: 10.1098/rspb.2014.2864.

[212] A. R. Ennos, J. R. E. Hickson, and A. Roberts, "Functional morphology of the vanes of the flight feathers of the pigeon Columba livia," *J. Exp. Biol.*, vol. 198, pp. 1219–1228, 1995, [Online]. Available: http://www.ncbi.nlm.nih.gov/pubmed/9319072.

[213] K. E. Crandell and B. W. Tobalske, "Aerodynamics of tip-reversal upstroke in a revolving pigeon wing.," *J. Exp. Biol.*, vol. 214, no. Pt 11, pp. 1867–73, Jun. 2011, doi: 10.1242/jeb.051342.

[214] Tucker, "Gliding Birds: The Effect of Variable Wing Span," *J. Exp. Biol.*, vol. 133, no. 1, 1987.

[215] P. C. Withers, "An aerodynamic analysis of bird wings as fixed aerofoils," *J. Exp. Biol.*, vol. 90, pp. 143–162, 1981.

[216] A. M. Berg, A. A. Biewener, and C. P. Ellington, "Wing and body kinematics of takeoff and landing flight in the pigeon (Columba livia).," *J. Exp. Biol.*, vol. 213, no. Pt 10, pp. 1651–8, May 2010, doi: 10.1242/jeb.038109.

[217] V. Tucker, "Drag reduction by wing tip slots in a gliding Harris' hawk, Parabuteo unicinctus," *J. Exp. Biol.*, vol. 198, no. Pt 3, pp. 775–81, 1995, [Online]. Available: http://www.ncbi.nlm.nih.gov/pubmed/9318544.

[218] Tucker, "Drag reduction by wing tip slots in a gliding Harris' hawk, Parabuteo unicinctus," *J. Exp. Biol.*, vol. 198, no. 3, 1995.

[219] M. Fluck and C. Crawford, "A lifting line model to investigate the influence of tip feathers on wing performance," *Bioinspiration and Biomimetics*, vol. 9, no. 4, p. 46017, 2014, doi: 10.1088/1748-3182/9/4/046017.

[220] W. P. Henderson and B. J. Holmes, "Induced Drag - Historical Perspective," Sep. 1989, doi: 10.4271/892341.

[221] M. Munk, "The minimum induced drag of aerofoils.," 1923. [Online]. Available: https://ntrs.nasa.gov/search.jsp?-R=19800006779%5Cnhttp://www.engbrasil.eng.br/index_arquivos/art73.pdf.

[222] C. D. Cone, "The Theory of Induced Lift and Minimum Induced Drag of Non-planar Lifting Systems.," *Nasa Tr R-139*, 1962.

[223] K. Ilan, M. John, and S. Stephen C., "Highly Nonplanar Lifting Systems," 1995. Accessed: May 24, 2018. [Online]. Available: http://aero.stanford.edu/reports/nonplanarwings/nonplanarwings.html.

[224] S. V. Lyapunov, "Nonplanar wings with minimum induced drag," *Fluid Dyn.*, vol. 28, no. 2, pp. 238–243, 1993, doi: 10.1007/BF01051213.

[225] H. Zimmer, "The Aerodynamic Optimization of Wings at Subsonic Speeds and the Influence of Wingtip Design. Thesis," May 1987. Accessed: May 24, 2018. [Online]. Available: https://ntrs.nasa.gov/search.jsp?R=19870013194.

[226] M. Degen, A. R. Johnson, and W. E. Thompson, "Aerodynamic characteristics of ring wings and ringwing-body combinations," 1957.

[227] J. E. Hackett, "Vortex drag reduction by aft-mounted diffusing vanes," *ICAS*, vol. 80, 1980.

[228] L. U. Roche and S. Palffy, "Wing-grid, a novel device for reduction of induced drag on wings," in *ICAS 20thCongress*, 1996, pp. 2303–2309.

[229] J. J. Spillman, "The use of wing tip sails to reduce vortex drag," *Aeronaut. J.*, vol. 82, no. 813, pp. 387–395, 1978, doi: 10.1017/s0001924000091168.

[230] G. W. Webber and T. Dansby, "Wing tip devices for energy conversion and other purposes," *Can. Aeronaut. Sp. J.*, vol. 29, no. 2, pp. 105–120, 1983.

[231] V. A. Tucker and G. C. Parrott, "Aerodynamics of gliding flight in a falcon and other birds," *J. Exp. Biol.*, vol. 52, no. 2, pp. 345–367, 1970, [Online]. Available: http://jeb.biologists.org/content/52/2/345.short.

[232] C. J. Pennycuick, "A Wind-Tunnel Study of Gliding Flight in the Pigeon Columba Livia," *J. Exp. Biol.*, vol. 49, no. 3, 1968, Accessed: Aug. 15, 2019. [Online]. Available: https://jeb.biologists.org/content/49/3/509.

[233] V. A. Tucker, "Gliding Birds: Descending Flight of the Whitebacked Vulture, Gyps Africanus," *J. Exp. Biol.*, vol. 140, no. 1, 1988.

[234] A. Balmford, I. L. Jones, and A. L. R. Thomas, "On Avian Asymmetry: Evidence of Natural Selection for Symmetrical Tails and Wings in," 1993. Accessed: Aug. 15, 2019. [Online]. Available: https://www-jstor-org.uproxy.library.dc-uoit.ca/stable/pdf/49887.pdf?refreqid=excelsior%3A5fdf6614d1ee97116e78f10094616bc5.

[235] C. P. Ellington, C. van den Berg, A. P. Willmott, and A. L. R. Thomas, "Leading-edge vortices in insect flight," *Nature*, vol. 384, no. 6610, pp. 626–630, Dec. 1996, doi: 10.1038/384626a0.

[236] M. Rosén and A. Hedenström, "Gliding flight in a jackdaw: a wind tunnel study.," *J. Exp. Biol.*, vol. 204, no. Pt 6, pp. 1153–66, Mar. 2001, Accessed: Aug. 15, 2019. [Online]. Available: http://www.ncbi.nlm.nih.gov/pubmed/11222131.

[237] D. Lentink *et al.*, "How swifts control their glide performance with morphing wings," *Nature*, vol. 446, no. 7139, pp. 1082–1085, Apr. 2007, doi: 10.1038/nature05733.

[238] D. Lentink and R. de Kat, "Gliding Swifts Attain Laminar Flow over Rough Wings," *PLoS One*, vol. 9, no. 6, p. e99901, Jun. 2014, doi: 10.1371/journal.pone.0099901.

[239] M. R. Voloojerdi and M. Mani, "Aerodynamic Characteristics of Conventional and Innovative High Lift Swept Wings," *J. Bionic Eng.*, vol. 16, no. 3, pp. 432–441, May 2019, doi: 10.1007/s42235-019-0035-2.

[240] G. Sachs, "Aerodynamic yawing moment characteristics of bird wings," *J. Theor. Biol.*, vol. 234, pp. 471–478, 2005, doi: 10.1016/j.jtbi.2004.12.001.

[241] P. Krus and P. Krus, "Natural methods for flight stability in birds," in *1997 World Aviation Congress*, Oct. 1997, doi: 10.2514/6.1997-5653.

[242] G. Sachs, "Yaw stability in gliding birds," *J. Ornithol.*, vol. 146, no. 3, pp. 191–199, Jul. 2005, doi: 10.1007/s10336-005-0078-5.

[243] M. A. Moelyadi and G. Sachs, *Simulation of Dynamic Yaw Stability Derivatives of a Bird Using CFD*. 2007.

[244] W. Liebe, "Der Auftrieb am Tragugel: Entstehung und Zusammenbruch," *Aerokurier*, vol. 12, pp. 1520–3, 1979.

[245] R. Griffin, "Design of a passive flow control device derived from bird wing aerodynamics," Mechanical Engineering, 2012.

[246] K. Kernstine, C. Moore, A. Cutler, and R. Mittal, "Initial Characterization of Self-Activated Movable Flaps, "Pop-Up Feathers"," in *46th AIAA Aerospace Sciences Meeting and Exhibit*, Jan. 2008, doi: 10.2514/6.2008-369.

[247] J. U. Schluter, "Lift Enhancement at Low Reynolds Numbers Using Self-Activated Movable Flaps," *J. Aircr.*, vol. 47, no. 1, pp. 348–351, Jan. 2010, doi: 10.2514/1.46425.

[248] R. Barakat, "Incompressible Flow Around Porous Two-Dimensional Sails and Wings," *J. Math. Phys.*, vol. 47, no. 1–4, pp. 327–349, Apr. 1968, doi: 10.1002/sapm1968471327.

[249] C. S. Ventres and R. Barakat, "Aerodynamics of Airfoils with Porous Trailing Edges," *Aeronaut. Q.*, vol. 30, no. 2, pp. 387–399, May 1979, doi: 10.1017/S000192590000860X.

[250] G. . Savu and 0. Trifu, "Porous Airfoils in Transonic Flow," *AIAA J.*, vol. 22, no. 7, pp. 989–991, Jul. 1984, doi: 10.2514/3.48535.

[251] H. D. Gruschka, I. U. Borchers, and J. G. Coble, "Aerodynamic Noise produced by a Gliding Owl," *Nature*, vol. 233, no. 5319, pp. 409–411, Oct. 1971, doi: 10.1038/233409a0.

[252] G. Iosilevskii, "Aerodynamics of permeable membrane wings," *Eur. J. Mech. - B/Fluids*, vol. 30, no. 5, pp. 534–542, Sep. 2011, doi: 10.1016/J.EUROMECHFLU.2011.05.003.

[253] G. Iosilevskii, "Aerodynamics of permeable membrane wings. Part 2: Seepage drag," *Eur. J. Mech. - B/Fluids*, vol. 39, pp. 32–41, May 2013, doi: 10.1016/J.EUROMECHFLU.2012.11.004.

[254] D. Venkataraman and A. Bottaro, "Numerical modeling of flow control on a symmetric aerofoil via a porous, compliant coating," *Phys. Fluids*, vol. 24, no. 9, p. 093601, Sep. 2012, doi: 10.1063/1.4748962.

[255] T. Bachmann and A. Winzen, "OWL INSPIRED SILENT FLIGHT," 2014, pp. 695–717.

[256] T. Geyer, E. Sarradj, and C. Fritzsche, "Nature-Inspired Porous Airfoils for Sound Reduction," Springer, Berlin, Heidelberg, 2012, pp. 355–370.

[257] A. Winzen, M. Klaas, and W. Schröder, "High-Speed Particle Image Velocimetry and Force Measurements of Bio-Inspired Surfaces," *J. Aircr.*, vol. 52, no. 2, pp. 471–485, Mar. 2015, doi: 10.2514/1.C032742.

[258] A. Winzen, M. Klaas, and W. Schröder, "High-speed PIV measurements of the near-wall flow field over hairy surfaces," *Exp. Fluids*, vol. 54, no. 3, p. 1472, Mar. 2013, doi: 10.1007/s00348-013-1472-z.

[259] H. Wagner, M. Weger, M. Klaas, and W. Schröder, "Features of owl wings that promote silent flight," *Interface Focus*, vol. 7, no. 1, p. 20160078, Feb. 2017, doi: 10.1098/rsfs.2016.0078.

[260] M. Aldheeb, W. Asrar, E. Sulaeman, and A. A. Omar, "Aerodynamics of porous airfoils and wings," *Acta Mech.*, vol. 229, no. 9, pp. 3915–3933, Sep. 2018, doi: 10.1007/s00707-018-2203-6.

[261] K. Malik *et al.*, "Effects of Bio-Inspired Surface Roughness on a Swept Back Tapered NACA 4412 Wing," *J. Aerosp. Technol. Manag.*, vol. 11, 2019, doi: 10.5028/jatm.v11.1021.

[262] R. T. Whitcomb, "A design approach and selected wind tunnel results at high subsonic speeds for wing-tip mounted winglets," *Nasa Tn D-8260*, no. July, pp. 1–33, 1976, [Online]. Available: http://ntrs.nasa.gov/archive/nasa/casi.ntrs.nasa.gov/-19760019075.pdf.

[263] Tucker, "Gliding birds: reduction of induced drag by wing tip slots between the primary feathers," *J. Exp. Biol.*, vol. 180, no. 1, 1993.

[264] J. P. Swaddle and R. Lockwood, "Wingtip shape and flight performance in the European starling Sturnus vulgaris," *Ibis (Lond. 1859).*, vol. 145, no. 3, pp. 457–464, 2003, doi: 10.1046/j.1474-919X.2003.00189.x.

[265] G. Sachs and M. A. Moelyadi, "Effect of slotted wing tips on yawing moment characteristics," *J. Theor. Biol.*, vol. 239, no. 1, pp. 93–100, 2006, doi: 10.1016/j.jtbi.2005.07.016.

[266] J. E. Guerrero, D. Maestro, and A. Bottaro, "Biomimetic spiroid winglets for lift and drag control," *Comptes Rendus - Mec.*, vol. 340, no. 1–2, pp. 67–80, 2012, doi: 10.1016/j.crme.2011.11.007.

[267] J. E. Guerrero and D. Maestro, "Biomimetic spiroid winglets for lift and drag control," *Comptes Rendus Mécanique*, vol. 340, no. 1–2, pp. 67–80, Jan. 2012, doi: 10.1016/J.CRME.2011.11.007.

[268] M. Lynch, B. Mandadzhiev, and A. Wissa, "Bioinspired wingtip devices: a pathway to improve aerodynamic performance during low Reynolds number flight," *Bioinspir. Biomim.*, vol. 13, no. 3, p. 036003, Mar. 2018, doi: 10.1088/1748-3190/aaac53.

[269] N. Siddiqui, M. Aldeeb, W. Asrar, and E. Sulaeman, "Experimental investigation of a new spiral wingtip," *Int. J. Aviat. Aeronaut. Aerosp.*, vol. 5, no. 2, Mar. 2018, doi: 10.15394/ijaaa.2018.1213.

[270] A. Wissa, A. K. Han, and M. R. Cutkosky, "Wings of a feather stick together: Morphing wings with barbule-inspired latching," in *Lecture Notes in Computer Science (including subseries Lecture Notes in Artificial Intelligence and Lecture Notes in Bioinformatics)*, 2015, vol. 9222, pp. 123–134, doi: 10.1007/978-3-319-22979-9_13.

[271] S. J. Portugal *et al.*, "Upwash exploitation and downwash avoidance by flap phasing in ibis formation flight," *Nature*, vol. 505, no. 7483, pp. 399–402, Jan. 2014, doi: 10.1038/nature12939.

[272] H. Chen, F. Rao, X. Shang, D. Zhang, and I. Hagiwara, "Biomimetic Drag Reduction Study on Herringbone Riblets of Bird Feather," *J. Bionic Eng.*, vol. 10, no. 3, pp. 341–349, Sep. 2013, doi: 10.1016/S1672-6529(13)60229-2.

[273] T. McKeag, "Auspicious Forms: Designing the Sanyo Shinkansen 500-Series Bullet Train," *Zygote Q.*, no. 2, pp. 12–36, 2012.

[274] AskNature, "Shinkansen Train," *AskNature*, 2017. https://asknature.org/idea/shinkansen-train/ (accessed Sep. 08, 2019).

[275] B. Wiltgen and A. K. Goel, "Functional Model Simulation for Evaluating Design Concepts," 2016. Accessed: Sep. 08, 2019. [Online]. Available: www.asknature.org.

[276] M. Hildebrand, "Motions of the Running Cheetah and Horse," *J. Mammal.*, vol. 40, no. 4, p. 481, Nov. 1959, doi: 10.2307/1376265.

[277] Blaine Friedlander, "When tiger beetles chase prey at high speeds they go blind temporarily, Cornell entomologists learn | Cornell Chronicle," *Cornell Chronicle*, 1998. http://news.cornell.edu/stories/1998/01/tiger-beetles-go-blind-chasing-prey-high-speeds (accessed Aug. 19, 2019).

[278] A. M. Wilson, J. C. Lowe, K. Roskilly, P. E. Hudson, K. A. Golabek, and J. W. McNutt, "Locomotion dynamics of hunting in wild cheetahs," *Nature*, vol. 498, no. 7453, pp. 185–189, Jun. 2013, doi: 10.1038/nature12295.

[279] E. Muybridge, *Animals in motion*. Dover Publications, 1957.

[280] M. Hildebrand, "Further Studies on Locomotion of the Cheetah," *J. Mammal.*, vol. 42, no. 1, p. 84, Feb. 1961, doi: 10.2307/1377246.

[281] P. E. Hudson, S. A. Corr, R. C. Payne-Davis, S. N. Clancy, E. Lane, and A. M. Wilson, "Functional anatomy of the cheetah (Acinonyx jubatus) hindlimb," *J. Anat.*, vol. 218, no. 4, pp. 363–374, Apr. 2011, doi: 10.1111/j.1469-7580.2010.01310.x.

[282] A. Patel, "Understanding the Motions of the Cheetah Tail Using Robotics," UNIVERSITY OF CAPE TOWN , 2014.

[283] A. Patel, E. Boje, C. Fisher, L. Louis, and E. Lane, "Quasi-steady state aerodynamics of the cheetah tail.," *Biol. Open*, vol. 5, no. 8, pp. 1072–6, Aug. 2016, doi: 10.1242/bio.018457.

[284] A. J. Spence, A. S. Thurman, M. J. Maher, and A. M. Wilson, "Speed, pacing strategy and aerodynamic drafting in Thoroughbred horse racing," *Biol. Lett.*, vol. 8, no. 4, p. 678, Aug. 2012, doi: 10.1098/RSBL.2011.1120.

[285] Anonymous, "Horse Racing Position Cuts Drag by up to 66%," *Australasian Science*, p. 11, Feb. 2015.

[286] Anne Marie Helmenstine, "How Fast Can a Cheetah Run?," *ThoughtCo.*, 2019. https://www.thoughtco.com/how-fast-can-a-cheetah-run-4587031 (accessed May 25, 2021).

[287] S. Peng, X. Liu, Z. Li, and F. Jiang, "Application of Bionics of Tiger Beetle to Aerodynamic Optimization of MIRA Fastback Model," in *International Conference on Computer Science and Application Engineering*, 2017, pp. 1–10.

[288] S. O. Kang *et al.*, "actively translating a rear diffuser device for the aerodynamic drag reduction of a passenger car," *Int. J. Automot. Technol.*, vol. 13, no. 4, pp. 583–592, 2012.

[289] T. Heinemann, M. Springer, H. Lienhart, S. Kniesburges, C. Othmer, and S. Becker, "Active flow control on a 1:4 car model," *Exp. Fluids*, vol. 55, no. 5, pp. 1–11, May 2014, doi: 10.1007/s00348-014-1738-0.

[290] R. Mestiri, A. Ahmed-Bensoltane, L. Keirsbulck, F. Aloui, and L. Labraga, "Active flow control at the rear end of a generic car model using steady blowing," *J. Appl. Fluid Mech.*, vol. 7, no. 4, pp. 565–571, 2014, doi: 10.36884/jafm.7.04.21752.

[291] M. Rouméas, P. Gilliéron, and A. Kourta, "Analysis and control of the near-wake flow over a square-back geometry," *Comput. Fluids*, vol. 38, no. 1, pp. 60–70, Jan. 2009, doi: 10.1016/j.compfluid.2008.01.009.

[292] E. Wassen and F. Thiele, "Drag reduction for a generic car model using steady blowing," in *4th AIAA Flow Control Conference*, 2008, doi: 10.2514/6.2008-3771.

[293] D. Krentel, R. Muminovic, A. Brunn, W. Nitsche, and R. King, "Application of active flow control on generic 3d car models," *Notes Numer. Fluid Mech. Multidiscip. Des.*, vol. 108, pp. 223–239, 2010, doi: 10.1007/978-3-642-11735-0_15.

[294] E. Wassen, S. Eichinger, and F. Thiele, "Simulation of active drag reduction for a square-back vehicle," *Notes Numer. Fluid Mech. Multidiscip. Des.*, vol. 108, pp. 241–255, 2010, doi: 10.1007/978-3-642-11735-0_16.

[295] S. Aubrun, J. McNally, F. Alvi, and A. Kourta, "Separation flow control on a generic ground vehicle using steady microjet arrays," *Exp. Fluids*, vol. 51, no. 5, pp. 1177–1187, Nov. 2011, doi: 10.1007/s00348-011-1132-0.

[296] J. McNally *et al.*, "Drag reduction on a flat-back ground vehicle with active flow control," *J. Wind Eng. Ind. Aerodyn.*, vol. 145, pp. 292–303, Oct. 2015, doi: 10.1016/j.jweia.2015.03.006.

[297] H. Park, J. H. Cho, J. Lee, D. H. Lee, and K. H. Kim, "Aerodynamic Drag Reduction of Ahmed Model Using Synthetic Jet Array," *SAE Int. J. Passeng. Cars - Mech. Syst.*, vol. 6, no. 1, pp. 1–6, Mar. 2013, doi: 10.4271/2013-01-0095.

[298] A. Kourta and C. Leclerc, "Characterization of synthetic jet actuation with application to Ahmed body wake," *Sensors Actuators, A Phys.*, vol. 192, pp. 13–26, 2013, doi: 10.1016/j.sna.2012.12.008.

[299] N. Tounsi, R. Mestiri, L. Keirsbulck, H. Oualli, S. Hanchi, and F. Aloui, "Experimental study of flow control on bluff body using piezoelectric actuators," *J. Appl. Fluid Mech.*, vol. 9, no. 2, pp. 827–838, 2016, doi: 10.18869/acadpub.jafm.68.225.24488.

[300] P. Joseph, X. Amandolèse, and J.-L. Aider, "Drag reduction on the 25° slant angle Ahmed reference body using pulsed jets," *Exp. Fluids*, vol. 52, no. 5, pp. 1169–1185, May 2012, doi: 10.1007/s00348-011-1245-5.

[301] P. Gilliéron *et al.*, "Drag reduction by pulsed jets on strongly unstructured wake: towards the square back control," *Int. J. Aerodyn.*, vol. 1, no. 3/4, p. pages 282-298, 2011.

[302] P. Gillieron and A. Kourta, "Massive separation control analysis of the pulsed jet actuators effects | Mechanics & Industry | Cambridge Core," *Mech. Ind.*, vol. 14, no. 6, pp. 441–445, Feb. 2013, Accessed: Apr. 11, 2020. [Online]. Available: https://www.cambridge.org/core/journals/mechanics-and-industry/article/massive-separation-control-analysis-of-the-pulsed-jet-actuators-effects/6F226CECB8B9F259035F63B2D106E94E.

[303] A. Kourta and P. Gilliéron, "Impact of the automotive aerodynamic control on the economic issues," *J. Appl. Fluid Mech.*, vol. 2, no. 2, pp. 69–75, 2009.

[304] B. Lehugeur, P. Gilliéron, and A. Kourta, "Experimental investigation on longitudinal vortex control over a dihedral bluff body," *Exp. Fluids*, vol. 48, no. 1, pp. 33–48, Jan. 2010, doi: 10.1007/s00348-009-0707-5.

[305] E. Wassen and F. Thiele, "Road vehicle drag reduction by combined steady blowing and suction," in *39th AIAA Fluid Dynamics Conference*, 2009, doi: 10.2514/6.2009-4174.

[306] J. T. Whiteman and M. Zhuang, "Active flow control schemes for bluff body drag reduction," in *American Society of Mechanical Engineers, Fluids Engineering Division (Publication) FEDSM*, Dec. 2016, vol. 1A-2016, doi: 10.1115/FEDSM2016-7520.

[307] V. Boucinha, R. Weber, and A. Kourta, "Drag reduction of a 3D bluff body using plasma actuators," *Int. J. Aerodyn.*, vol. 1, no. 3/4, p. 262, 2011, doi: 10.1504/ijad.2011.038845.

[308] S Shadmani, S. M. Mousavi Nainiyan, Ramin Ghasemiasl, and Masoud Mirzaei, "Experimental Study of Flow Control Over an Ahmed Body Using Plasma Actuator," *Mech. Mech. Eng.*, vol. 22, no. 1, pp. 239–251, Jun. 2018, Accessed: Apr. 11, 2020. [Online]. Available: https://www.researchgate.net/publication/325847753_Experimental_Study_of_Flow_Control_Over_-an_Ahmed_Body_Using_Plasma_Actuator.

[309] B. Khalighi, J. Ho, J. Cooney, B. Neiswander, T. C. Corke, and T. Han, "Aerodynamic drag reduction investigation for a simplified road vehicle using plasma flow control," in *American Society of Mechanical Engineers, Fluids Engineering Division (Publication) FEDSM*, Dec. 2016, vol. 1A-2016, doi: 10.1115/FEDSM2016-7927.

[310] J. L. Aider, J. F. Beaudoin, and J. E. Wesfreid, "Drag and lift reduction of a 3D bluff-body using active vortex generators," *Exp. Fluids*, vol. 48, no. 5, pp. 771–789, May 2010, doi: 10.1007/s00348-009-0770-y.

[311] I. Kim and H. Chen, "Reduction of aerodynamic forces on a minivan by a pair of vortex generators of a pocket type," *Int. J. Veh. Des.*, vol. 53, no. 4, pp. 300–316, Jul. 2010, doi: 10.1504/IJVD.2010.034103.

[312] G. Pujals, S. Depardon, and C. Cossu, "Drag reduction of a 3D bluff body using coherent streamwise streaks," *Exp. Fluids*, vol. 49, no. 5, pp. 1085–1094, Nov. 2010, doi: 10.1007/s00348-010-0857-5.

[313] G. Filip, K. Maki, P. Bachant, and R. Lietz, "Simulation of Flow Control Devices in Support of Vehicle Drag Reduction," in *SAE Technical Papers*, Apr. 2018, vol. 2018-April, doi: 10.4271/2018-01-0713.

[314] S. Krajnović, "Large eddy simulation exploration of passive flow control around an Ahmed body," *J. Fluids Eng. Trans. ASME*, vol. 136, no. 12, Dec. 2014, doi: 10.1115/1.4027221.

[315] Walid Ibrahim Mazyan, "Numerical simulations of drag-reducing devices for ground vehicles ," American University of Sharjah, Sharjah, 2013.

[316] G. Shankar and G. Devaradjane, "Experimental and computational analysis on aerodynamic behavior of a car model with vortex generators at different yaw angles," *J. Appl. Fluid Mech.*, vol. 11, no. 1, pp. 285–295, 2018, doi: 10.29252/jafm.11.01.28357.

[317] I. Kim, H. Chen, and R. C. Shulze, "A rear spoiler of a new type that reduces the aerodynamic forces on a mini-van," in *SAE Technical Papers*, Apr. 2006, doi: 10.4271/2006-01-1631.

[318] J.-F. Beaudoin and J.-L. Aider, "Drag and lift reduction of a 3D bluff body using flaps," *Exp. Fluids*, vol. 44, no. 4, pp. 491–501, Apr. 2008, doi: 10.1007/s00348-007-0392-1.

[319] J. Tian, Y. Zhang, H. Zhu, and H. Xiao, "Aerodynamic drag reduction and flow control of Ahmed body with flaps," *Adv. Mech. Eng.*, vol. 9, no. 7, pp. 1–17, 2017, doi: 10.1177/1687814017711390.

[320] J. Marklund, L. Lofdahl, H. Danielsson, and G. Olsson, "Performance of an Automotive Under-Body Diffuser Applied to a Sedan and a Wagon Vehicle," *SAE Int. J. Passeng. Cars - Mech. Syst.*, vol. 6, no. 1, pp. 293–307, Apr. 2013, doi: 10.4271/2013-01-0952.

[321] J. Cho, T. K. Kim, K. H. Kim, and K. Yee, "Comparative investigation on the aerodynamic effects of combined use of underbody drag reduction devices applied to real sedan," *Int. J. Automot. Technol.*, vol. 18, no. 6, pp. 959–971, Dec. 2017, doi: 10.1007/s12239-017-0094-5.

[322] K. S. Song *et al.*, "Aerodynamic design optimization of rear body shapes of a sedan for drag reduction," *Int. J. Automot. Technol.*, vol. 13, no. 6, pp. 905–914, Oct. 2012, doi: 10.1007/s12239-012-0091-7.

[323] X. Hu *et al.*, "Automotive shape optimization using the radial basis function model based on a parametric surface grid," *Proc. Inst. Mech. Eng. Part D J. Automob. Eng.*, vol. 230, no. 13, pp. 1808–1821, Nov. 2016, doi: 10.1177/0954407015624042.

[324] C. H. Bruneau, E. Creusé, D. Depeyras, P. Gilliéron, and I. Mortazavi, "Coupling active and passive techniques to control the flow past the square back Ahmed body," *Comput. Fluids*, vol. 39, no. 10, pp. 1875–1892, Dec. 2010, doi: 10.1016/j.compfluid.2010.06.019.

[325] . B., . H., E. A. Kosasih, R. F. Karim, and J. Julian, "Drag reduction by combination of flow control using inlet disturbance body and plasma actuator on cylinder model," *J. Mech. Eng. Sci.*, vol. 13, no. 1, pp. 4503–4511, Mar. 2019, doi: 10.15282/jmes.13.1.2019.12.0382.

[326] A. Evrard, O. Cadot, C. Sicot, V. Herbert, D. Ricot, and R. Vigneron, "Comparative effects of vortex generators on Ahmed's squareback and minivan car models," *Proc. Inst. Mech. Eng. Part D J. Automob. Eng.*, vol. 231, no. 9, pp. 1287–1293, Aug. 2017, doi: 10.1177/0954407016681696.

[327] M. O. L. Hansen *et al.*, "Aerodynamically shaped vortex generators," *Wind Energy*, vol. 19, no. 3, pp. 563–567, Mar. 2016, doi: 10.1002/we.1842.

[328] J. C. Lin, F. G. Howard, and G. V. Selbyt, "Small submerged vortex generators for turbulent flow," *J. Spacecr. Rockets*, vol. 27, no. 5, pp. 503–507, 1990, doi: 10.2514/3.26172.

[329] P. Martínez-Filgueira, U. Fernandez-Gamiz, E. Zulueta, I. Errasti, and B. Fernandez-Gauna, "Parametric study of low-profile vortex generators," *Int. J. Hydrogen Energy*, vol. 42, no. 28, pp. 17700–17712, Jul. 2017, doi: 10.1016/j.ijhydene.2017.03.102.

[330] G. Fourrié, L. Keirsbulck, L. Labraga, and P. Gilliéron, "Bluff-body drag reduction using a deflector," *Exp. Fluids*, vol. 50, no. 2, pp. 385–395, Feb. 2011, doi: 10.1007/s00348-010-0937-6.

[331] W. Hanfeng, Z. Yu, Z. Chao, and H. Xuhui, "Aerodynamic drag reduction of an Ahmed body based on deflectors," *J. Wind Eng. Ind. Aerodyn.*, vol. 148, pp. 34–44, Jan. 2016, doi: 10.1016/j.jweia.2015.11.004.

[332] A. Altaf, A. A. Omar, and W. Asrar, "Passive drag reduction of square back road vehicles," *Jnl. Wind Eng. Ind. Aerodyn.*, vol. 134, pp. 30–43, 2014, doi: 10.1016/j.jweia.2014.08.006.

[333] C.-H. Bruneau, I. Mortazavi, and P. Gilliéron, "Passive Control Around the Two-Dimensional Square Back Ahmed Body Using Porous," *J. fluid Eng.*, vol. 130, no. 6, pp. 1–12, 2008, doi: 10.1115/1.2917423.

[334] S. R. Ahmed, G. Ramm, and G. Faltin, "Some Salient Features Of The Time-Averaged Ground Vehicle Wake," *SAE Trans.*, vol. 93, no. 2, pp. 473–503, Feb. 1984, doi: 10.4271/840300.

[335] H. B. Evans *et al.*, "Engineered bio-inspired coating for passive flow control," *Proc. Natl. Acad. Sci. U. S. A.*, vol. 115, no. 6, pp. 1210–1214, Feb. 2018, doi: 10.1073/pnas.1715567115.

[336] R. Bansal and R. B. Sharma, "drag reduction of a generic passenger car using vortex generator with different yaw angles," *Int. J. Automob. Eng. Res. Dev.*, vol. 3, no. 2, pp. 73–80, 2013.

[337] S. Mohandas, R. Krishna Siddharth, and B. John, "Reduction of wave drag on parameterized blunt bodies using spikes with varied tip geometries," *Acta Astronaut.*, vol. 160, pp. 25–35, Jul. 2019, doi: 10.1016/j.actaastro.2019.04.017.